SAND2019-4442PE

Molecular Level Details of Dynamics, Domain Structure and Transport in Polymers using NMR Spectroscopy

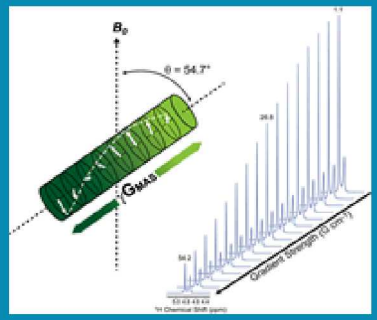

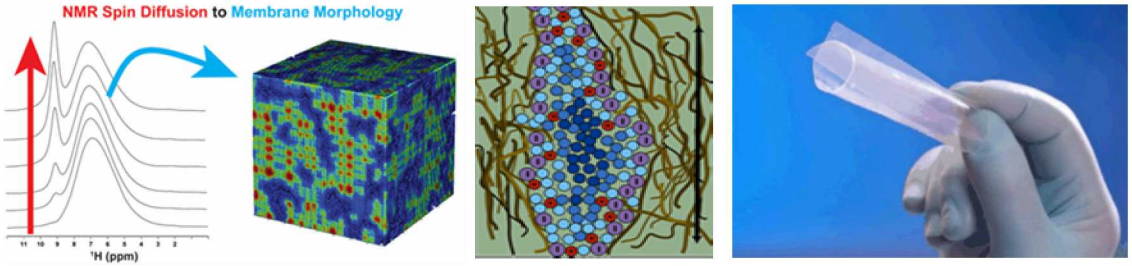

Macromolecules Institute's Solvay Seminar
Virginia Tech Chemistry and Chemical Engineering
April 24th 2019

PRESENTED BY

Dr. Todd M. Alam

Organic Materials Science Department
Sandia National Laboratories
Albuquerque, NM 87185

LDRD
LABORATORY DIRECTED RESEARCH & DEVELOPMENT

Sandia National Laboratories is a multimission laboratory managed and operated by National Technology and Engineering Solutions of Sandia LLC, a wholly owned subsidiary of Honeywell International Inc. for the U.S. Department of Energy's National Nuclear Security Administration under contract DE-NA0003525.

SAND2019-XXXXXX

SANDIA'S HISTORY IS TRACED TO THE MANHATTAN PROJECT

…In my opinion you have here an opportunity to render an exceptional service in the national interest.

- July 1945
  Los Alamos creates Z Division
- Nonnuclear component engineering
- November 1, 1949
  Sandia Laboratory established
- AT&T: 1949–1993
- Martin Marietta: 1993–1995
- Lockheed Martin: 1995–2017
- Honeywell: 2017–present

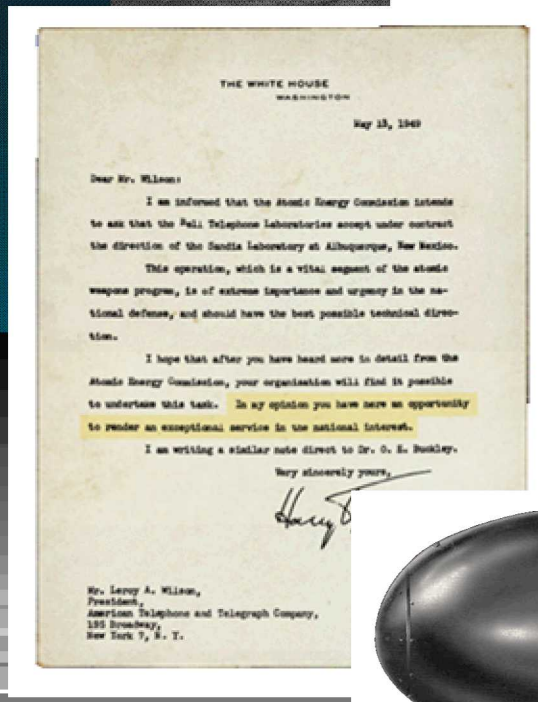

THE WHITE HOUSE
WASHINGTON

May 13, 1949

Dear Mr. Wilson:

I am informed that the Atomic Energy Commission intends to ask that the Bell Telephone Laboratories accept under contract the direction of the Sandia Laboratory at Albuquerque, New Mexico.

This operation, which is a vital segment of the atomic weapons program, is of extreme importance and urgency in the national defense, and should have the best possible technical direction.

I hope that after you have heard more in detail from the Atomic Energy Commission, your organization will find it possible to undertake this task. In my opinion you have here an opportunity to render an exceptional service in the national interest.

I am writing a similar note direct to Dr. O. E. Buckley.

Very sincerely yours,

Mr. Leroy A. Wilson,
President,
American Telephone and Telegraph Company,
195 Broadway,
New York 7, N. Y.

SANDIA HAS FACILITIES ACROSS THE NATION

Activity locations

- Kauai, Hawaii
- Waste Isolation Pilot Plant, Carlsbad, New Mexico
- Pantex Plant, Amarillo, Texas
- Tonopah, Nevada

Main sites

- Albuquerque, New Mexico
- Livermore, California

PURPOSE STATEMENT DEFINES WHAT WE DO

Multiple research thrust areas at Sandia

Energy

Energy Research

ARPAe, BES Chem Sciences, ASCR, CINT, Geo Bio Science, BES Material Science

Climate & Environment

Measurement & Modeling, Carbon Management, Water & Environment, and Biofuels

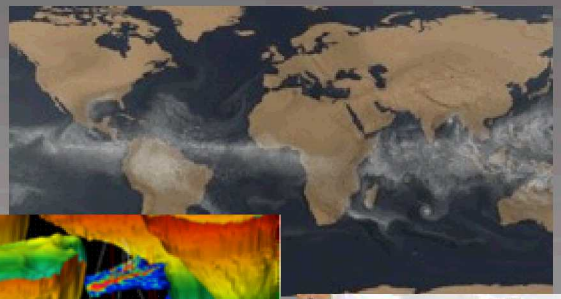

Nuclear Energy & Fuel Cycle

Commercial Nuclear Power & Fuel, Nuclear Energy Safety & Security, DOE Managed Nuclear Waste Disposal

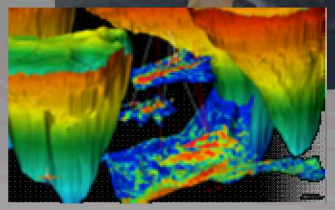

Renewable Systems & Energy Infrastructure

Renewable Energy, Energy Efficiency, Grid and Storage Systems

Transportation Energy & Systems

Vehicle Technologies, Biomass, Fuel Cells & Hydrogen Technology

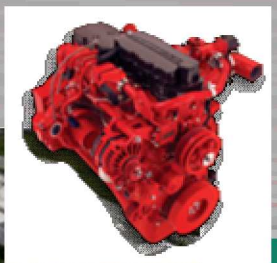

NMR Centric…. Biased View

Home Land Security

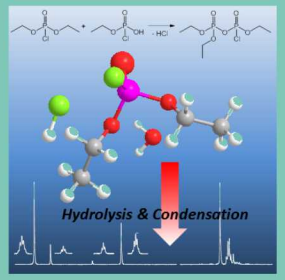

Bulk decontamination of bulk CWAs

Materials

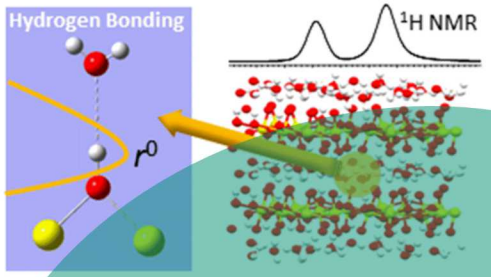

Dynamics in uranyl capsules

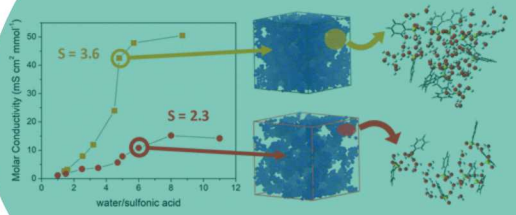

Fuel cell membranes

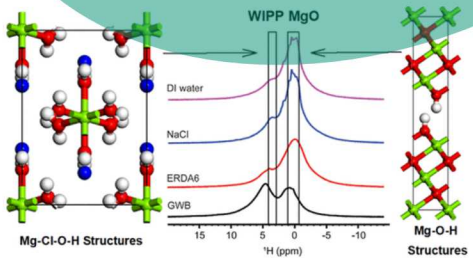

Intermediate phases in MgO hydration

NMR Spectroscopy

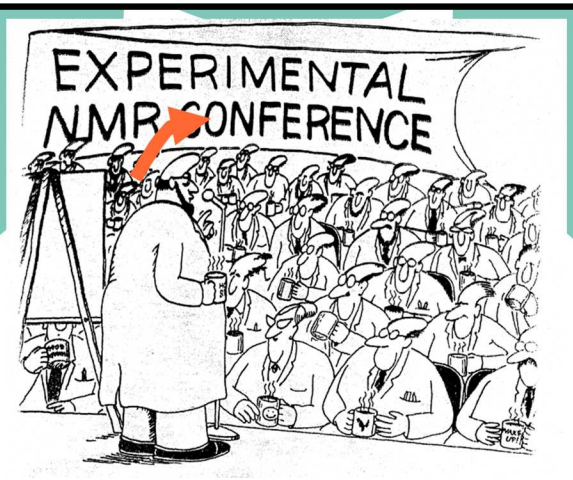

"Therefore we can draw the conclusion that long term exposure to high magnetic fields has no known harmful physical effect"

NMR Diffusometry

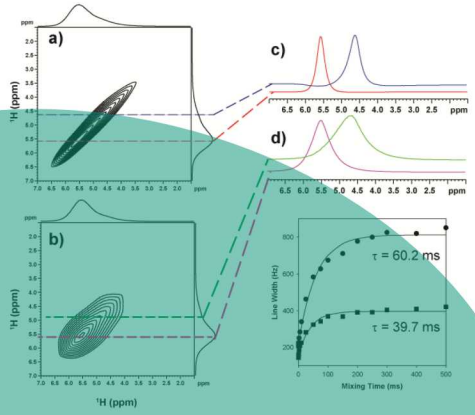

Solvent diffusion in nanocarbon

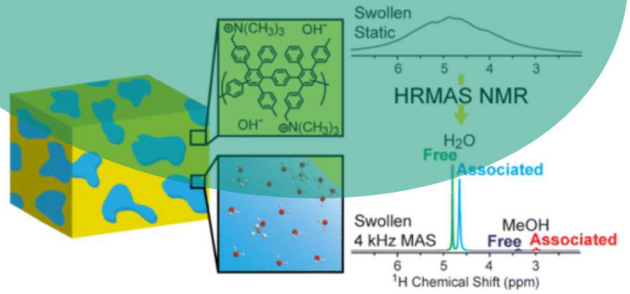

Diffusion in PEMs and AEMs

Outline

Transport in PEMS SDAPP membranes

- Motivation for SDAPP
- MD Simulations of Nanomorphology
- Characterization (NMR and SAXS)
- NMR Diffusometry

Chain dynamics in Ferrocene cured thermosets

- Cure stress in cross-linked polymers
- ^{1}H NMR of chain dynamics

Fuel Cells – Emerging Technology
"Old Technology – Material Advances Lead the Way"

- Convert chemical energy (fuel) to electricity using oxygen.
- Different types of fuels (hydrogen, methanol, ethanol…).
- Can produce electricity as *long as there is fuel* (unlike batteries)….remote locations.
- Power generation (backup), including remote sites, military, automobile.
- Higher efficiency (60 – 85%) than combustion systems (30%).

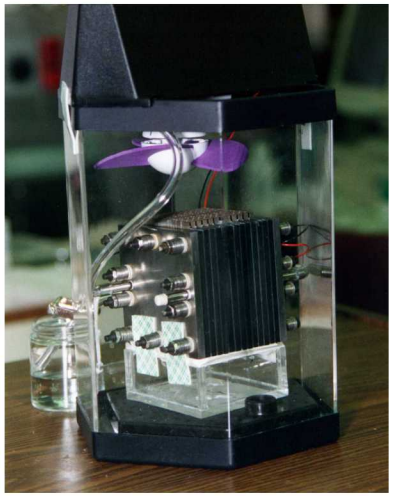

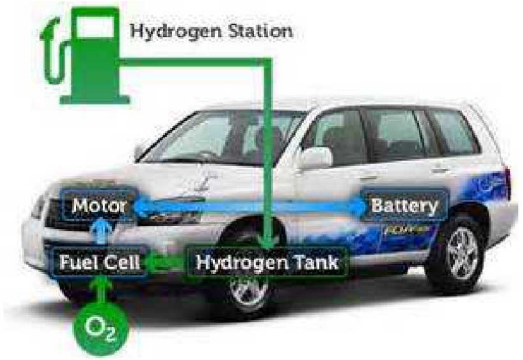

Polymer Exchange Membranes (PEM) at Sandia

Proton exchange membranes

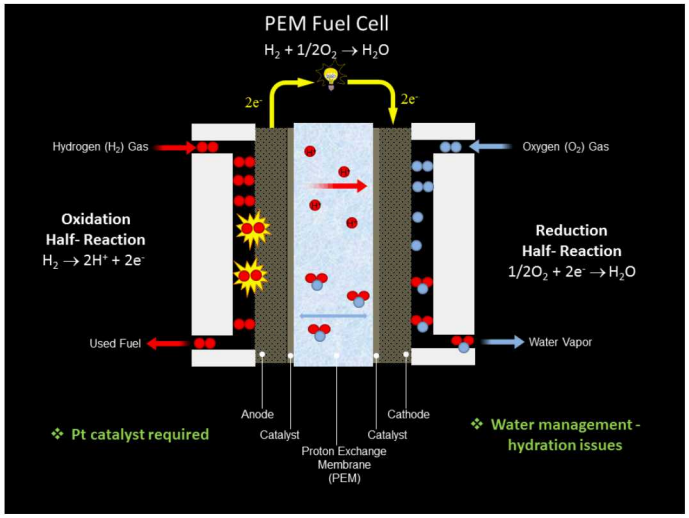

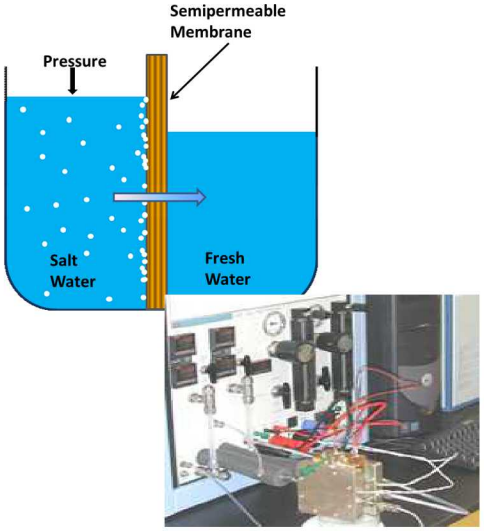

- Fuel Cells (PEMs and AEM)
- Battery Separators
- Flow Batteries (V, Na, Fe *etc.*)
- Catalyst Support Binder

- Desalination
- Reverse Osmosis
- Electrolysis
- Ion Selective Electrodes

"Development of new membranes materials for a wide range of technological applications ultimately based on fundamental understanding of transport…"

Sulfonated Diels Alder Polyphenylene (SDAPP) Membranes

Nafion

(perfluoronated membranes)

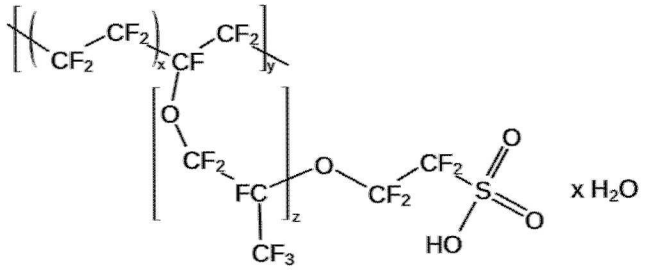

- Good conductivity at low temperatures.
- The present industry standard.

SDAPP

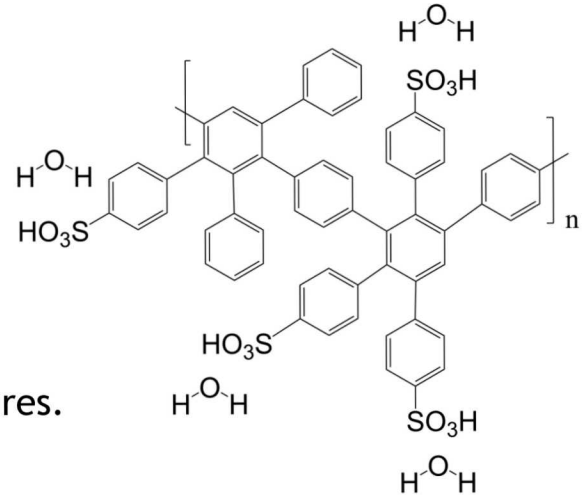

- Stable in alkaline environments.
- High T_g (~350 °C).
- Easily processed.
- Wide range of functionalities.
- Promising alternative to Nafion.
- No F (i.e. HF) during aging

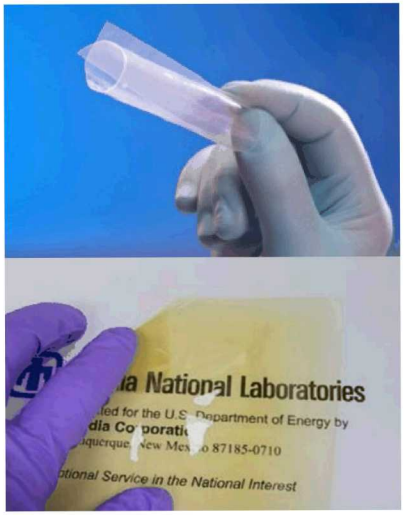

SDAPP Analogues

AEM (Anion Exchange Membranes)

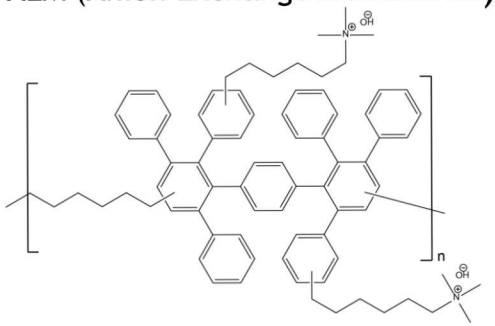

MeOH fuel cell (Hibbs, SNL)

SDAPP-FDPS Copolymers

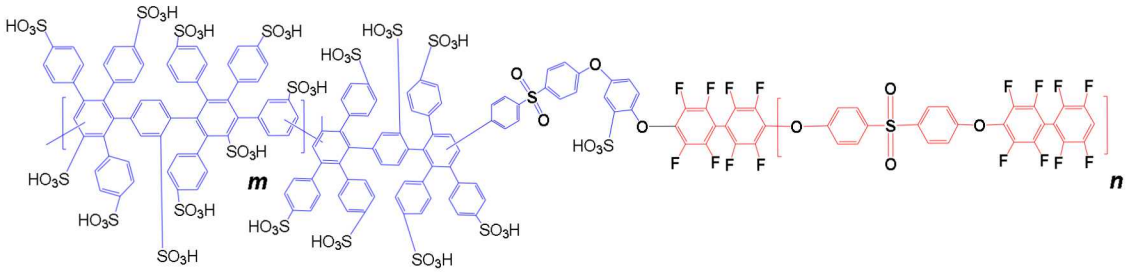

Fujimoto, C. H., Hickner, M. A., Cornelius, C. J., Loy, D. A., Macromolecules 2005, 38 (12), 5010-5016.

Diels Alder Polymerization

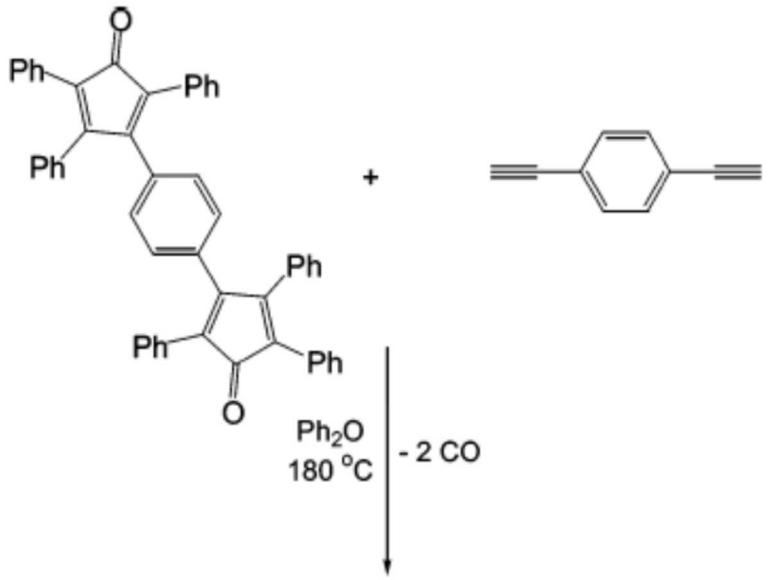

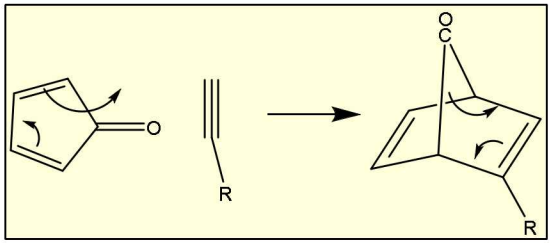

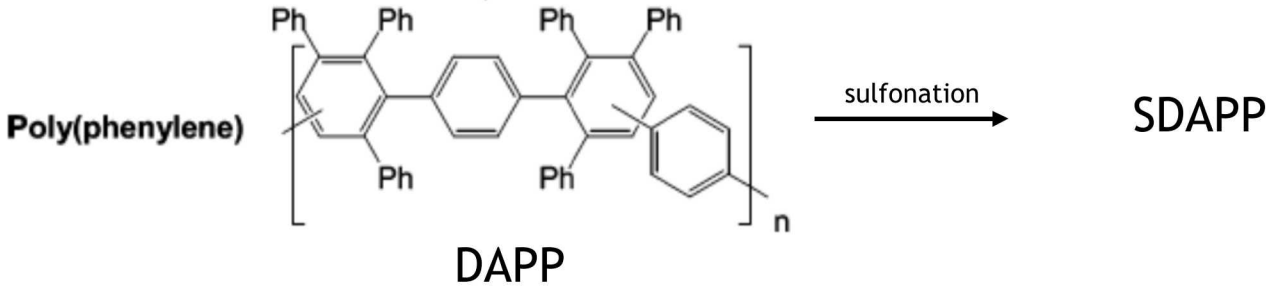

DAPP

SDAPP

Sulfonated Diels Alder Polyphenylene (SDAPP) Membranes

SDAPP

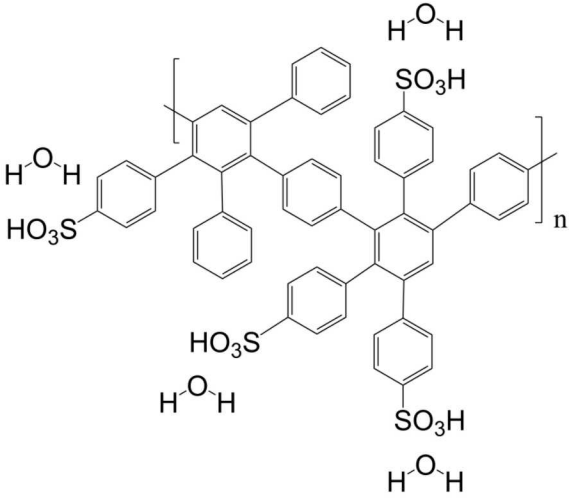

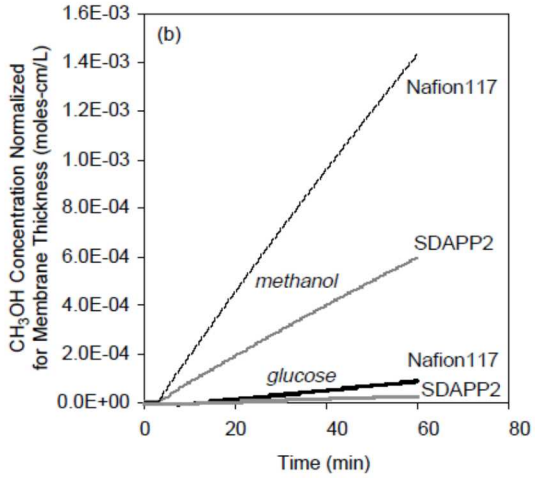

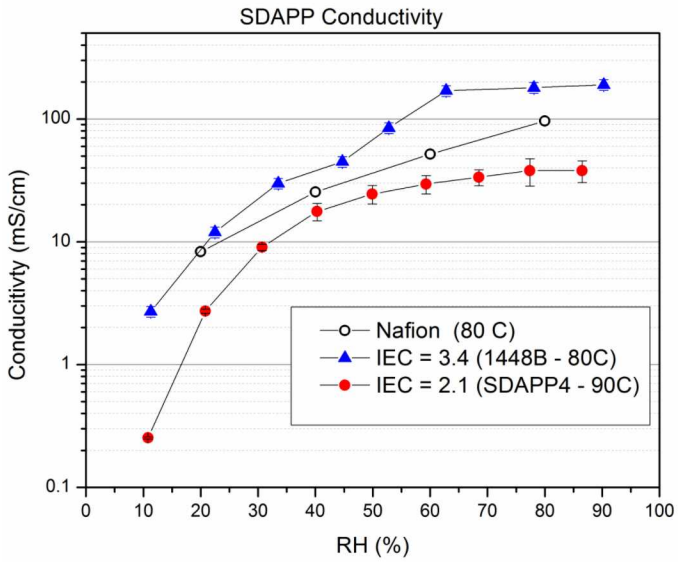

- Conductivity equal to Nafion.
- Can run at higher temperatures.
- Improved fuel barrier.
- Can reach high ion exchange capacity (IEC ~ 3.8) without solubility issues.
- Improved H conductivity over wide RH%.
- No heteronuclear atoms – aging impact.

M. A. Hickner, C. H. Fujimoto, C. J. Cornelius, Polymer 47 (2006) 4238-4244

What is Controlling SDAPP Conductivity?

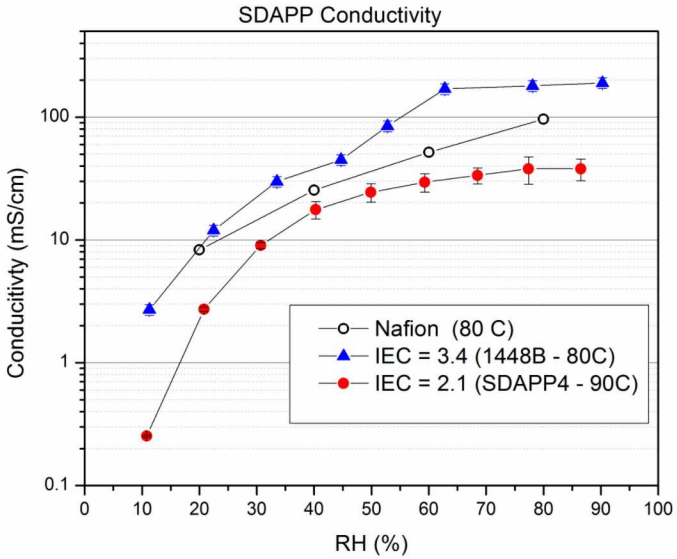

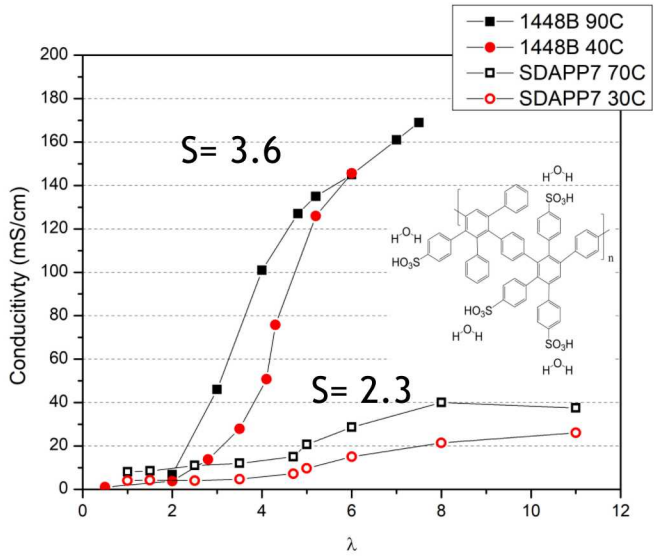

Questions we would like to answer

- Why the different conductivity versus hydration behavior with increasing sulfonation (S)?
- Why the low temperature variation in the fluorinated coblock polymer?
- Why the low conductivity temperature variations?

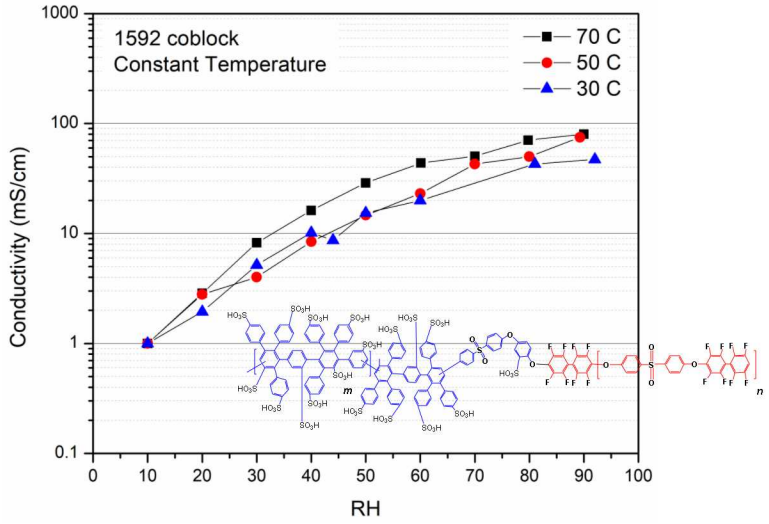

Nanoscale Morphology Impacts Design Principals for Improved Performance of Hydrocarbon Based PEMs

II. Morphology Control is Essential (Gross, 2009)

- Produce morphologies that provide percolation/transport pathways.
- Bicontinuous/random morphologies with numerous contacts between hydrophilic domains.
- Positional dependent diffusion constant (PDDC).
- Anisotropic directional alignment added benefit.

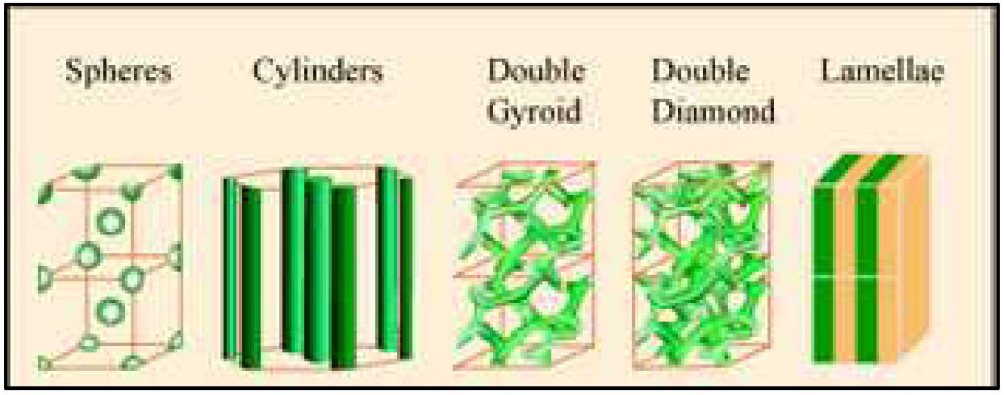

[1]

[2]

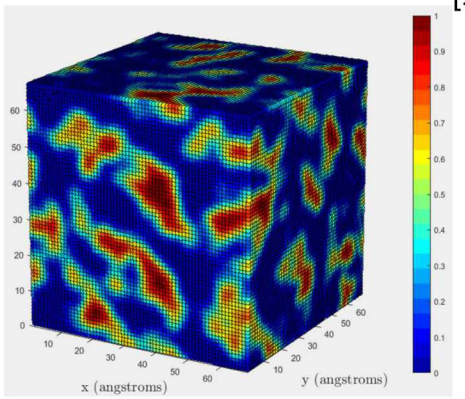

[3]

[5]

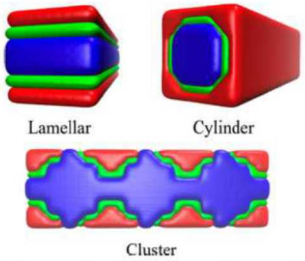

[4]

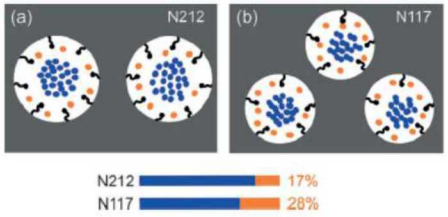

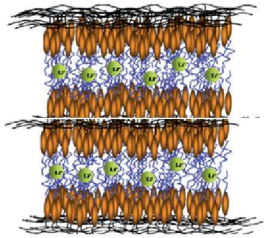

[1] Prof. Thomas, Figure by MIT OpenCourseWare. [2] Liu, S.; Savage, J.; Voth, G. A., Mesoscale Study of Proton Transport in Proton Exchange Membranes: Role of Morphology. The Journal of Physical Chemistry C 2015, 119 (4), 1753-1762. [3] Lauren J. Abbott and Amalie L. Frischknecht,"Nanoscale Structure and Morphology of Sulfonated Polyphenylenes via Atomistic Simulations" *Macromolecules 2017, 50(3), 1184-1192*. [4] Ling, X.; Bonn, M.; Parekh, S. H.; Domke, K. F., Nanoscale Distribution of Sulfonic Acid Groups Determines Structure and Binding of Water in Nafion Membranes. Angewandte Chemie International Edition 2016, 55 (12), 4011-4015. [5] P. W. Majewski *et al.*, "Anisotropic Ionic Conductivity in Block Copolymer Membranes by Magnetic Field Alignment" (2010), J. Am. Chem. Soc., 132, 17516-17522.

SDAPP Nanoscale Morphology Expected to be Different than Nafion

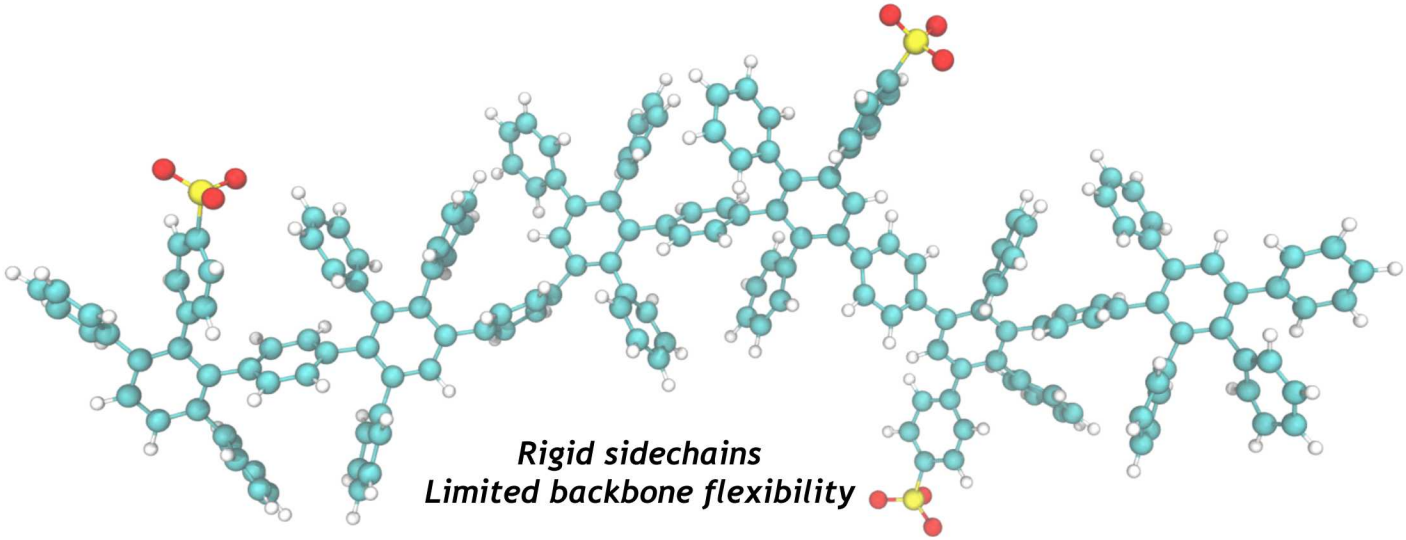

Combination of Efforts

- Quantum calculation of water binding energetics.
- MD simulations of nanoscale morphology.
- X-ray Scattering of SDAPP Membranes
- NMR spin diffusion domain size measurements.
- Connecting MD and experimental NMR spin diffusion.
- NMR Diffusometry

SDAPP Molecular (MD) Simulations

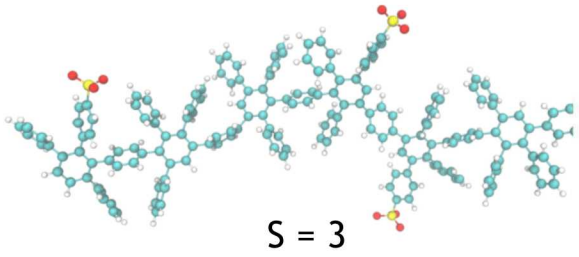

- Local structure depends on the degree of sulfonation (S) and the hydration (λ) levels.
- Cluster domain shape depends on how it is defined: distance based versus density based methods.
- Increasing S and λ resulted in larger and more spherical cluster sizes, with the formation of fully percolated ionic domains.

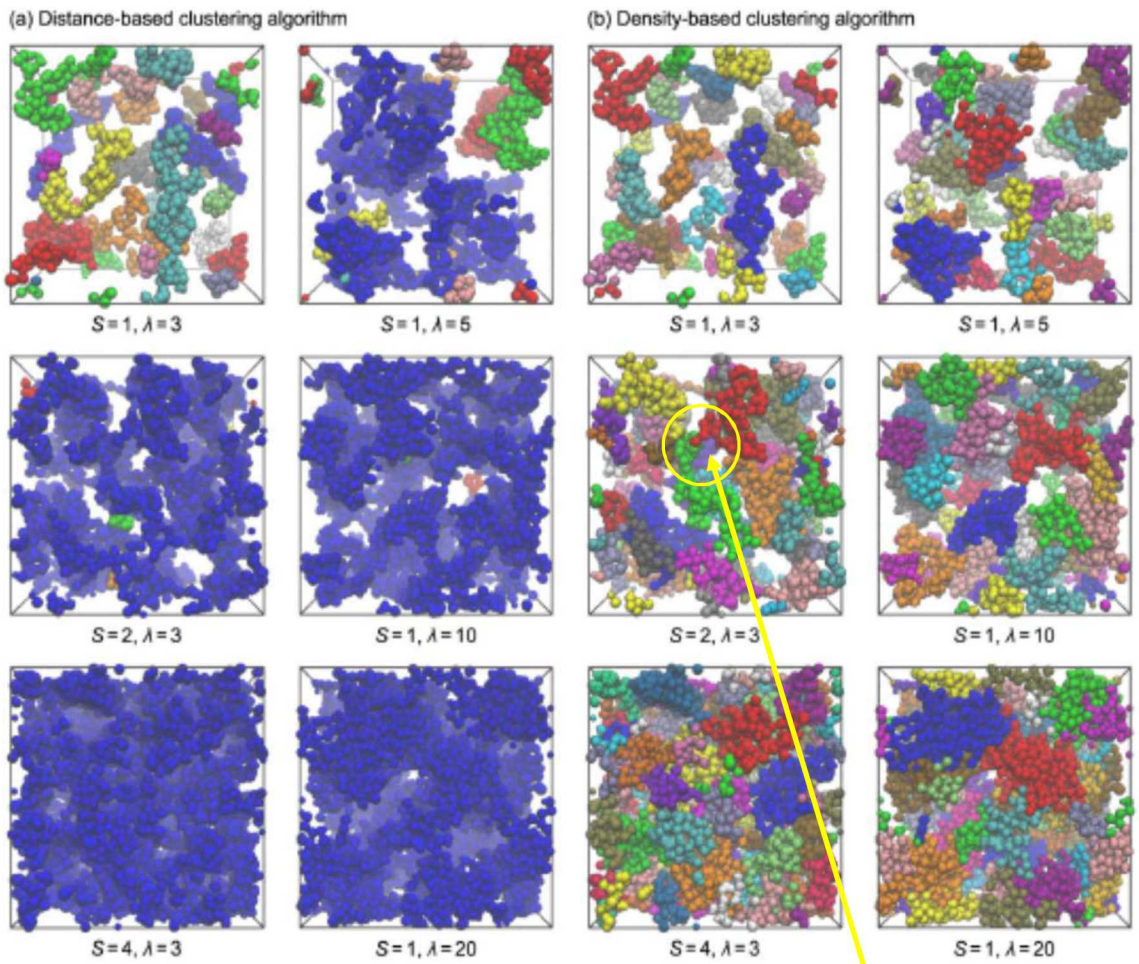

Thin connections are not considered a domain in density based algorithm.

L. A. Abbott, A. Frischknecht, *Macromolecules*, 50(3), 1184-1192, **2017**.

SDAPP Molecular (MD) Simulations

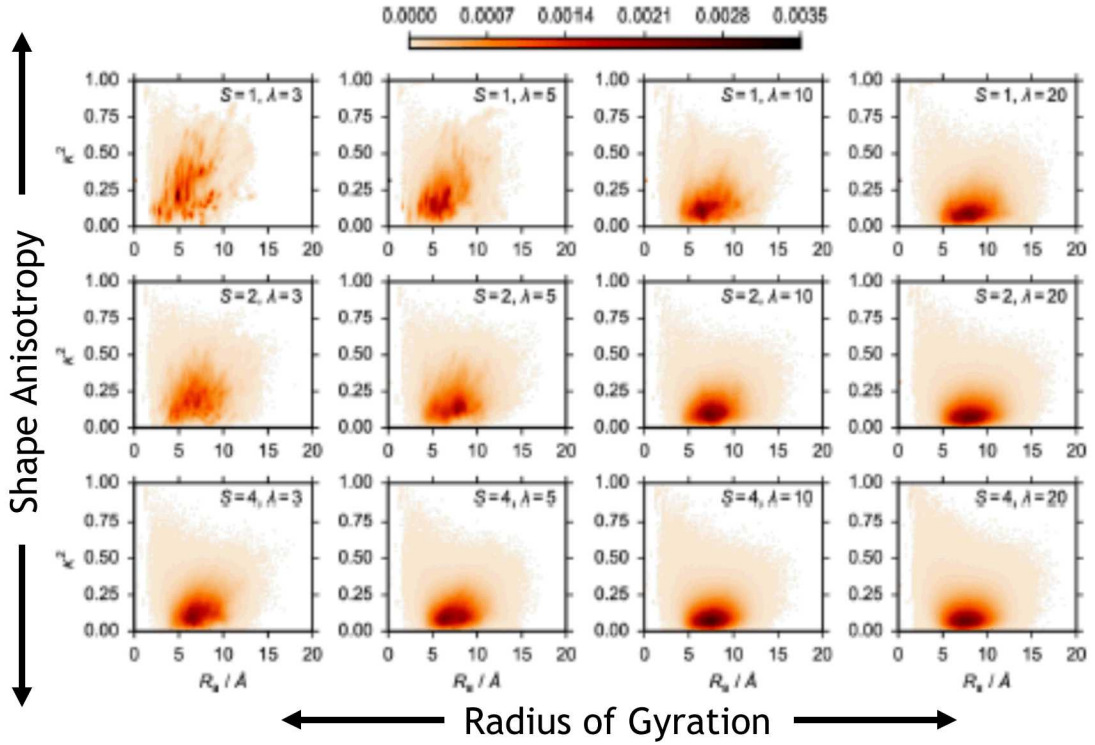

- At low sulfonation (S) and hydration (λ) levels, the ionic clusters elongated in shape and poorly connected.
- The sulfonate groups became more hydrated at higher S and λ, producing more solvated contact ion pairs (CIPs).
- These changes are predicted to produce improved proton transport.

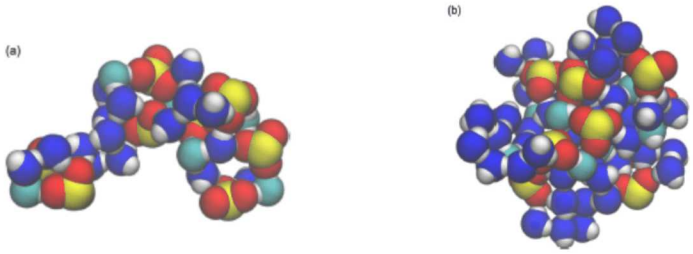

Can we obtain experimental verification of these proposed domain structures and changes in the structure with increasing hydration?

L. A. Abbott, A. Frischknecht, *Macromolecules*, 50(3), 1184-1192, **2017**.

SAXS scattering MD structure

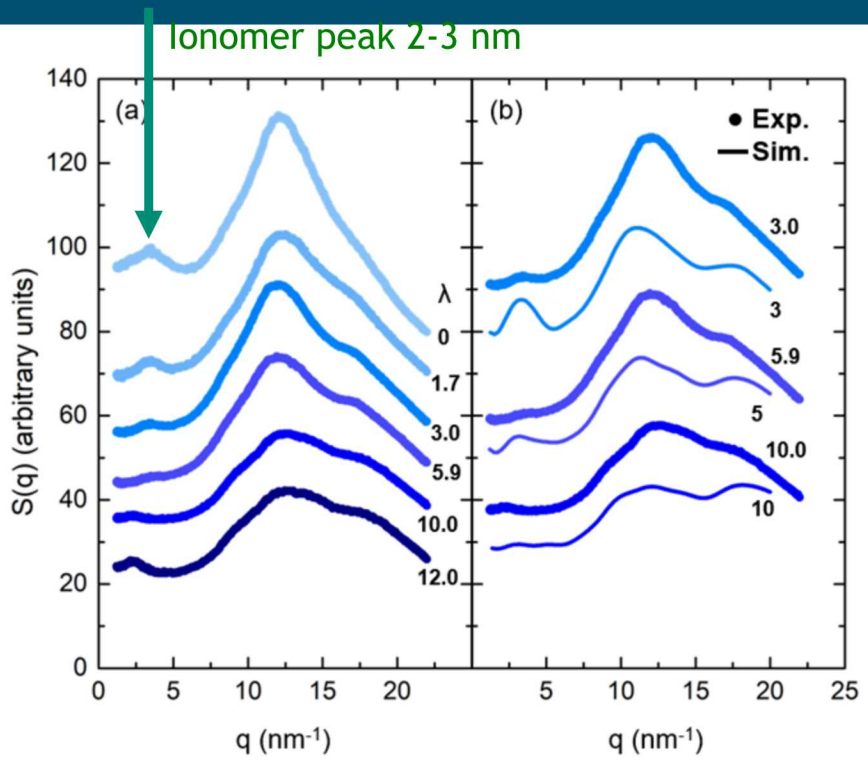

14-48B (S=3.6) versus S=4 (MD)

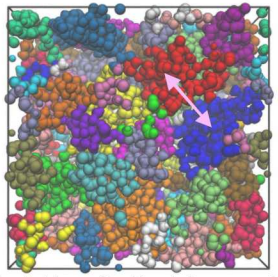

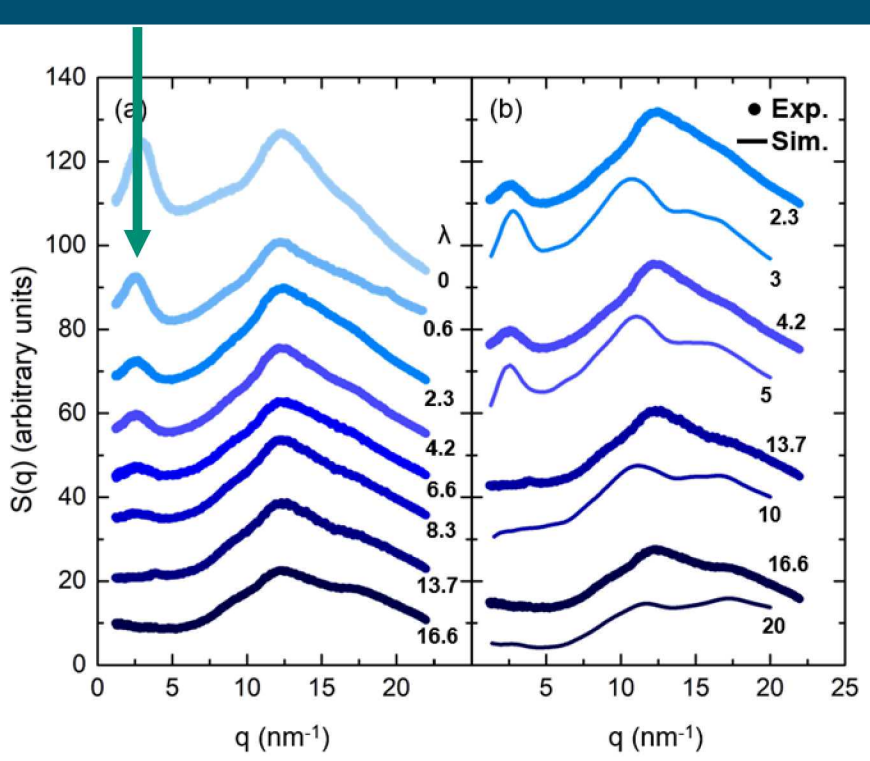

SDAPP7 (S=2.3) versus S=2 (MD)

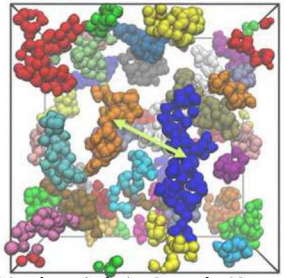

Eric G. Sorte, Benjamin A. Paren, Christina G. Rodriguez, Cy Fujimoto, Cassandria Poirier, Lauren J. Abbott, Nathaniel A. Lynd, Karen I. Winey, Amalie L. Frischknecht, and Todd M. Alam, "Impact of Hydration and Sulfonation on the Morphology and Ionic Conductivity of Sulfonated Poly(phenylene) Proton Exchange Membranes", Macromolecules 52, 857-876 (2019).
DOI: 10.1021/acs.macromol.8b02013

Loss of Ionomer peak in SAXS…

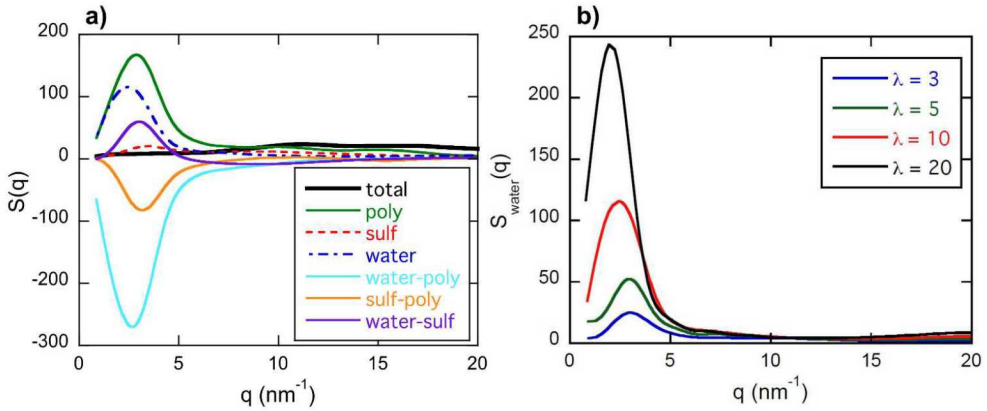

a) Partial structure factors from SDAPP MD simulation for S = 2, λ= 10; b) Water partial structure factors (S_{water}) for S = 2, for λ = 3 (blue), λ = 5 (green), λ = 10 (red), and λ = 20 (black).

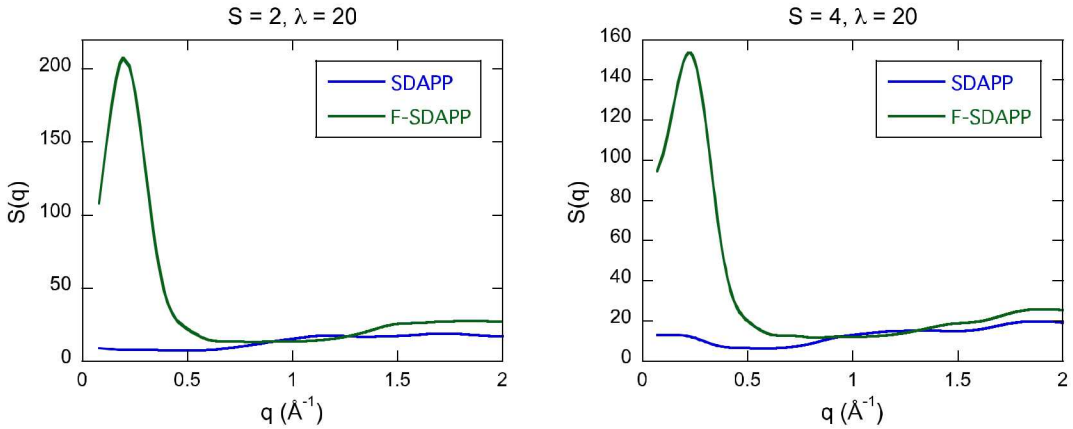

Sorte et al., Macromolecules 52, 857-876 (2019). DOI:10.1021/acs.macromol.8b02013

Total structure factors from MD simulation, using the atomic scattering coefficients for SDAPP (blue), and replacing the aromatic hydrogen scattering coefficients with those for fluorine (green).

Reduction in ionomer peak is NOT due to loss of nanophase separation but is scattering contrast related.

^{1}H NMR Spin Diffusion Experiments

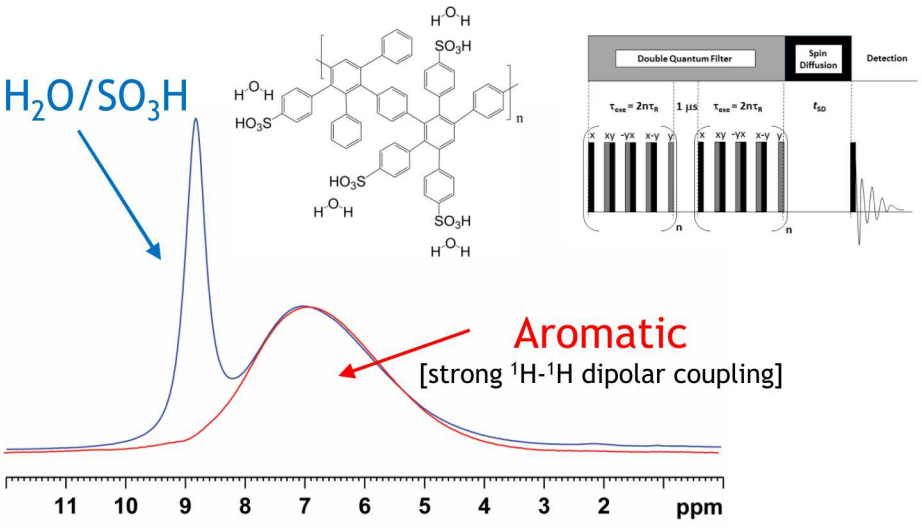

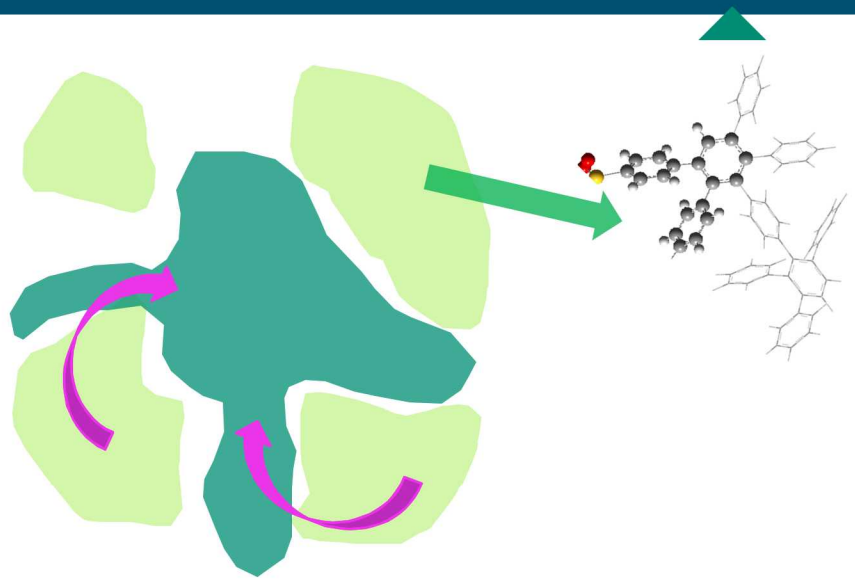

Spin Diffusion Experiment

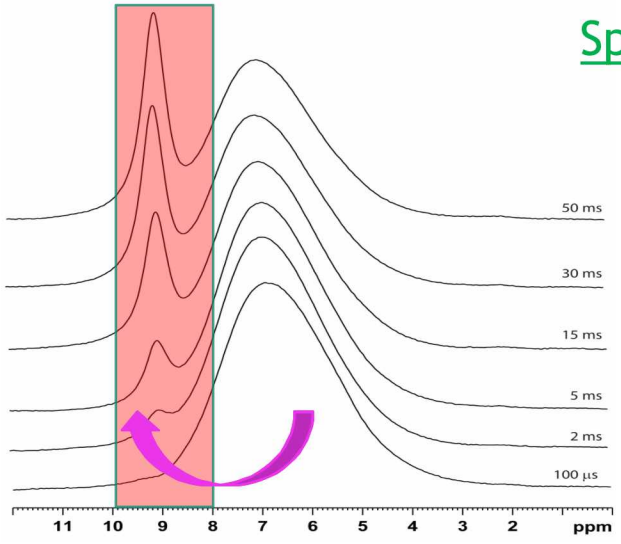

"spin temperature" equilibration

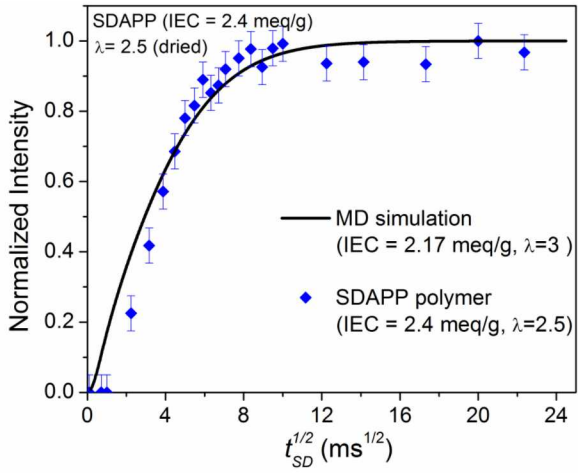

Connecting Models to NMR Spin Diffusion

- Analytical solutions for the simplest cases.
- Solutions become unwieldy for distribution of more complex structures!!
- Would like to simulate structured from MD and Course Grain simulations.

- Developed the program (NMR_DIFFSIM) to simulate any proposed structure.
- Used to estimate domain size in SDAPP polymer membranes.

Sorte, E. G., Lauren J. Abbott, Mark Wilson, Amalie Frischknecht, and Todd M. Alam, "Hydrophilic Domain Structure in Polymer Exchange membranes: Simulation of NMR Spin Diffusion Experiments to Address Ability for Model Discrimination", J. Polym. Sci., Part B: Polym. Phys. 2018, **56**, 62-78.

3D
(3 diffusion dimensions)

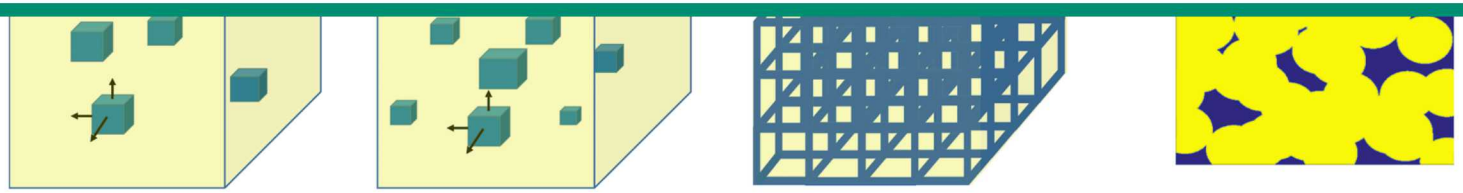

MD → Spin Diffusion Experiments

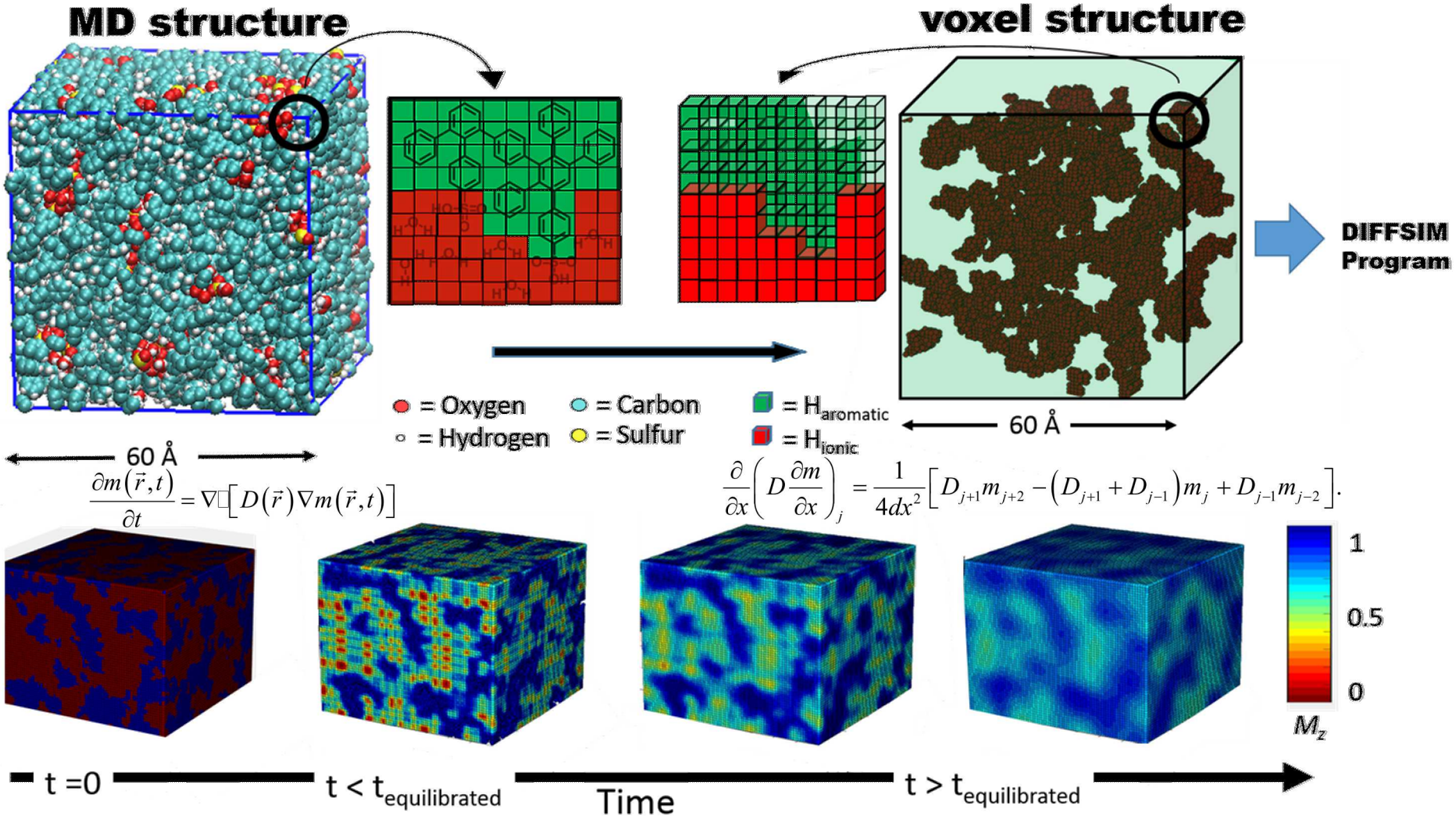

Sorte, E. G., Lauren J. Abbott, Mark Wilson, Amalie Frischknecht, and Todd M. Alam, "Hydrophilic Domain Structure in Polymer Exchange membranes: Simulation of NMR Spin Diffusion Experiments to Address Ability for Model Discrimination", J. Polym. Sci., Part B: Polym. Phys. 2018, **56**, 62-78.

Connecting MD to Spin Diffusion Experiments

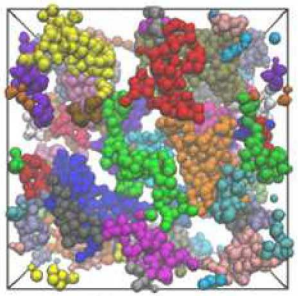

S = 2, λ = 3

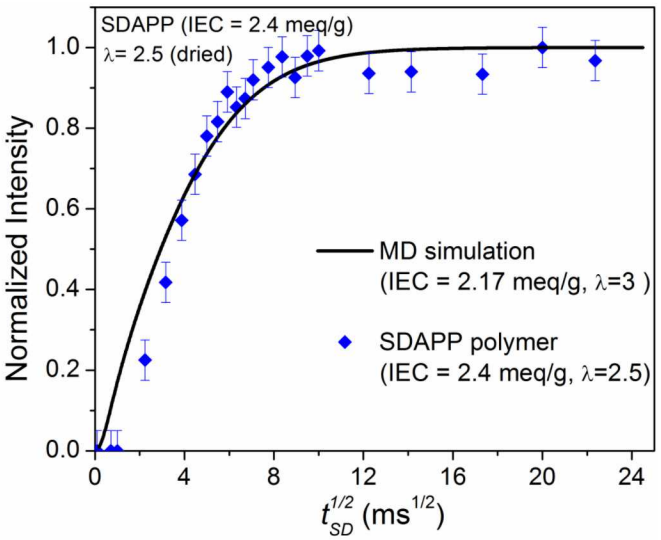

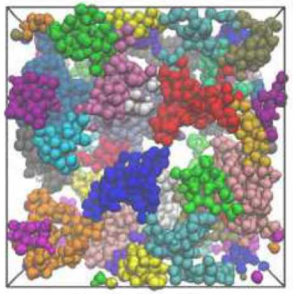

S = 2, λ = 10

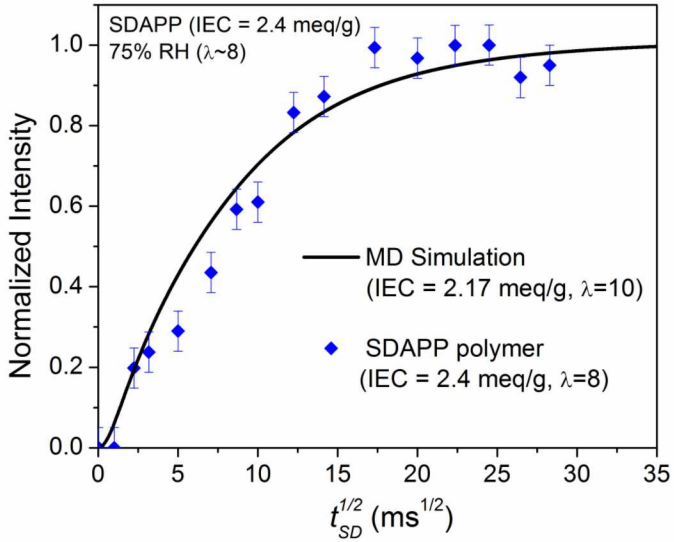

- MD structure (morphology from simulation)
- Spin diffusion constants, volume fractions, etc. are fixed.
- No adjustable parameters in these fits!!!!
- Deviations at higher hydration levels [finite simulation size]

Sorte, E. G., Lauren J. Abbott, Mark Wilson, Amalie Frischknecht, and Todd M. Alam, "Hydrophilic Domain Structure in Polymer Exchange membranes: Simulation of NMR Spin Diffusion Experiments to Address Ability for Model Discrimination", J. Polym. Sci., Part B: Polym. Phys. 2018, **56**, 62-78.

Estimation of Domain Size

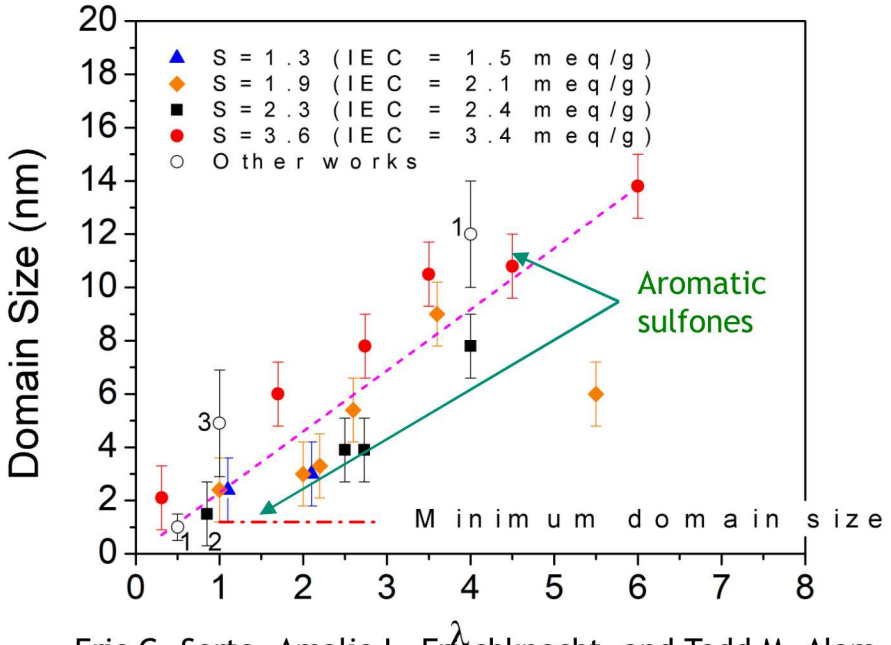

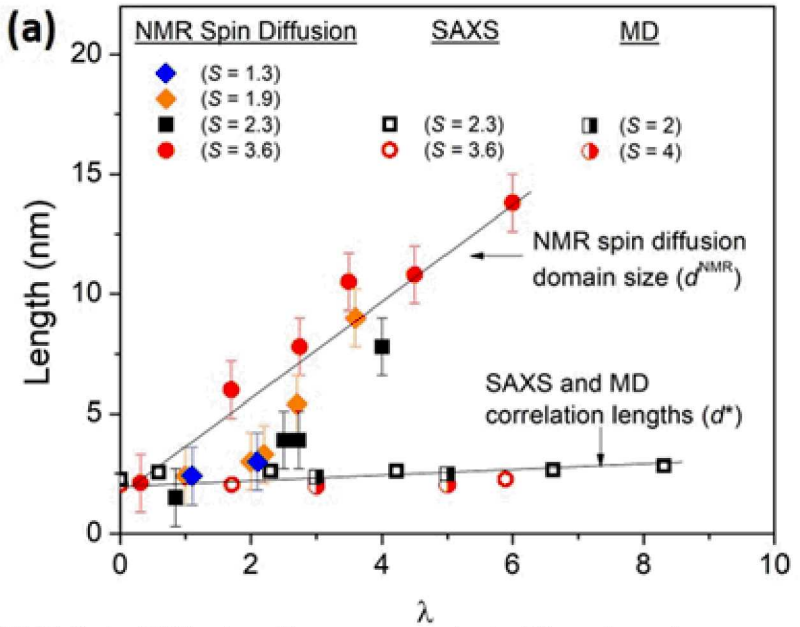

Eric G. Sorte, Amalie L. Frischknecht, and Todd M. Alam, "NMR Spin Diffusion Measurements in Disordered Polymers: Insights and Limitations", Physical Review Materials, ASAP (2019).

- Continuous variation with hydration level (factor of 7) – no step with λ.
- Different than Nafion.
- NMR spin diffusion seems appears to represent the distance based description of the hydrophilic domain.
- NMR spin diffusion does not give a clear indicator of shape or anisotropy.

NMR Spin Diffusion and Models

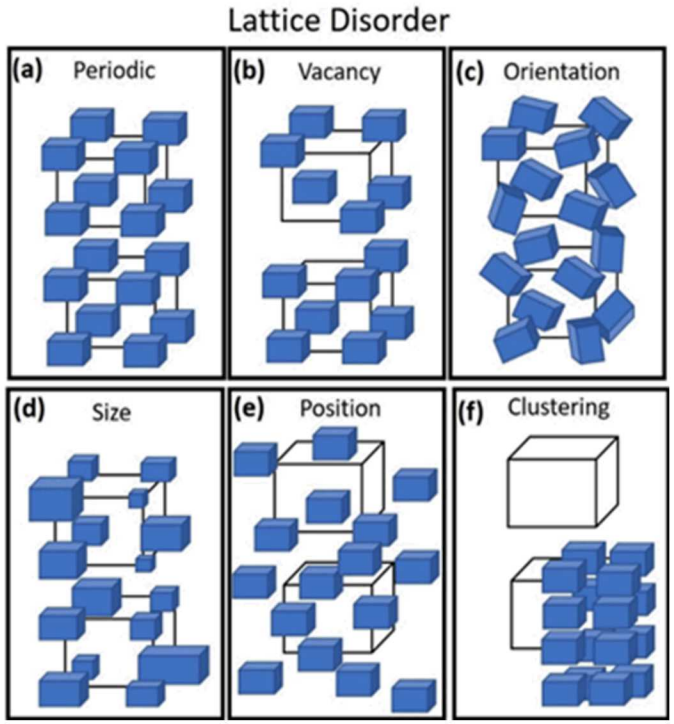

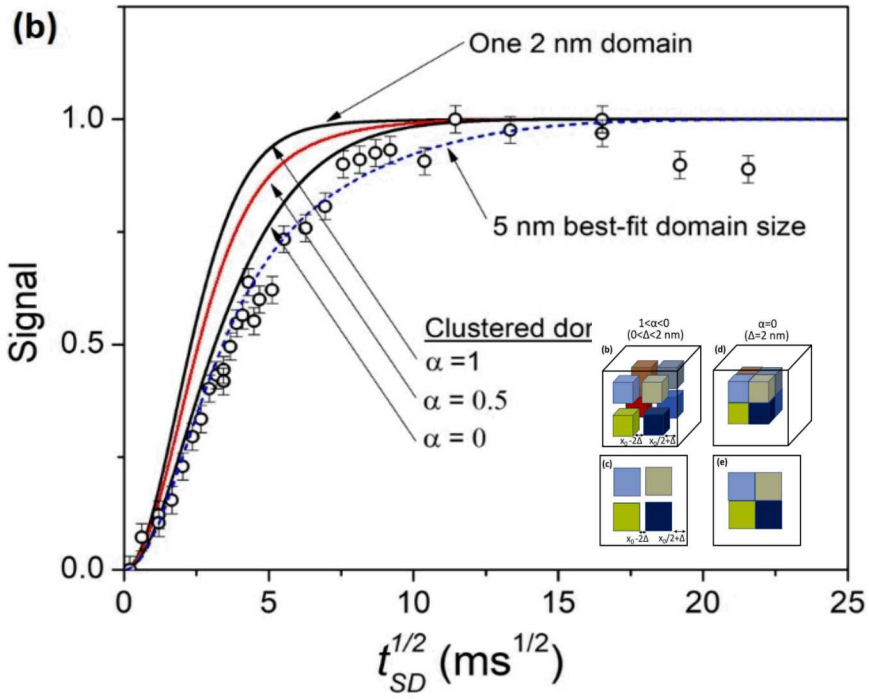

Eric G. Sorte, Amalie L. Frischknecht, and Todd M. Alam, "NMR Spin Diffusion Measurements in Disordered Polymers: Insights and Limitations", Physical Review Materials, ASAP (2019).

- Heterogeneous domain structure (i.e. disorder) can have significant impact on the NMR spin diffusion experiments.
- Need guidance for structural model (MD, SAXS, Imaging etc.)

NMR Diffusometry - Water in SDAPP Membranes

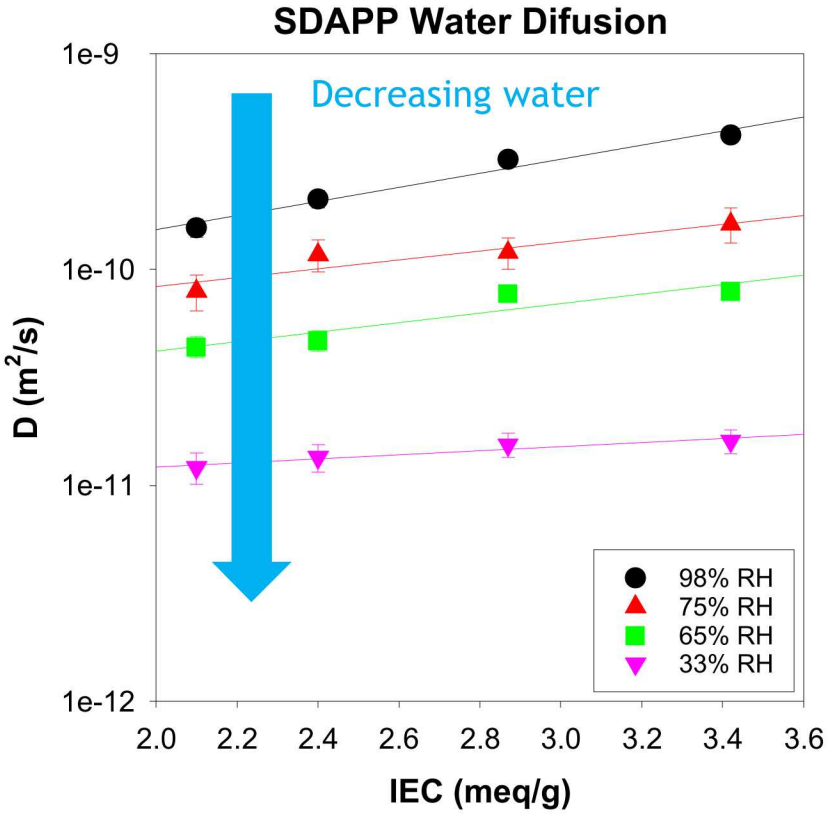

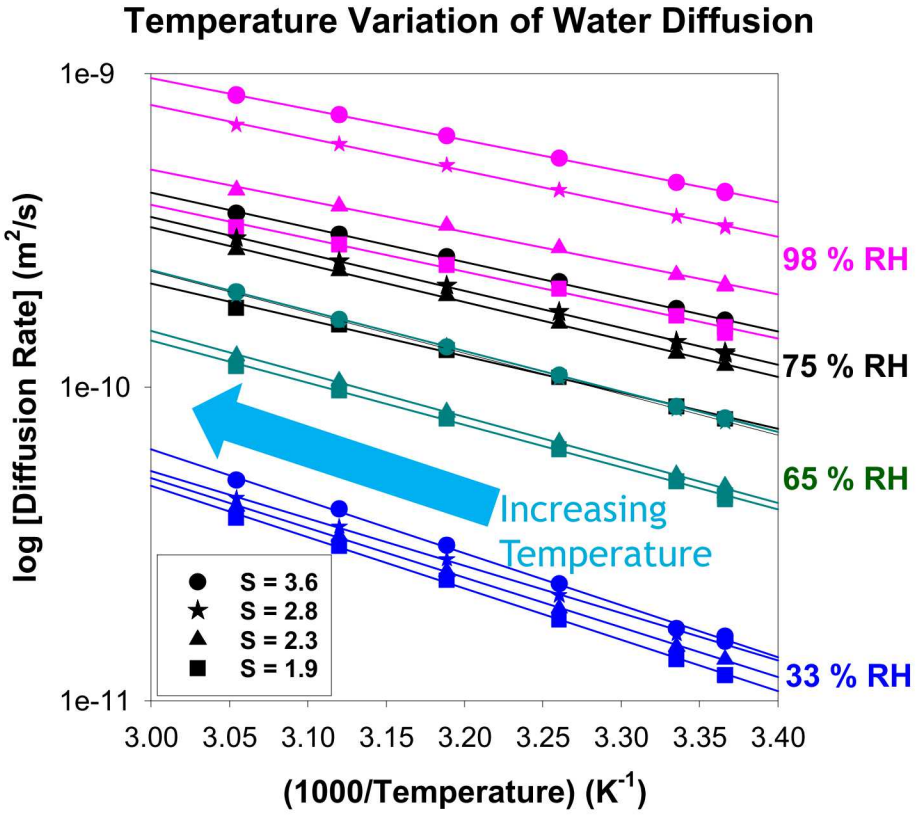

Sample	E_a (kJ/mol)			
	33%	65%	75%	98%
S = 1.9	31.3	25.8	22.2	20.4
S = 2.3	30.4	26.4	22.9	19.1
S = 2.8	29.0	24.7	22.6	20.1
S = 3.6	31.8	24.7	21.1	19.0

- E_a similar to other PEMs at higher hydration levels.
- At < 33% RH increasing E_a.
- PFG NMR not obtainable at low RH%

Conductivity and Diffusion

Nernst-Einstein Equation

$$\sigma = \frac{F^2 c\left(D_+ + D_-\right)}{RT} \xrightarrow{\text{Only involves } H^+ \text{ (or } OH^-\text{)}} \sigma = \frac{F^2 c\left(D_+\right)}{RT}$$

Surface Grotthuss Vehicular

$$\sigma = \frac{F^2}{RT}\left(D_{H^+}^{Surf} C_{H^+}^{Surf} + D_{H^+}^{Grott} C_{H^+}^{Grott} + D_{H^+}^{Veh} C_{H^+}^{Veh}\right)$$

The transport of H^+ in PEMs can also be discussed in terms of different diffusion environments.

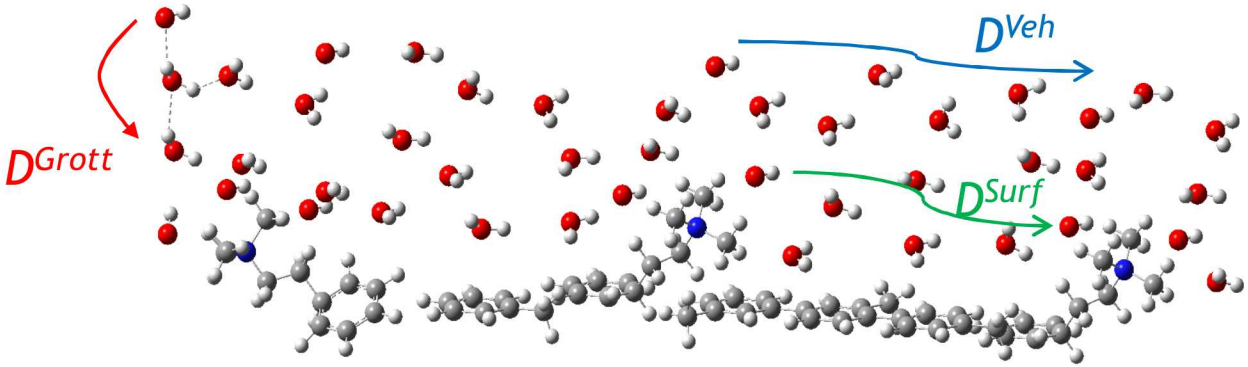

If we can measure diffusion individually, we can evaluate different contributions.

SDAPP Conductivity from Diffusivity

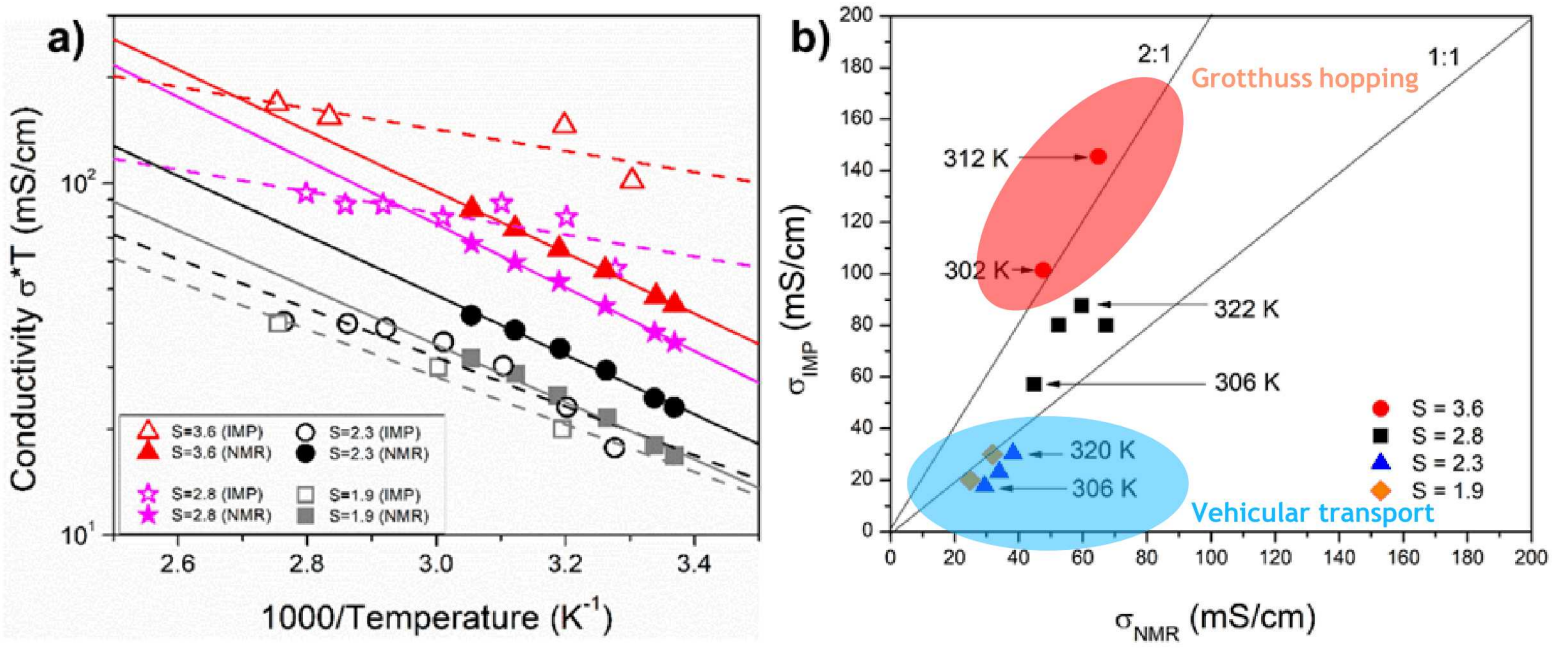

- At low-moderate S conductivity controlled by water vehicular transport at full hydration.
- With increasing S, Grotthuss mechanism becomes significant and leads to increased conductivity beyond simple diffusion.
- Membrane design rule strive for the highest D^{veh}, but H^+ requires an environment (hydrogen bond strength) allowing Grotthuss hopping.

Eric G. Sorte, Benjamin A. Paren, Christina G. Rodriguez, Cy Fujimoto, Cassandria Poirier, Lauren J. Abbott, Nathaniel A. Lynd, Karen I. Winey, Amalie L. Frischknecht, and Todd M. Alam, "Impact of Hydration and Sulfonation on the Morphology and Ionic Conductivity of Sulfonated Poly(phenylene) Proton Exchange Membranes", Macromolecules 52, 857-876 (2019).
DOI: 10.1021/acs.macromol.8b02013

Conclusions

- **SDAPP membranes are shown to have H conductivity equivalent to Nafion, but with improved thermal behavior and reduced membrane solubility in water.**
- **Combined experimental and computation studies used to probe the nanostructure of SDAPP membranes.**
- **The loss of the ionomer peak in the SAXS is shown to be due to loss of scattering contrast NOT a loss of nanophase separation. MD simulations suggest an increasing degree of phase separation.**
- **Combining PFG NMR diffusometry and the H conductivity shows the evolution of the conductivity mechanism evolving from vehicular transport to a hybrid mechanism with increasing Grotthuss mechanism.**
- **Improved conductivity can be driven by increasing the degree of sulfonation (S > 3.5) and exceeds the simple increase in the H^+ concentration.**

Outline

Transport in PEMS SDAPP membranes

- Motivation for SDAPP
- MD Simulations of Nanomorphology
- Characterization (NMR and SAXS)
- NMR Diffusometry

Chain dynamics in Ferrocene cured thermosets

- Cure stress in cross-linked polymers
- ^{1}H NMR of chain dynamics

Motivation: Stress Relief in Thermoset Polymers

Cure Stress Variation

Epon 828 + MDA (C, methylenedianaline) or IPD (D, isophorene diamine) [1]

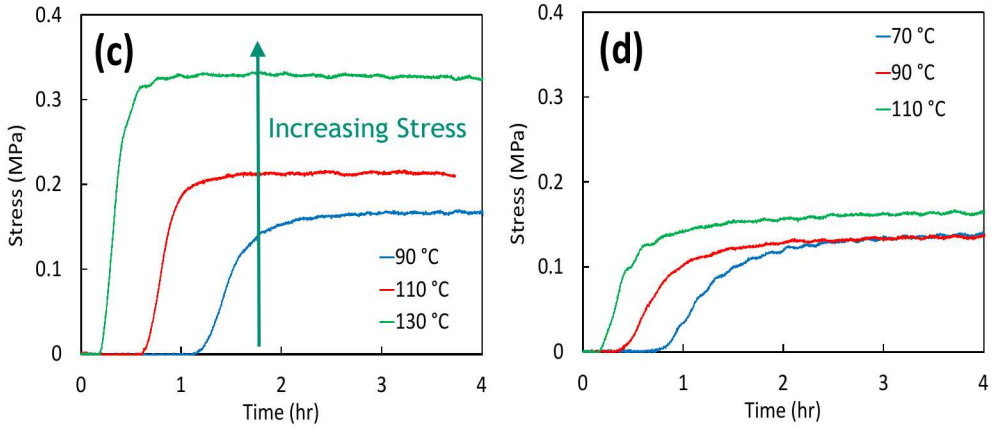

[2]

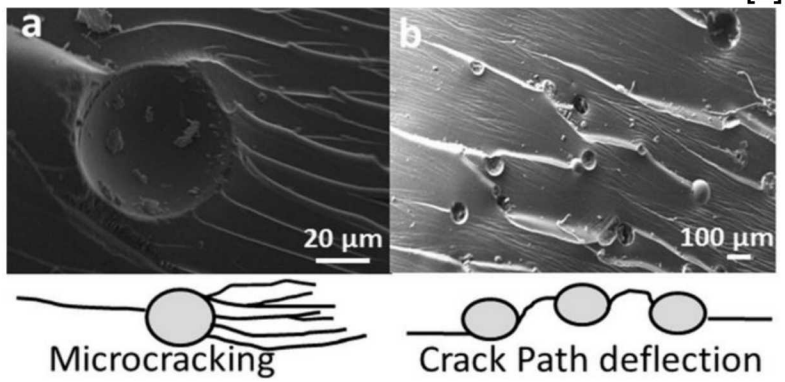

[3]

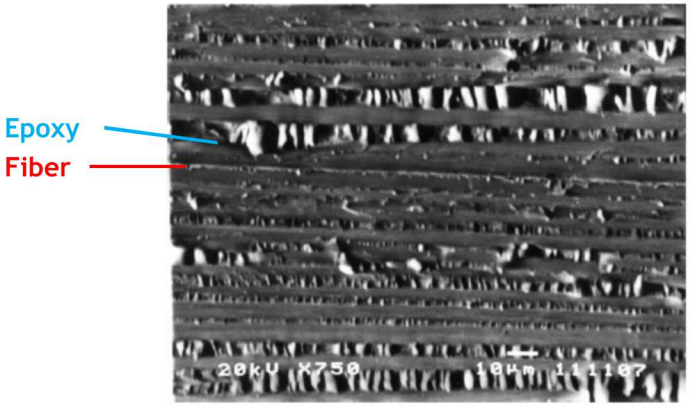

- Cure stress due to polymerization shrinkage.
- Crosslinks prevent terminal viscoelastic behavior (flow).
- Stress formation a function of cure temperature.
- Stress formation a function of the curing agent.

1. Brad H. Jones, David R. Wheeler, Hayden T. Black, Mark E. Stavig, Patricia S. Sawyer, Nicholas H. Giron, Mathias C. Celina, Timothy N. Lambert, and Todd M. Alam, "Stress Relaxation in Epoxy Thermosets via a Ferrocene-Based Amine Curing Agent", Macromolecules, 50(13), 5014-5024 (2017) DOI: 10.1021/acs.macromol.7b00501
2. S. Chaudhary, S. Parthasarathy, C. Rajagopal, P. Roy, D. Kumar "Simple toughening of epoxy thermosets by preformed thermoplastics", Plastics Research Online (2014) http://www.4spepro.org/view.php?article=005409-2014-04-09&category=Polymer+Modifiers
3. Yayla, P., Fracture Surface Morphology of Delamination Failure of Polymer Fiber Composites Under Different Failure Modes. Journal of Failure Analysis and Prevention 2016, 16 (2), 264-270.

Alternative Chemistries For Stress Mediation (Self Repair)

Volume Expandable

Spiro Ortho Carbonates [a]

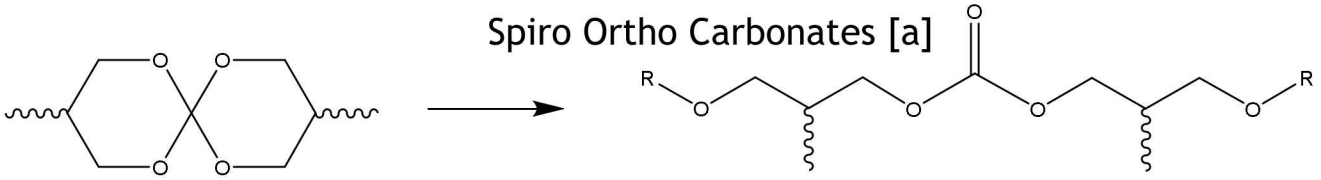

Covalent Adaptable Network (CAN)

Diels-Alder [1]

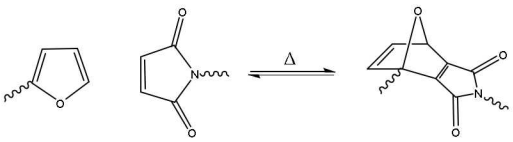

Catalyzed Olefin Metathesis [5]

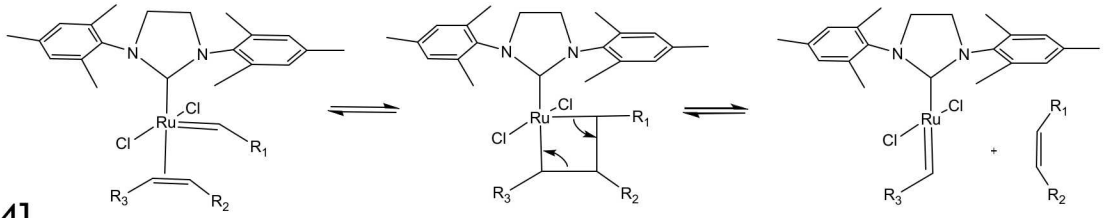

Addition-Fragmentation Chain Transfer [2,3,4]

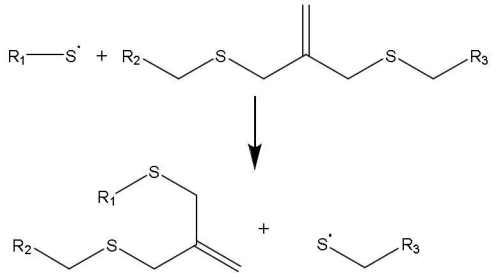

- Oxetane Ring Opening [6]
- Chain Exchange Reaction [7]
- Transesterfication [8]
- Transcarbamoylation
- Transamination
- Transalkylation

[a] Bailey, W. J., Matrices that expand on curing for high strength composites and adhesives. Materials Science and Engineering: A 1990, 126 (1-2), 271-279.; Alcoutlabi, M.; McKenna, G. B.; Simon, S. L., Analysis of the development of isotropic residual stresses in a bismaleimide/spiro orthocarbonate thermosetting resin for composite materials. Journal of Applied Polymer Science 2003, 88 (1), 227-244. [1] Chen, X.; Dam, M. A.; Ono, K.; Mal, A.; Shen, H.; Nutt, S. R.; Sheran, K.; Wudl, F., A Thermally Re-mendable Cross-Linked Polymeric Material. Science 2002, 295 (5560), 1698-1702. [2] Scott, T. F.; Schneider, A. D.; Cook, W. D.; Bowman, C. N., Photoinduced Plasticity in Cross-Linked Polymers. Science 2005, 308 (5728), 1615-1617. [3] Kloxin, C. J.; Scott, T. F.; Bowman, C. N., Stress Relaxation via Addition–Fragmentation Chain Transfer in a Thiol-ene Photopolymerization. Macromolecules 2009, 42 (7), 2551-2556. [4] Nicolaÿ, R.; Kamada, J.; Van Wassen, A.; Matyjaszewski, K., Responsive Gels Based on a Dynamic Covalent Trithiocarbonate Cross-Linker. Macromolecules 2010, 43 (9), 4355-4361. [5] Lu, Y.-X.; Tournilhac, F.; Leibler, L.; Guan, Z., Making Insoluble Polymer Networks Malleable via Olefin Metathesis. Journal of the American Chemical Society 2012, 134 (20), 8424-8427. [6] Ghosh, B.; Urban, M. W., Self-Repairing Oxetane-Substituted Chitosan Polyurethane Networks. Science 2009, 323 (5920), 1458-1460. [7] Montarnal, D.; Capelot, M.; Tournilhac, F.; Leibler, L., Silica-Like Malleable Materials from Permanent Organic Networks. Science 2011, 334 (6058), 965-968.[8] Capelot, M.; Montarnal, D.; Tournilhac, F.; Leibler, L., Metal-Catalyzed Transesterification for Healing and Assembling of Thermosets. Journal of the American Chemical Society 2012, 134 (18), 7664-7667.

Metallocene Curing Agents for Stress Relief

Ferrocene Fluxional Mechanism

No bond breakage

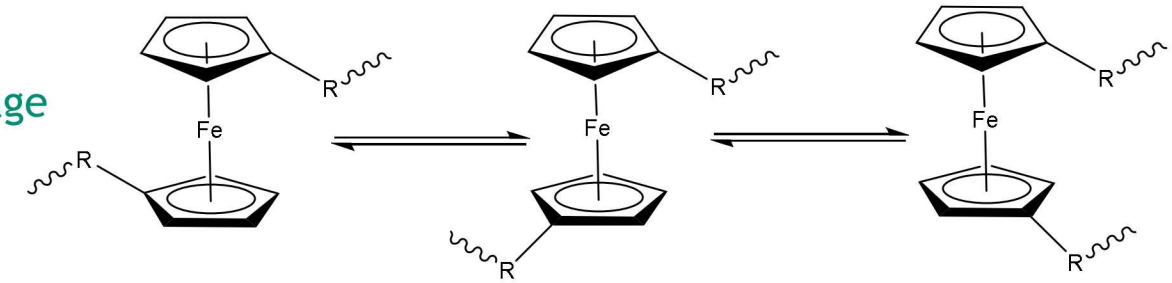

Linkages on both Ferrocene rings

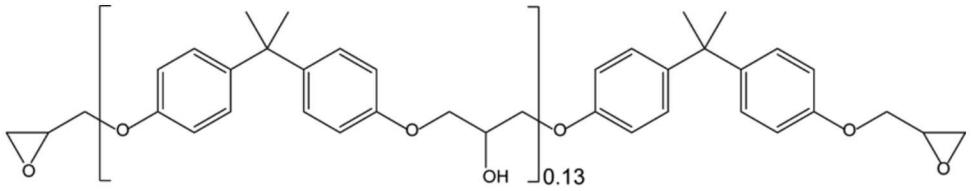

EPON 828

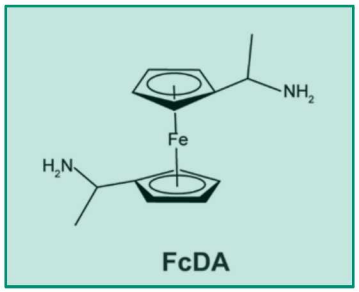

FcDA

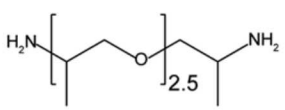

Jeffamine D-230

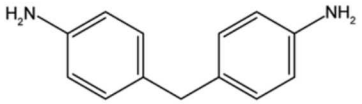

MDA

Brad H. Jones, David R. Wheeler, Hayden T. Black, Mark E. Stavig, Patricia S. Sawyer, Nicholas H. Giron, Mathias C. Celina, Timothy N. Lambert, and Todd M. Alam, "Stress Relaxation in Epoxy Thermosets via a Ferrocene-Based Amine Curing Agent", Macromolecules, 50(13), 5014-5024 (2017) DOI: 10.1021/acs.macromol.7b00501

Rotation Barriers in Ferrocene Derivatives

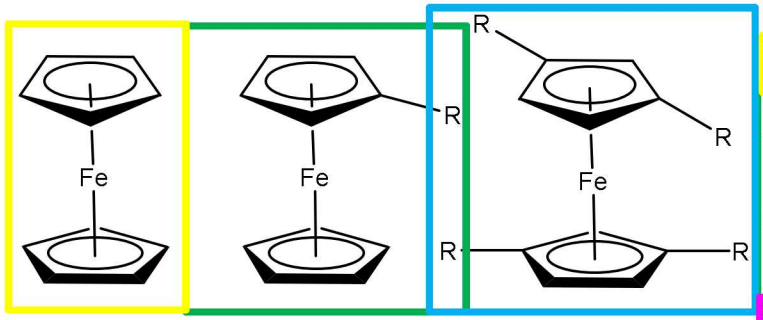

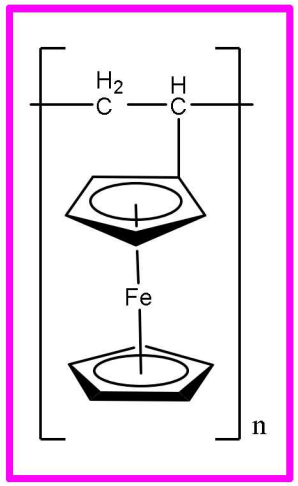

"Fe ball bearing"

Compound	$\Delta G^{\dagger}$ [E_a] kJ mol^{-1}	Ref.
$Fe(\eta^5\text{-}C_5H_5)_2$	4.4,5.4,7.5	
$Fe(\eta^5\text{-}C_5H_5)(\eta^5\text{-}C_5H_4CHO)$	15.2	[1]
$Fe(\eta^5\text{-}C_5H_5)(\eta^5\text{-}C_5H_4CMe_2Et)$	10.2 15.2	[2]
$Fe(\eta^5\text{-}C_5H_5)(\eta^5\text{-}C_5H_4Bu^n)$	8.0 11.7	[2]
PVFc	9.6	[3]
$Fe(\eta^5\text{-}C_5H_3(t\text{-}Bu)_4)$	55.6, 54.8	[4]
$Fe(\eta^5\text{-}C_5H_3(t\text{-}Pentyl)_4)$	56.7	[4]
$Fe(\eta^5\text{-}C_5H_2(TMS)_6)$	46.0	[4]
$Ru(\eta^5\text{-}C_5H_5)_2$	9.6	[5]
$Ru(\eta^5\text{-}C_5H_3(t\text{-}Pentyl)_2)$	45.7	[4]
$Ni(\eta^5\text{-}C_5H_5)_2$	7.5	[6]
$Co(\eta^5\text{-}C_5H_5)_2$	7.5	[6]
$Cr(\eta^5\text{-}C_5H_5)_2$	7.5	[6]

1. Pazur, R.J., et al., *Proton spin-lattice relaxation time studies and atom-atom non-bonded potential calculations on ferrocenecarbaldehyde (η^5-C_5H_5)Fe(η^5-C_5H_4CHO).* Canadian Journal of Chemistry, 1987. **65**(8): p. 1940-1944.
2. Mann, B.E., et al., *A determination of the activation energy of cyclopentadienyl group rotation and molecular tumbling in [Fe(h^5-C_5H_5)(h^5-C_5H_4R)](R = CMe_2Et or Bu^n) using carbon-13 nuclear magnetic resonance relaxation measurements.* Journal of the Chemical Society, Dalton Transactions, 1984(9): p. 2027-2028.
3. Appel, M.A., *Ring Rotation in Ferrocene and Ferrocene-Containing Polymers.* 2015, Technische Universität: Darmstadt, Germany. p. 137.
4. Abel, E.W., et al., *Dynamic NMR studies of ring rotation in substituted ferrocenes and ruthenocenes.* Journal of Organometallic Chemistry, 1991. **403**(1-2): p. 195-208.
5. Holm, C.H. and J.A. Ibers, *NMR Study of Ferrocene, Ruthenocene, and Titanocene Dichloride.* J. Chem. Phys., 1959. **30**(4): p. 885-888.
6. Luke, W.D. and A. Streitwieser, *Barriers to Ring Rotation in 1,1',4,4'-Tetra-tert-butyluranocene and 1,1',3,3'-tetra-tert-butylferrocene.* J. Am. Chem. Soc., 1981. **103**(12): p. 3241-3243.

Ferrocene in Polymers (Including Epoxies)

[1,2]

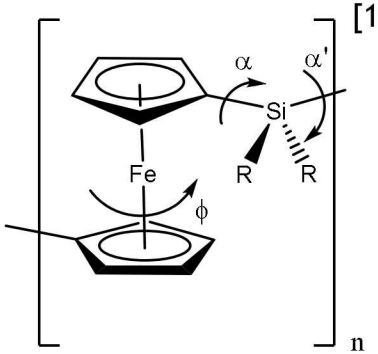

R = CH_3, OCH_3, OC_6H_{13}

[3]

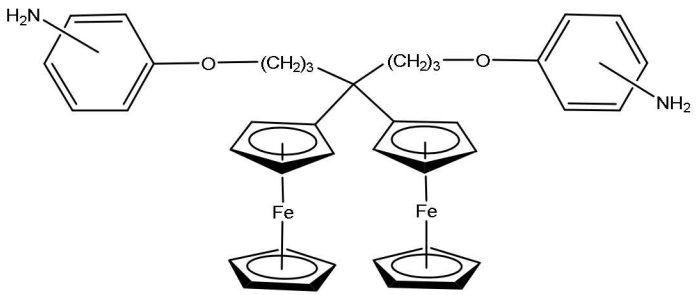

[4]

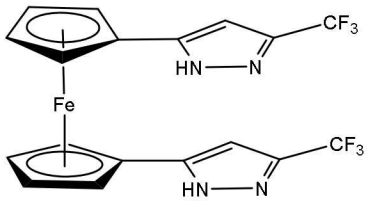

- Propellent Burn Rate Catalyst
- Conductivity
- Electrochemical
- Magnetic Ceramics
- Refractive Index
- Electron Beam Resistance
- Self Assembly (fluxional impact)

[5]

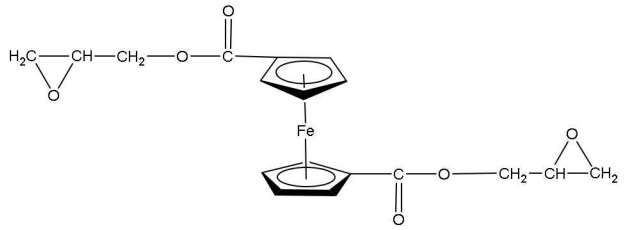

[6]

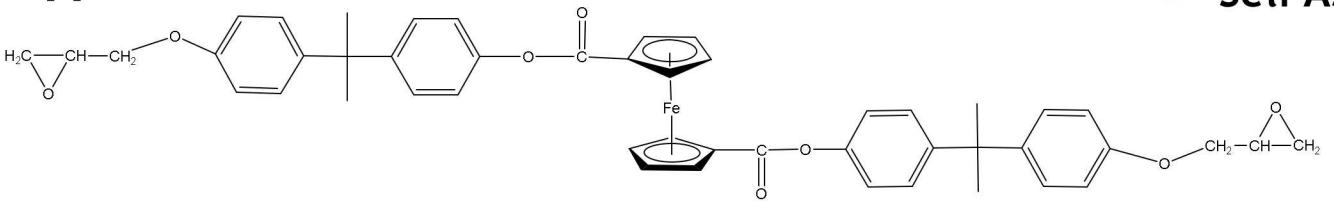

[1] Kulbaba, K.; Macdonald, P. M.; Manners, I., Molecular Motions in Poly(ferrocenes): Solid-State Deuterium NMR Studies of Poly(ferrocenylsilanes) near Their Glass Transition Temperature. Macromolecules 1999, 32 (4), 1321-1324. [2] Kulbaba, K.; Manners, I.; Macdonald, P. M., Molecular Motions in Metal-Containing Polymers: Solid-State Deuterium NMR Studies of Polyferrocenylsilanes near Their Glass Transition Temperature. Macromolecules 2002, 35 (27), 10014-10025. [3] Wright, M. E.; Laub, J.; Stafford, P. R.; Norris, W. P., Synthesis of new ferrocene containing diamines and their use in epoxy resins. Journal of Organometallic Chemistry 2001, 637-639, 837-840. [4] Veronelli, M.; Dechert, S.; Demeshko, S.; Meyer, F., 1,1′-Bis(pyrazol-3-yl)ferrocene: A Clip Ligand That Forms Supramolecular Aggregates and Prismatic Hexanuclear Coinage Metal Complexes. Inorganic Chemistry 2015, 54 (14), 6917-6927. [5] Yu, H.; Wang, L.; Huo, J.; Ding, J.; Tan, Q., Synthesis and Curing Behavior of a Novel Ferrocene-Based Epoxy Compound. J. Appl. Polymer Sci. 2008, 110, 1594-1599. [6] Yu, H.; Wang, L.; Huo, J.; Li, C.; Tan, Q., Synthesis of Glycidyl Ether of Poly(bisphenol-A-1,1′-ferrocene dicarboxylate) and Its Electrochemical Behavior. Designed Monomers and Polymers 2009, 12, 305-313.

Static ^{1}H NMR – Temperature Variations

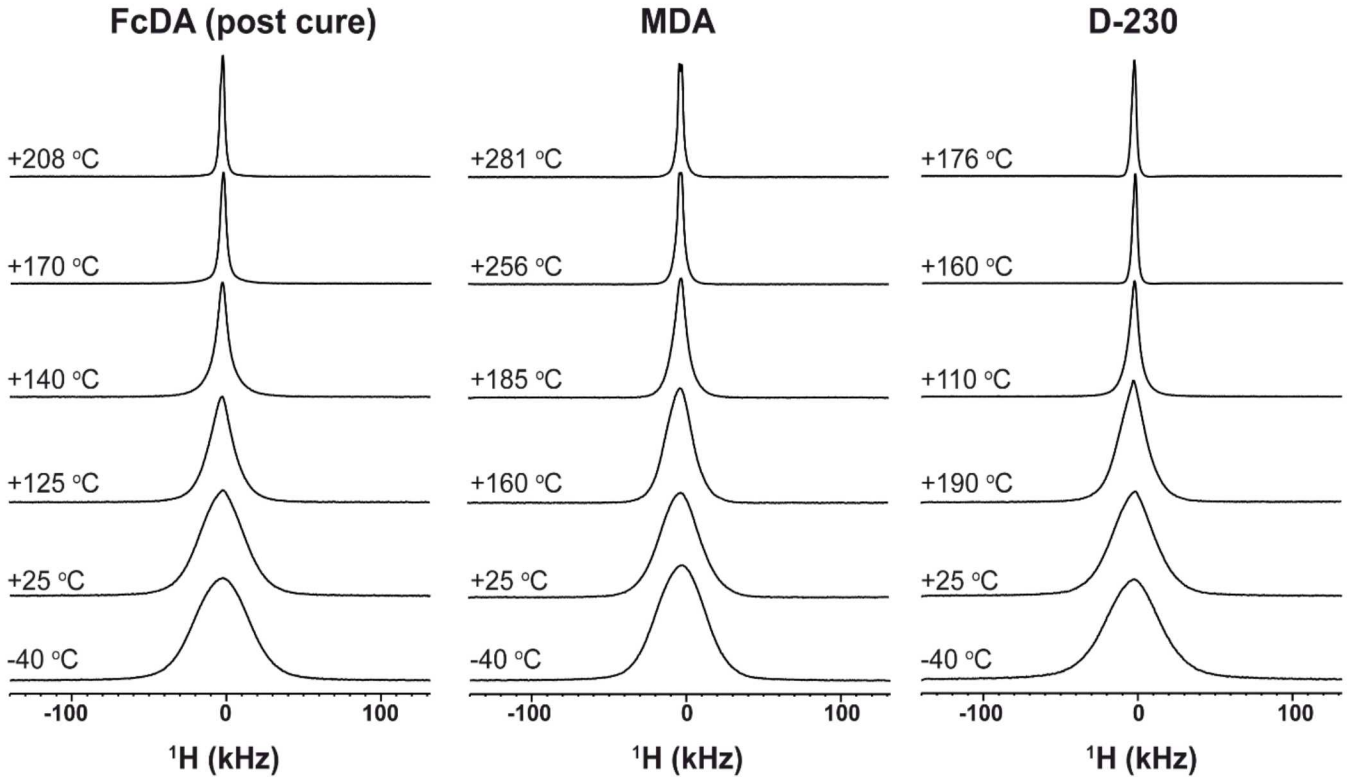

Dipolar Coupling and Motional Averaging

$$\omega_D^{ij} = \sqrt{\frac{3}{2}}\left[\frac{\mu_0 \gamma_I^2 \hbar}{4\pi r_{ij}^3}\right]\left(3\cos^2\theta - 1\right)$$

$$\left\langle \omega_D^{ij} \right\rangle = \sqrt{\frac{3}{2}}\left[\frac{\mu_0 \gamma_I^2 \hbar}{4\pi r_{ij}^3}\right]\left(3\cos^2\theta' - 1\right)\left\langle 3\cos^2\beta - 1\right\rangle \rightarrow \sqrt{\frac{3}{2}}\left[\frac{\mu_0 \gamma_I^2 \hbar}{4\pi r_{ij}^3}\right]\left(3\cos^2\theta' - 1\right) S_b$$

^{1}H NMR – Mapping Internal Polymer Motions

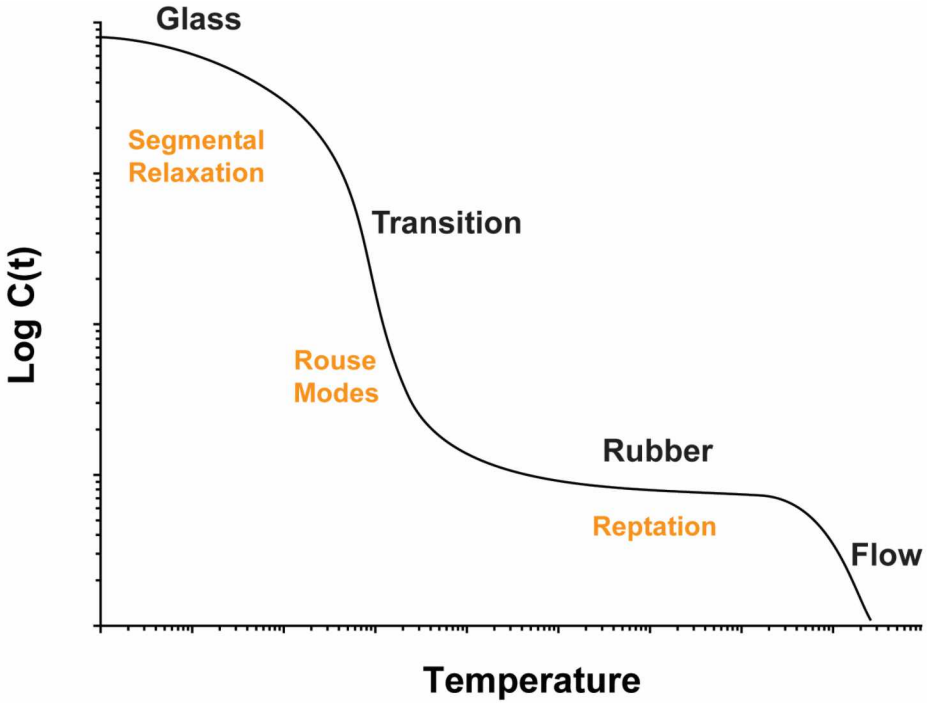

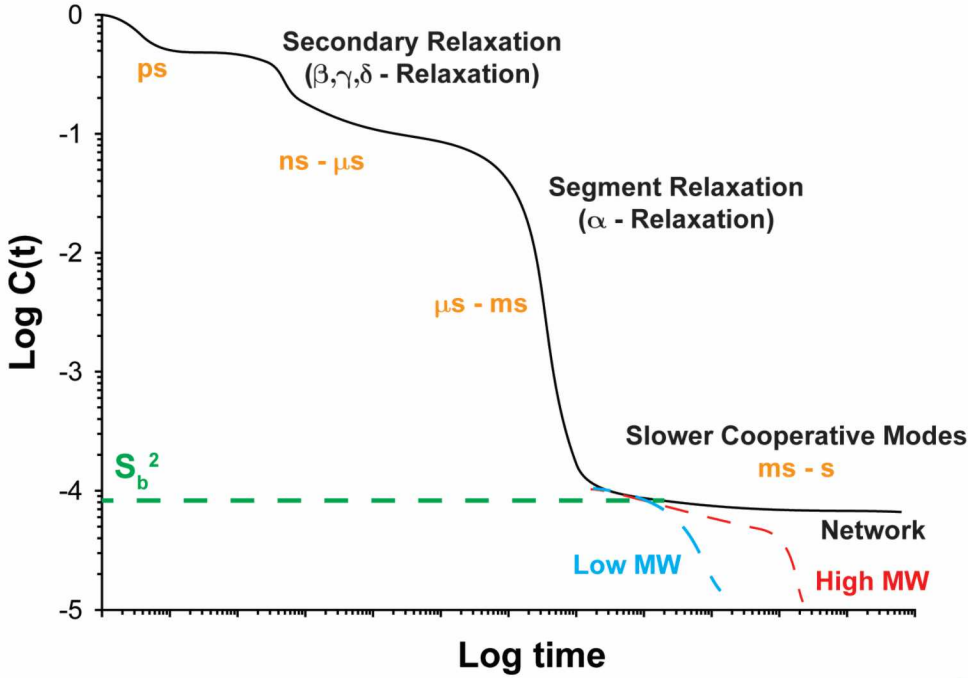

Leads to Concept of Time-Temperature Superposition

Static ^{1}H NMR Line Width - Dynamics

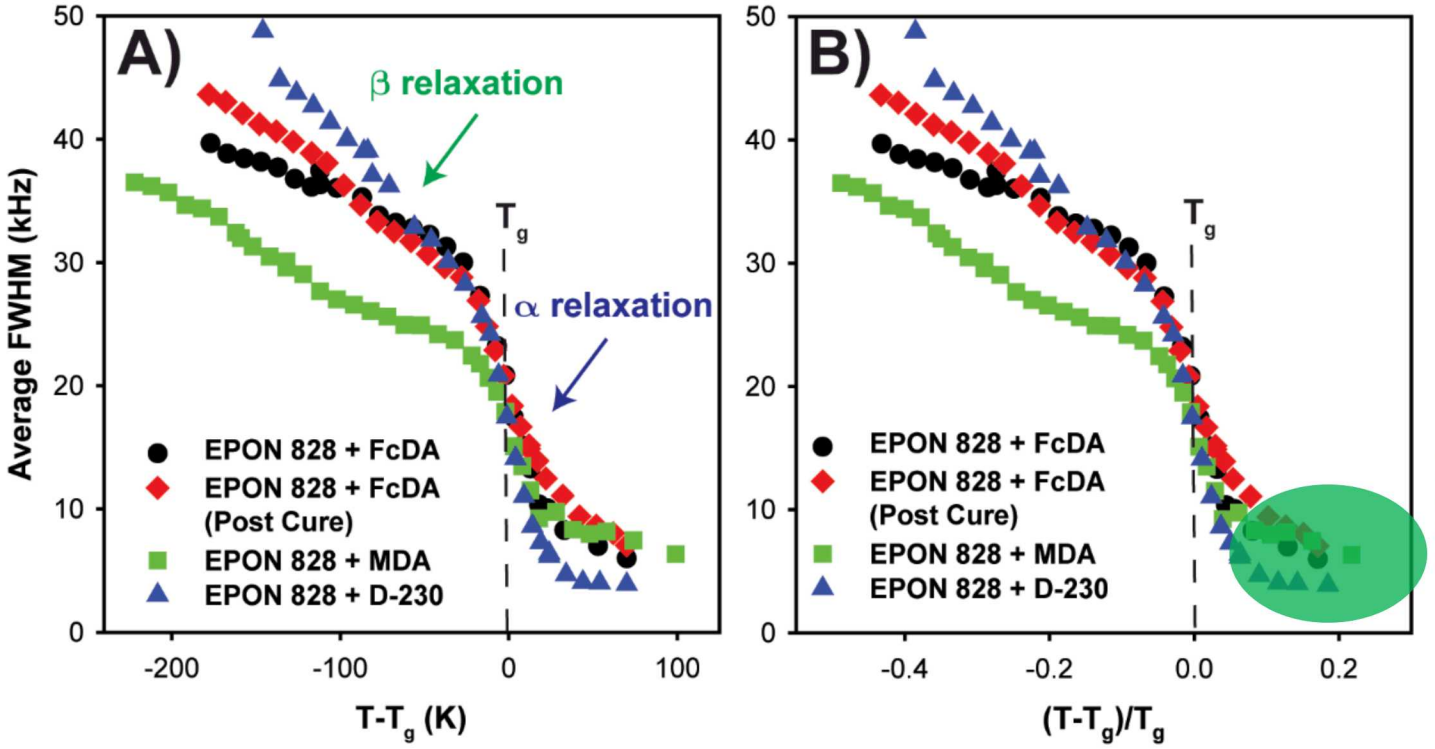

Reduced Temperature

$$\frac{T-T_g}{T_g}=\frac{\Delta T}{T_g}=\frac{T_g}{T}-1=\frac{1}{T_g}-\frac{1}{T}$$

$$\tau_i=\frac{1}{W_i}\tan\left[\frac{\pi}{2}\frac{W_i^2-\langle W\rangle^2}{W_0^2-\langle W\rangle^2}\right]$$

Structural Investigations by Means of Nuclear Magnetism. II. Hindered Rotation in Solids, H. S. Gutowsky and G. E. Pake, The Journal of Chemical Physics 18, 162 (1950); doi: 10.1063/1.1747580

Static ^{1}H NMR - Dynamics From Line Width

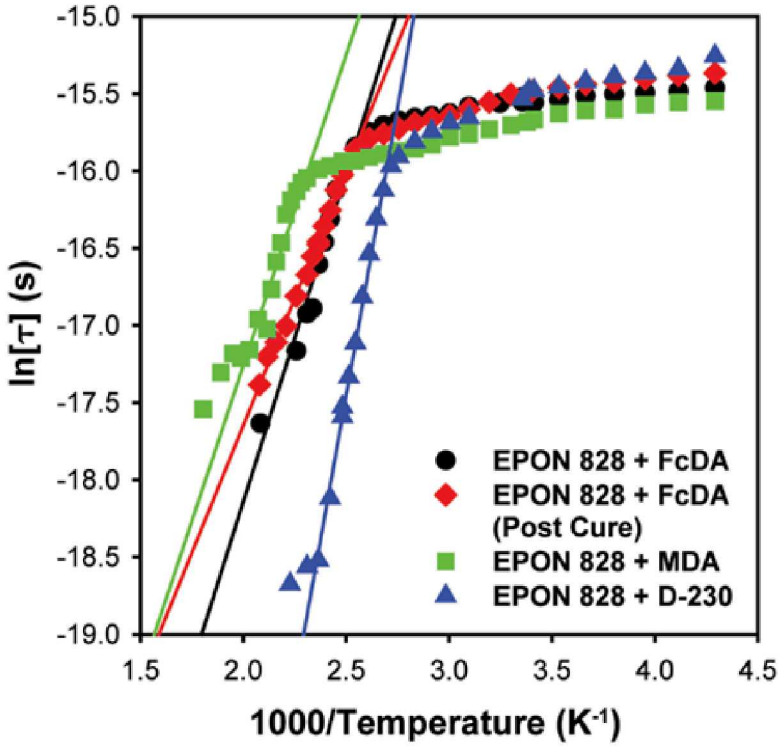

Temperature dependence of this molecular correlation time can be used to estimate T_g activation energy.

$$\tau_i = \tau_0 \exp\left[E_a / RT\right]$$

Epoxy Sample	T_g DSC (°C)	T_g NMR (°C)[a]	b[a]	T_g E_a (kJ/mol)[b]	Sub T_g E_a' (kJ/mol)[c]
EPON 828 + MDA	180	182	-11.1	33.5	2.8
EPON 828 + D230	90	106	-9.6	62.1	2.9
EPON 828 + FcDA	125	137	-13.8	35.3	1.8
* EPON 828 + FcDA (postcure)	113	138	-15.6	27.4	2.0

^{1}H NMR - Double Quantum (DQ) NMR

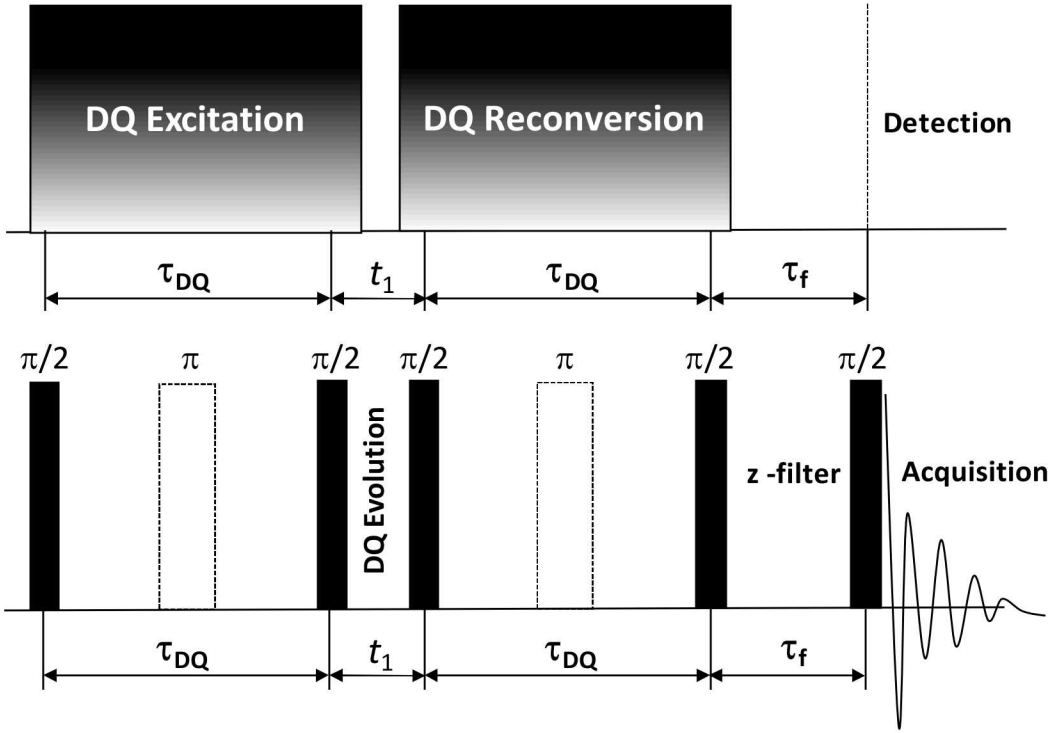

- 5 -pulse DQ sequence (Pines).
- π pulses for refocusing.
- Variation on τ_{DQ} for buildups.
- Not increased cycle number.
- Used extensively in rubbers for motions in the ms range.
- Cross link density in rubbers (industry - e.g. tires).

$$\omega_D^{ij} = \sqrt{\frac{3}{2}}\left[\frac{\mu_0 \gamma_I^2 \hbar}{4\pi r_{ij}^3}\right]\left(3\cos^2\theta - 1\right)$$

$$I_{nDQ} = \frac{I_{DQ}}{I_{DQ} + I_{ref} - B\exp\left[-2\tau_{DQ}/T_2\right]}$$

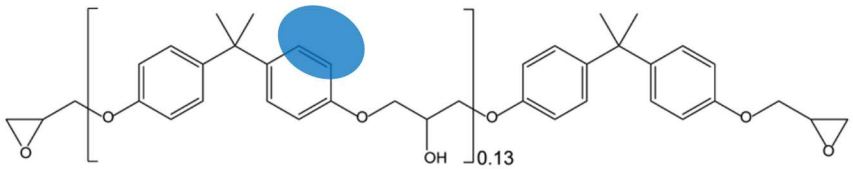

EPON 828

^{1}H NMR – DQ NMR Fully Cure

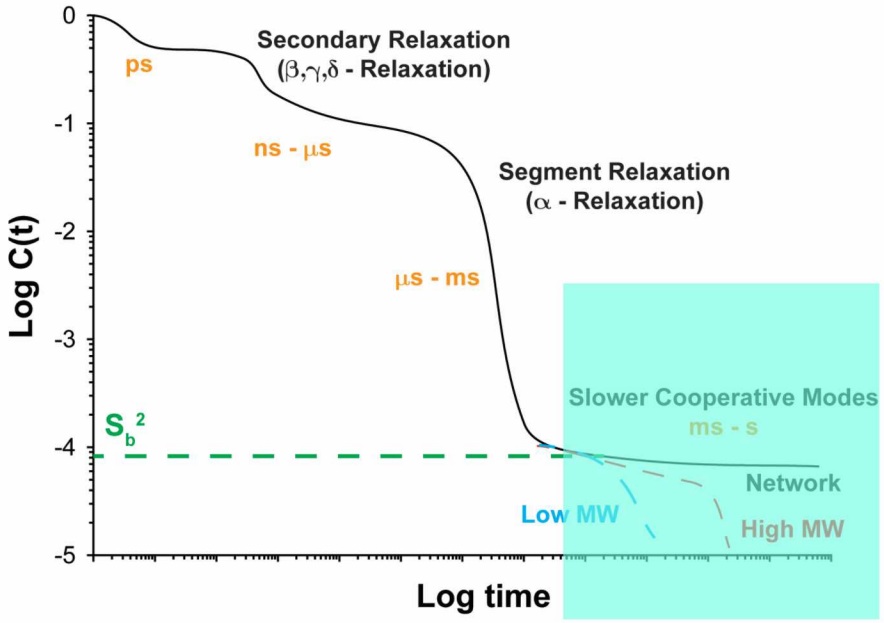

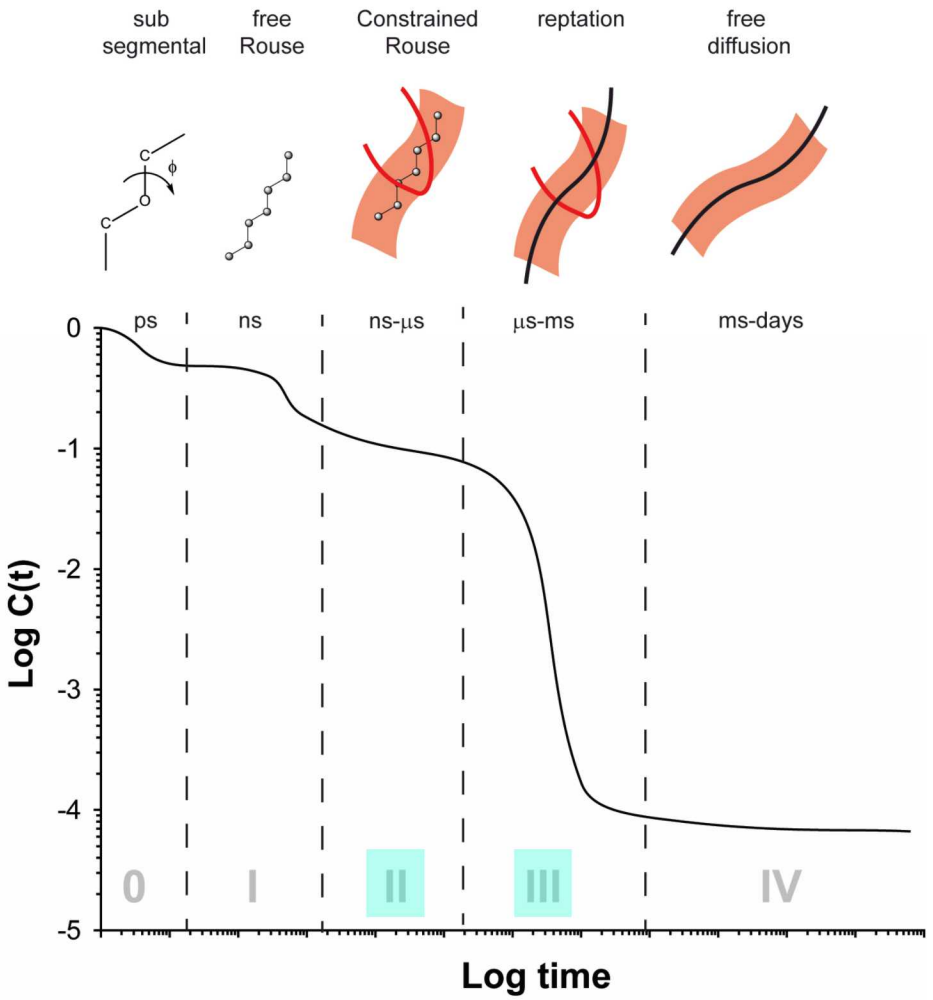

High temperature region $T > T_g$
DQ NMR directly measures S_b

DQ ^{1}H NMR – Fully Cure Epoxy Normalized DQ Buildups

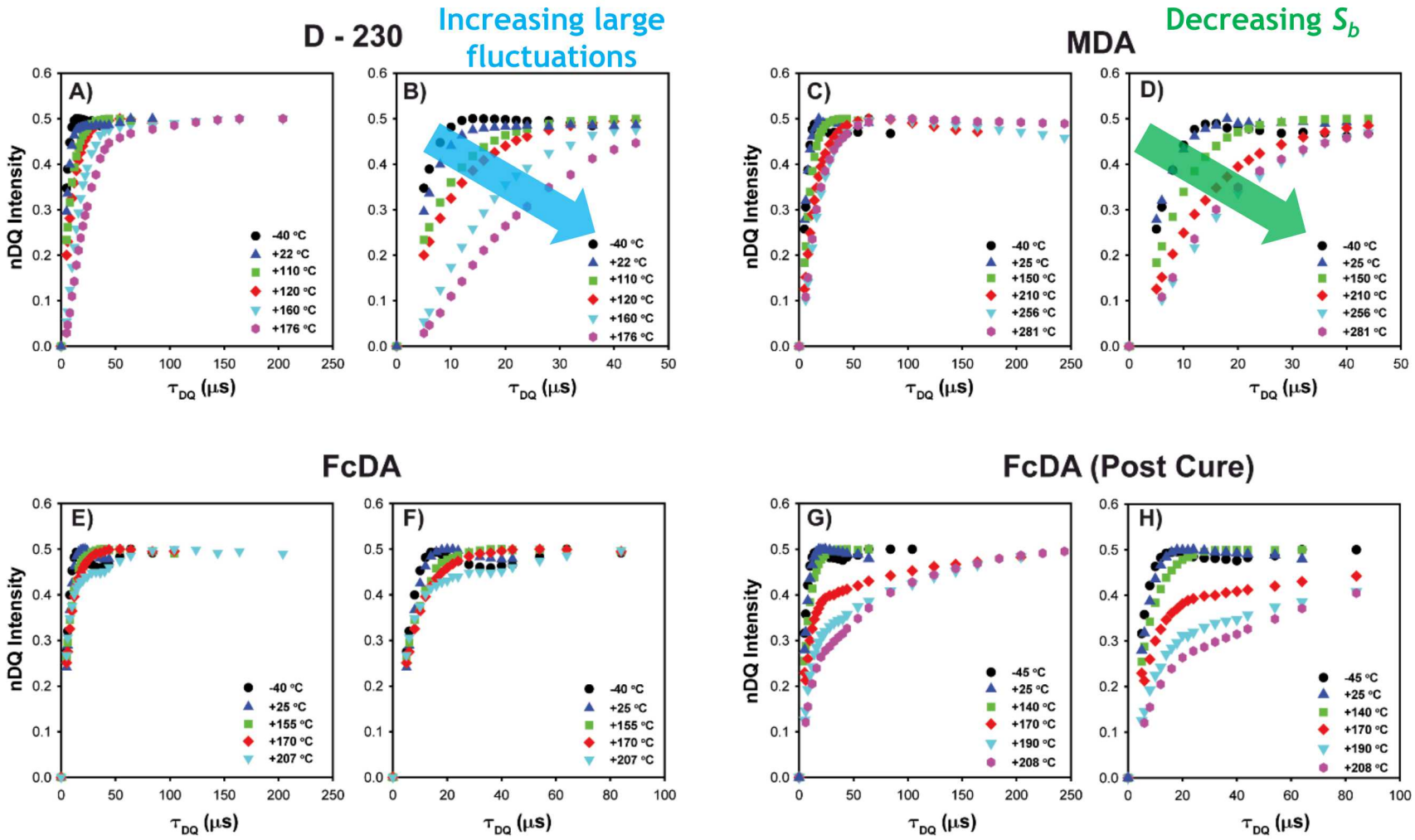

So What….
How is this Related to Polymer Physics?

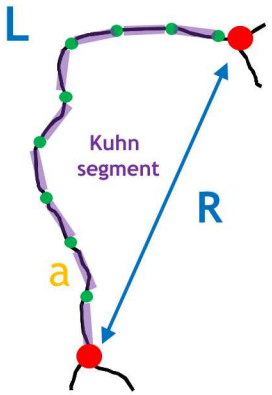

$$S_b = \left\langle P_2\left(\cos\theta_t\right)\right\rangle_t = k\frac{D_{res}}{D_{stat}}\frac{1}{\left\langle P_2\left(\cos\alpha\right)\right\rangle} = \frac{3}{5}\frac{\boldsymbol{R}^2}{L^2}$$

Freely Jointed Chain (FJC) Model

Scaling to N Kuhn segments of Length a
Follow Gaussian Statistics
Used to get cross link densities
Connects to Flory Constant C_∞
Connects to Freely Rotating Chain (FRC) and Hindered Rotation Models (HRC)

$$N_M l_M \longrightarrow Na$$

$$\boldsymbol{R}^2 = Na^2;\ L = Na;\ r = \boldsymbol{R}/\boldsymbol{R}_0$$

Has been used to measure cross-link densities

$$S_b = \frac{3}{5}\frac{\boldsymbol{R}^2}{L^2} = \frac{3}{5}\frac{r^2}{N}$$

$$\left\langle \boldsymbol{R}^2\right\rangle \sim C_n n l^2 \quad \left(Flexible\ Chain\right)$$

$$C_\infty = \lim_{N\to\infty} \boldsymbol{R}^2 / N_M l_M^2$$

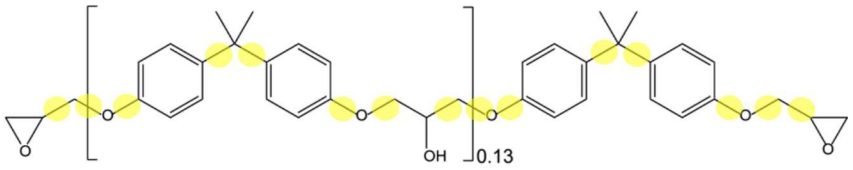

EPON 828

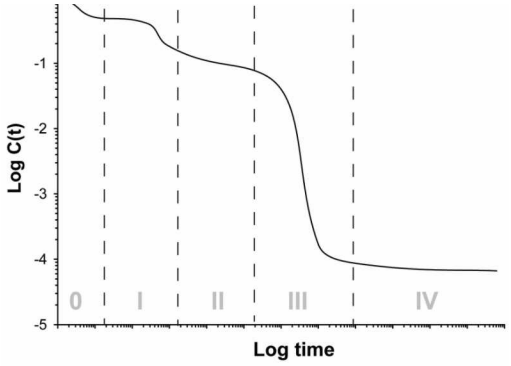

DQ ^{1}H NMR Derived Order Parameters

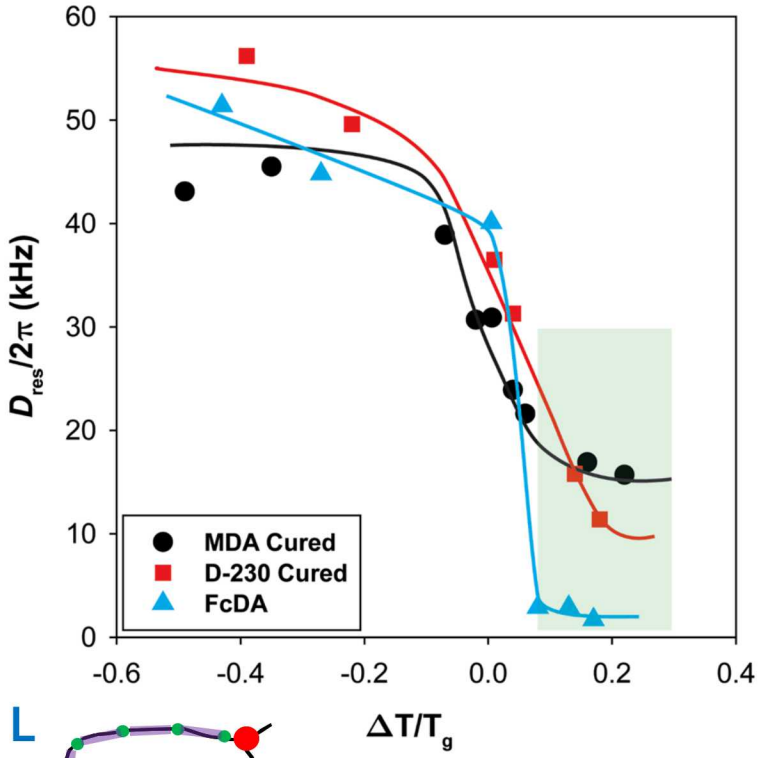

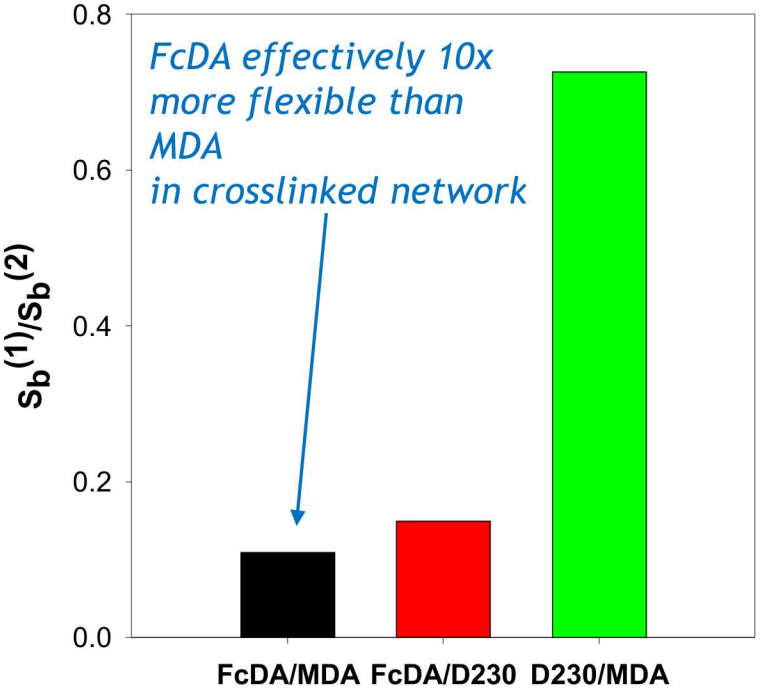

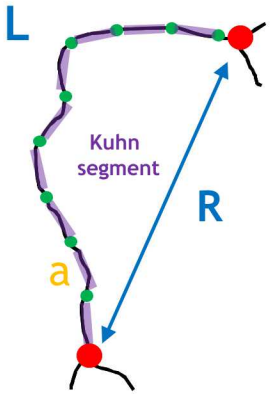

$$\frac{S_b^{(1)}}{S_b^{(2)}} = k\frac{D_{res}^{(1)}}{D_{stat}}\frac{1}{\langle P_2(\cos\alpha)\rangle} \Big/ k\frac{D_{res}^{(2)}}{D_{stat}}\frac{1}{\langle P_2(\cos\alpha)\rangle} \approx \frac{D_{res}^{(1)}}{D_{res}^{(2)}}$$

$$\frac{S_b^{(1)}}{S_b^{(2)}} \approx \frac{D_{res}^{(1)}}{D_{res}^{(2)}} = \left\{\frac{3}{5}\frac{r^2}{N^{(1)}}\right\} \Big/ \left\{\frac{3}{5}\frac{r^2}{N^{(2)}}\right\} = \frac{N^{(2)}}{N^{(1)}} = \frac{n^{(2)}C_\infty^{(1)}}{n^{(1)}C_\infty^{(2)}}$$

Conclusions

- ^{1}H NMR line width variation used to probe local polymer dynamics as a function of temperature.
- Allows evaluation of E_a for segmental motions at glass transition.
- DQ ^{1}H NMR can be used to look at epoxy curing from purely segmental motion viewpoint (S_b).
- For $T >> T_g$ the DQ build up curves allow the order parameter S_b in the rubber plateau to be measured.
- The FcDA cured epoxy shows a heterogeneous cross-link (dynamic) environment.
- Order parameters can be related to polymer models and crosslink properties.

Acknowledgements

Dr. Amalie Frischknecht (SNL) - MD Simulations

Prof. Janelle Jenkins (Prof. at E. Washington Univ.)

Dr. Lauren J. Abbott (SNL…now NASA) - MD Simulations

Dr. Eric Sorte (SNL) - DIFFSIM_NMR

Dr. Cy Fujimoto (SNL) - SDAPP Synthesis

Dr. Michael Hibbs (SNL) - AEM Synthesis

Dr. Brad Jones (SNL) - Epoxies

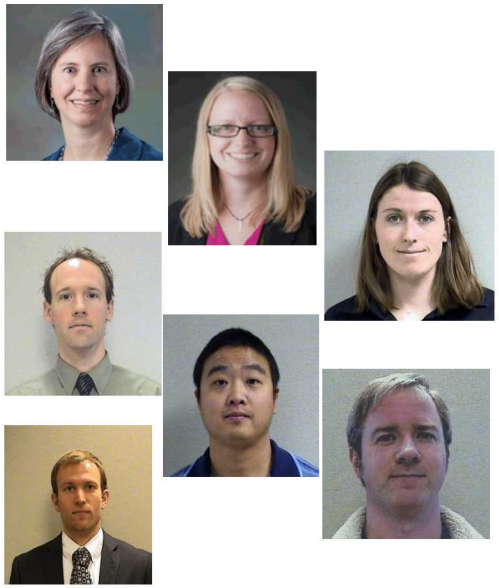

Prof. Karen Whiney (Univ. of Penn)

Ben Paren (Graduate Student, U. Penn)

Kim Childress (Graduate Student, UC-Boulder)

Randi Miller (NMR Facility Technician)

LDRD LABORATORY DIRECTED RESEARCH & DEVELOPMENT

Project funding through the Sandia LDRD program

Sandia Fellowships

Jill Hruby Fellowship (National Security Science)

- deadline Nov. 1st

Truman Fellowship (National Security Science and Engineering)

- deadline Nov. 1st

John von Neumann Fellowship (Computational Science)

- dealine Nov. 26th

NMR Postdoctoral Fellowship

A postdoctoral position will be available in the Organic Materials Science department and NMR facility at Sandia National Laboratories (SNL) in Albuquerque, NM. We are presently seeking highly motivated individuals to pursue research utilizing NMR spectroscopy in a national lab setting.
The postdoctoral position involves the use of solid state NMR and NMR diffusometry techniques to look at a variety of materials related issues. Candidate can become involved in a series of collaborative projects ranging from: 1) development of novel MAS NMR techniques to structure and dynamics in materials, 2) PFG NMR studies of transport in materials, 3) self-assembly phenomena, 4) NMR analysis of chemistry directed towards homeland security issues. Experience in either high resolution or solid state NMR spectroscopy as applied to materials science is desired.

The laboratory is well equipped for both solution and solid state NMR investigations. The position requires a Ph.D. in chemistry, physics, material science or closely related field. Excellent communication skills are required. Salary is industry-based, highly competitive and is for a 1-year position, with the possibility of extension. Interested parties should send a current CV to Dr. Todd M. Alam, tmalam@sandia.gov referencing. The ability to obtain a clearance security will be required. Interested candidates should also apply directly to https://www.sandia.gov/careers/students_postdocs/index.html Job ID # 665997

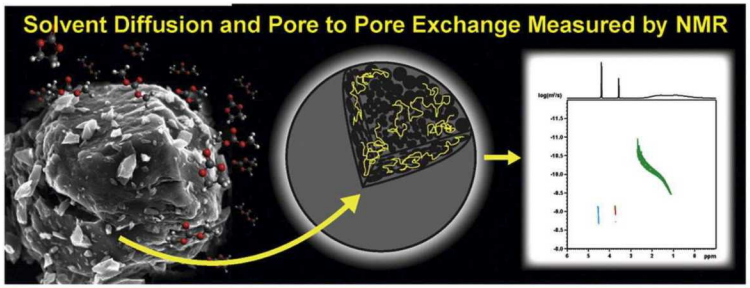

Backup Slides

NMR Diffusometry - SDAPP Membranes

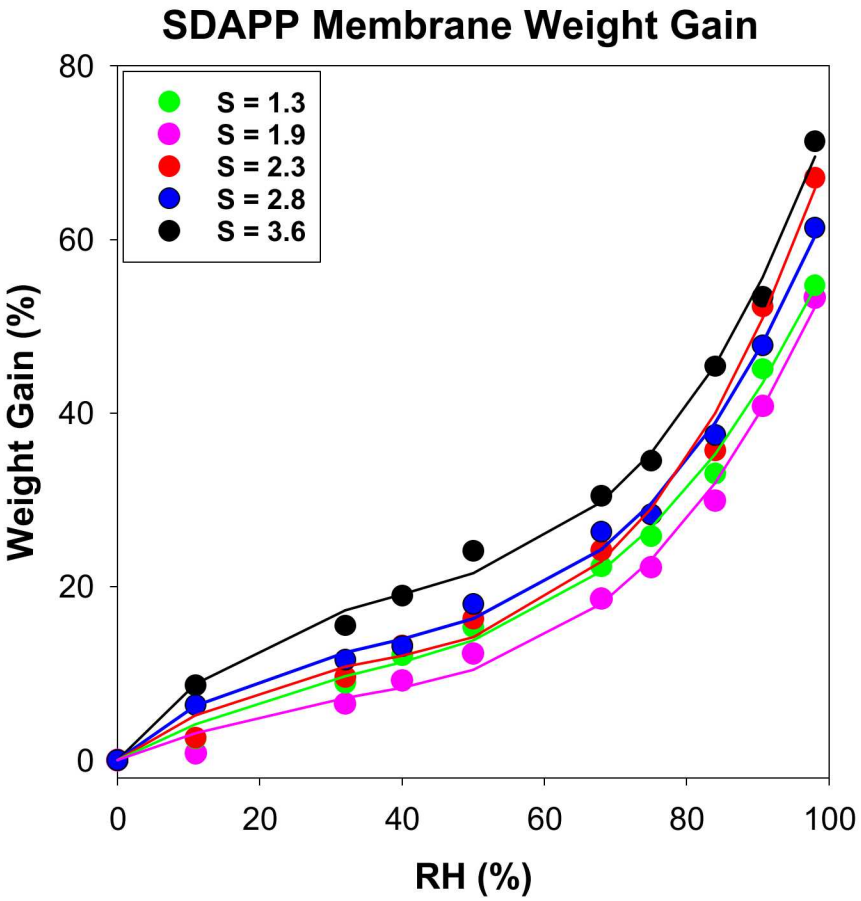

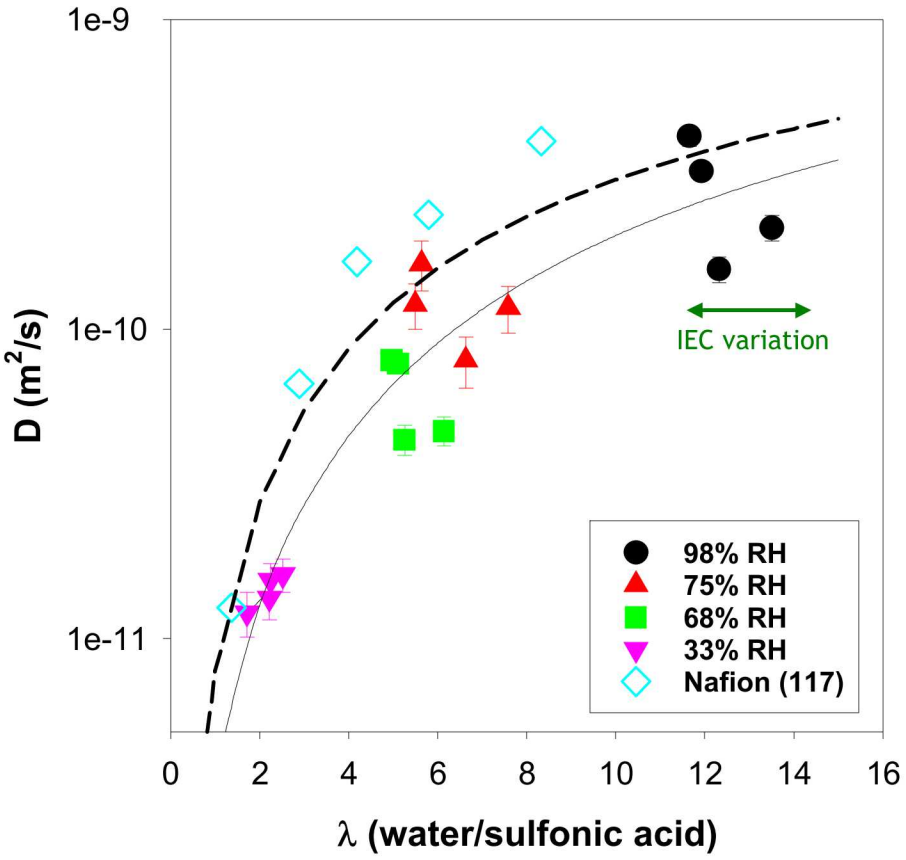

- Diffusion trends are same order of magnitude as Nafion.
- Small variations as a function of IEC.

High Resolution Magic Angle Spinning (HRMAS) Pulse Field Gradient (PFG) Diffusion Experiments

"Diffusometry NMR"

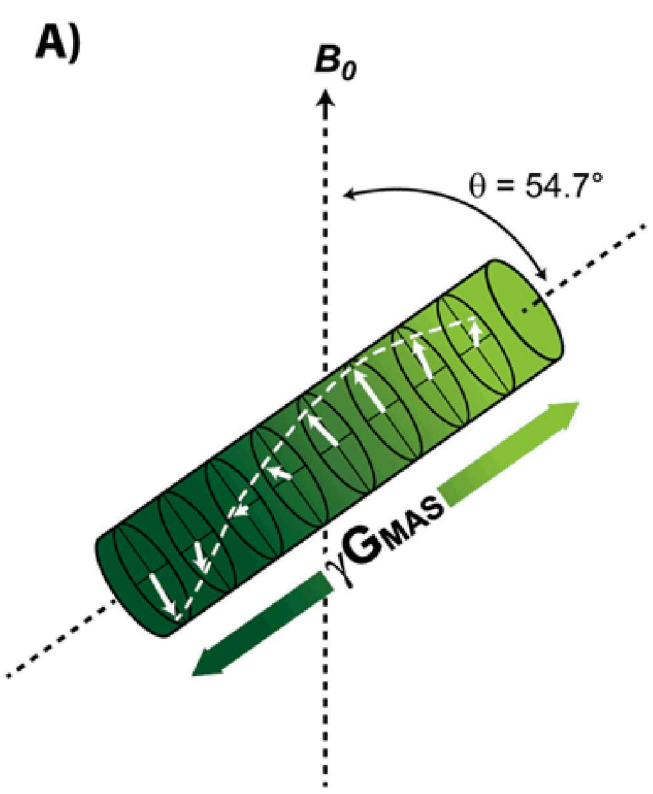

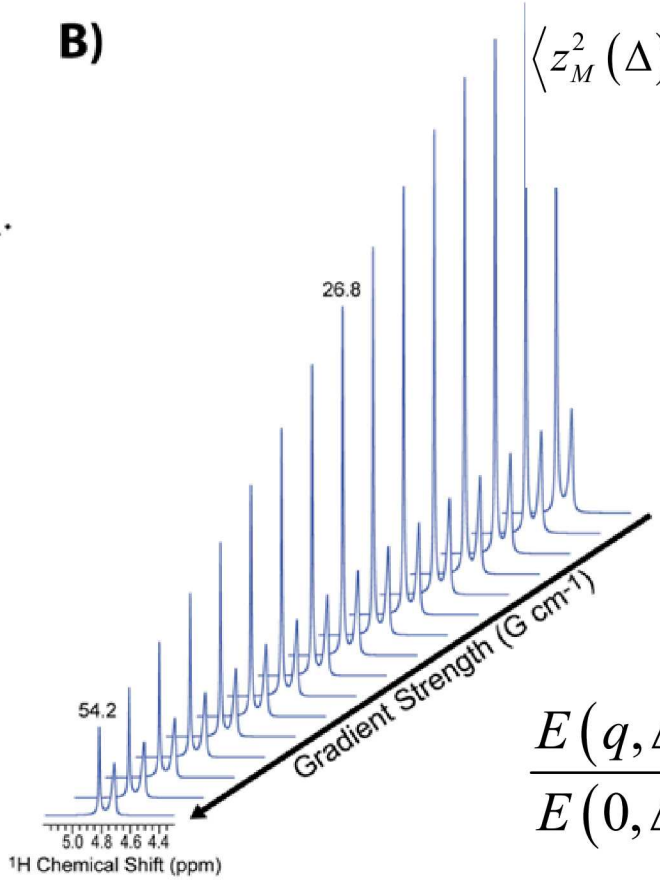

$$\left\langle z_M^2(\Delta)\right\rangle = -2\ln\left[E(q,\Delta)/E(0,\Delta)\right]/q^2$$

$$\left\langle z_M^2\right\rangle = 2D_\alpha t^\alpha$$

Diffusion Using Stejskal-Tanner Formula

$$\frac{E(q,\Delta)}{E(0,\Delta)} = \exp\left[-q^2 D\left(\Delta - \frac{\delta}{3}\right)\right]$$

Figure 8: A) Pictorial representation of the gradient produced along the magic angle of the rotor. B) The decay of two different water signals found in a 1N methanol solution of an AEM membrane with increasing gradient strength. Gradient strength values (G/cm) are shown above the stack plot.

NMR Diffusometry - Transport of Water Pulsed Field Gradient (PFG) NMR

Stimulated Echo (STE)

Spin Voxel is spatially "tagged"

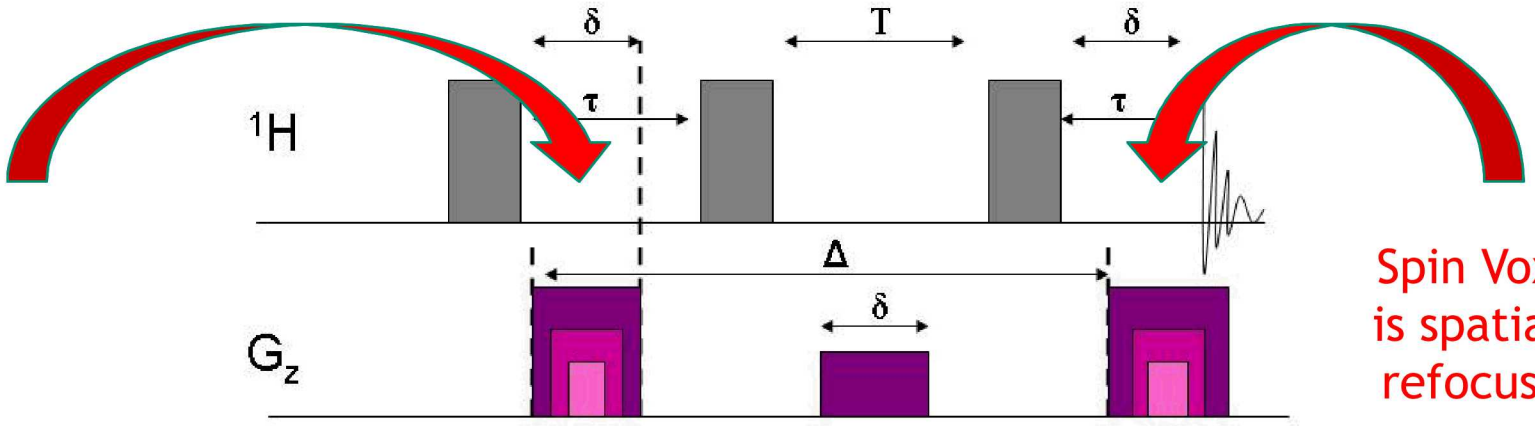

Spin Voxel is spatially refocused

Signal decay is measured by:

$$S(T+2\tau_1) = \frac{M_0}{2}\exp(-2\tau_1/T_2 - T/T_1)\exp\left[-D\gamma^2 g^2 \delta^2 (\Delta - \delta/3)\right]$$

Where:

- T_1 = spin-lattice relaxation time
- δ = length of gradient pulse
- g = gradient strength
- γ = gyromagnetic ratio
- T_2= spin-spin relaxation time
- Δ= inter pulse delay
- D= diffusion constant
- τ, T: inter-pulse spacing

Pulse Field Gradient (PFG) NMR provides one method for characterizing the self-diffusion transport of species within the membrane.

PFG NMR Diffusometry Equipment

Water cooled diffusion probe

Nucleus Specific

^{1}H, ^{2}H, ^{19}F, ^{7}Li, ^{13}C, ^{23}Na, ^{31}P....

Gradient control and B_0 emphasis unit

High power gradient unit

Visualization of Diffusion Process

Propagator

$$\bar{P}(\vec{r},t) = \int_V P(\vec{r}_1 + \vec{r}, \vec{r}_1, t)\, p_0(\vec{r}_1)\, d\vec{r}_1$$

$$\bar{P}(\vec{r},t) = \frac{1}{\sqrt{(4\pi D t)^3}} \exp\left(-\frac{(\vec{r}(t))^2}{4Dt}\right)$$

$$\left\langle \vec{r}^{\,2}(t) \right\rangle = \int_V P(\vec{r},t)\vec{r}^{\,2}\, d\vec{r}_1 = 6Dt$$

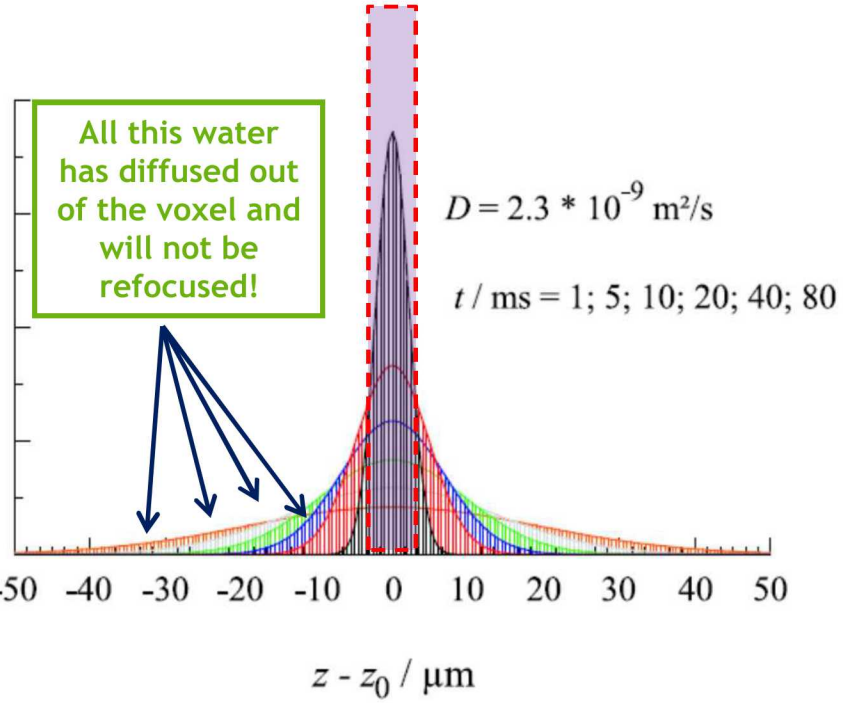

- Will use pulse field gradient (PFG) NMR (described next) to measure this self-diffusion constant (D).
- Signal from the PFG experiment is the FT of the diffusion propagator.

$$\Psi(g,\delta,\Delta) = \int \bar{P}(z,\Delta)\cos(\gamma g \delta z)\, dz$$

Site Resolution in MeOH Fuel Cell Membranes
"The Odyssey Begins"

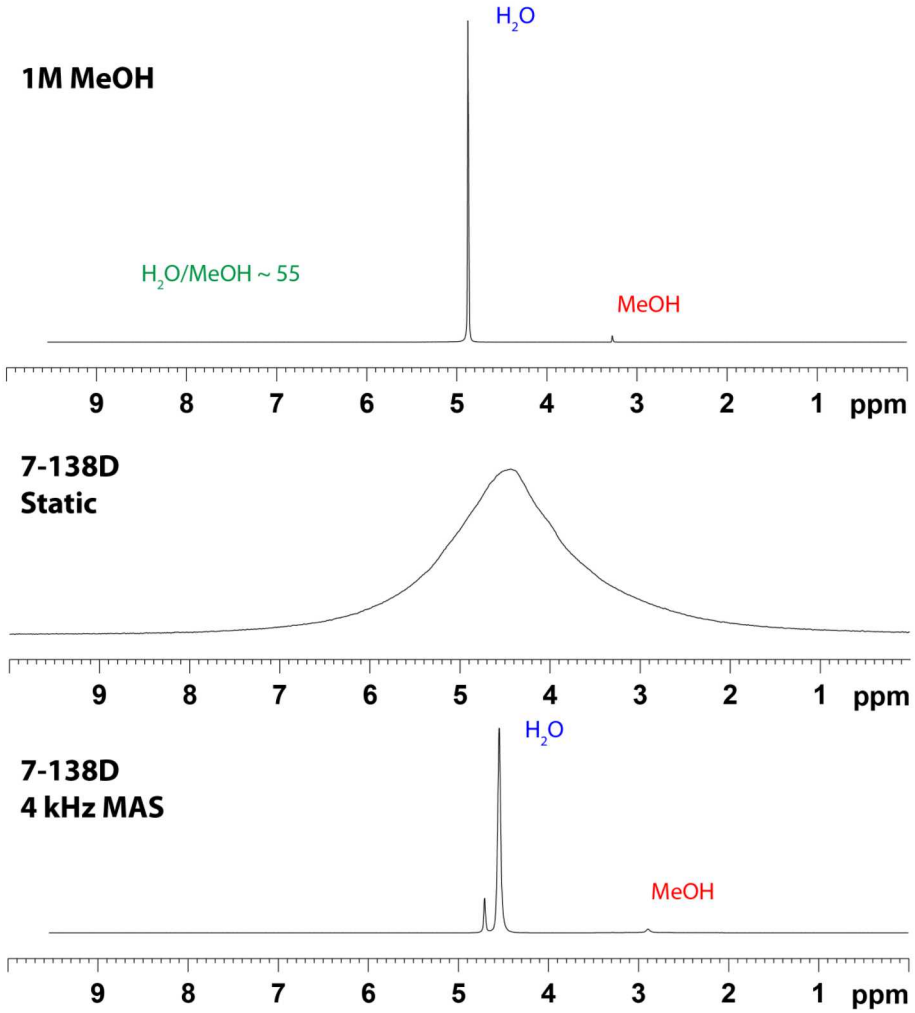

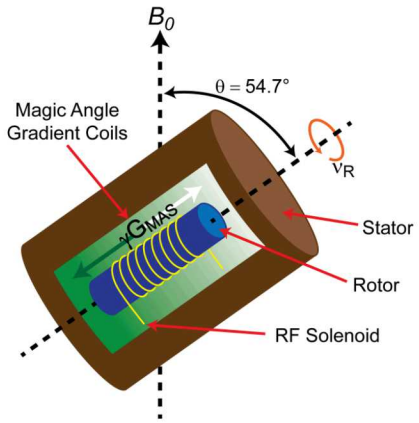

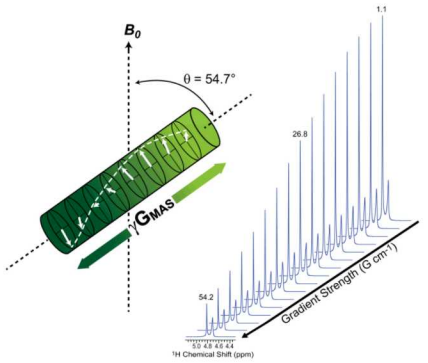

Different water environments in polymers

- Water in hot pressed Nafion, Jeong and Han, Bull. Korean Chem. Soc. (2009), 30, 1559.
- Water in PEEK, Baias *et al*, Chem. Phys. Lett. (2008), 456, 227; (2009) 473, 142. MAS with SSB with no chemical shift resolution.
- Mele *et al.*, J. Incl. Phenon. Macrocycl. Chem. (2011), 69, 403. HRMAS resolution.

High Resolution Magic Angle Spinning (HRMAS)

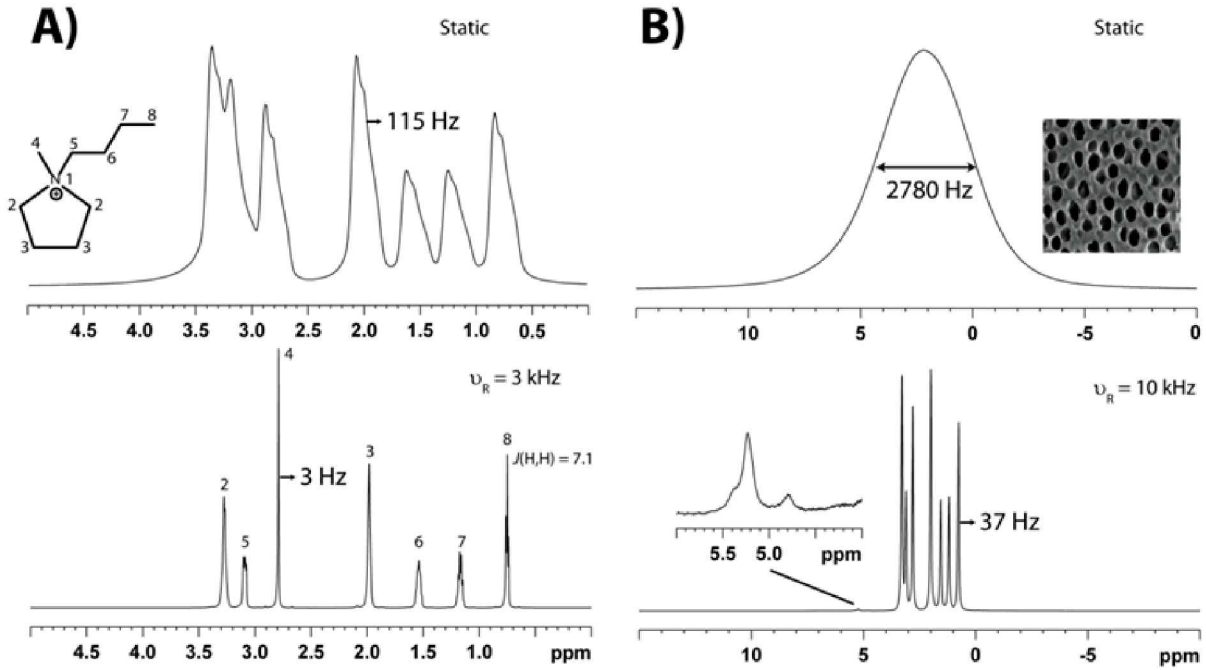

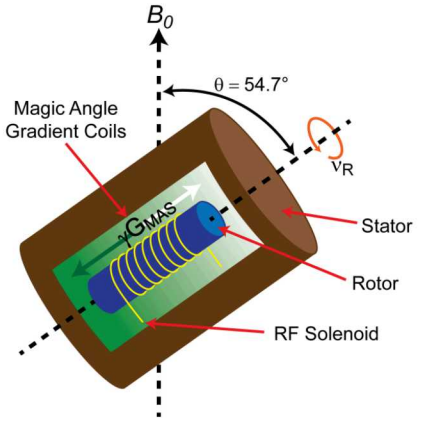

Reduce susceptibility effects in semi-solid materials:

- Combinatorial resins
- Tissues
- Cell dispersions
- Polymer gels

"Magic Angle Spinning"

$$\Delta B \sim P_2(\cos\theta) = 3\left(\cos^2\theta - \frac{1}{2}\right)$$

Hamiltonian same form as CSA and dipolar interactions!

Todd M. Alam and Janelle E. Jenkins, " HR-MAS NMR Spectroscopy in Material Science", in Advanced Aspects of Spectroscopy, Muhammad Akhyar Farrukh (Ed.), ISBN: 978-953-51-0715-6, InTech, (2012).

High Resolution Magic Angle Spinning (HRMAS)

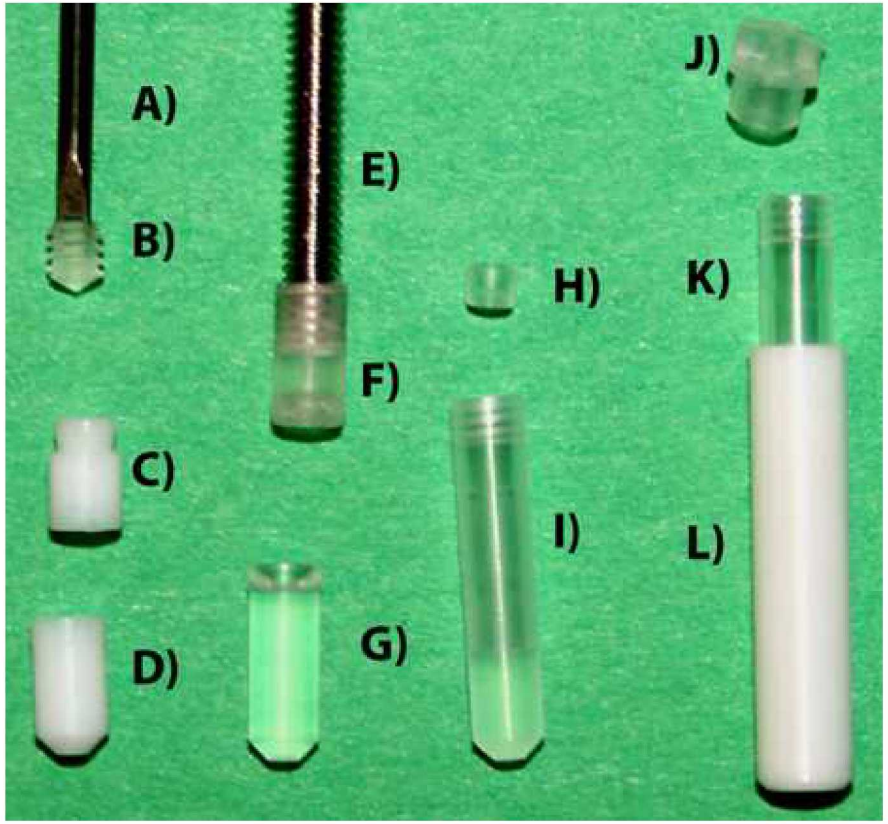

Figure 4: The tools and inserts used for HR-MAS NMR. These include A) the specialized tool for screw cap insertion, B) the sealing screw cap, C) the upper insert (Teflon®), D) lower Teflon® insert for 30 µL volume, E) screw for insertion/extraction of top insert, F) top Kel-F® insert, G) bottom Kel-F® insert for 12 µL sample volume, H) plug for disposable insert, I) disposable 30 uL Kel-F® insert, J) 4 mm rotor cap, K) disposable inserted partially in a 4 mm rotor, L) 4 mm zirconia MAS rotor. All these parts are for the Bruker HR-MAS system, and may vary between vendors.

- "Liquid like samples" need to retain liquid under MAS.
- Might need to consider centrifugation effects under MAS.

HRMAS PFG NMR and Site Resolution

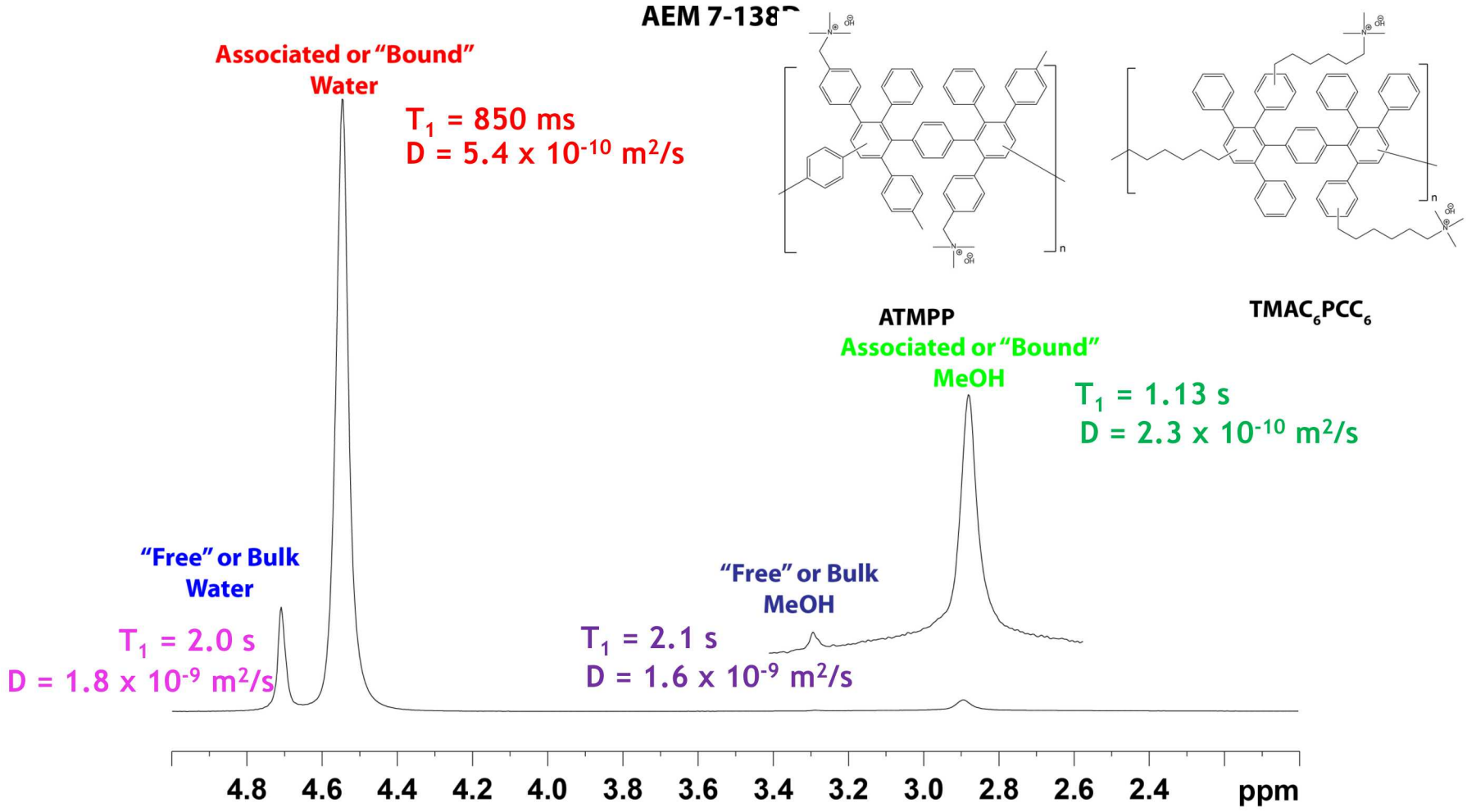

Resolution is always exciting! ***Can ask questions about differences between MeOH and water association with the membrane.***

^{1}H HRMAS NMR of Different AEM Membranes

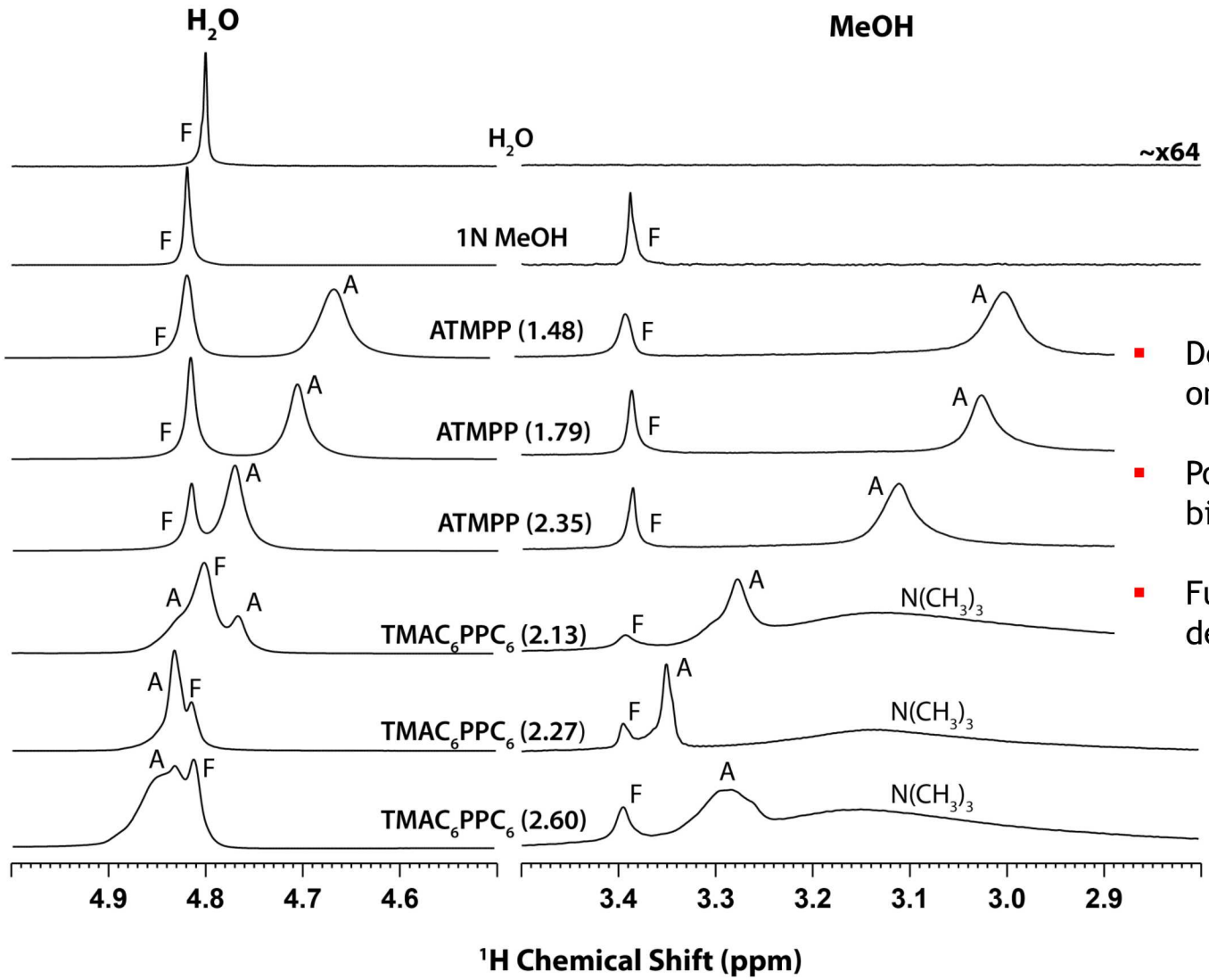

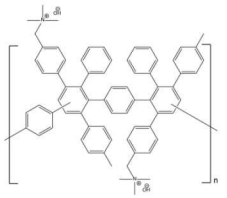

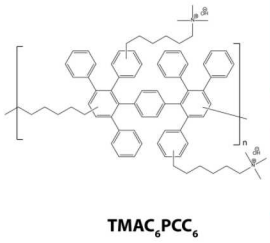

- Desired differential impact on MeOH transport.
- Polymer membrane for binding of Pt catalyst.
- Function of both polymer design and IEC.

Where are these Associated Species?

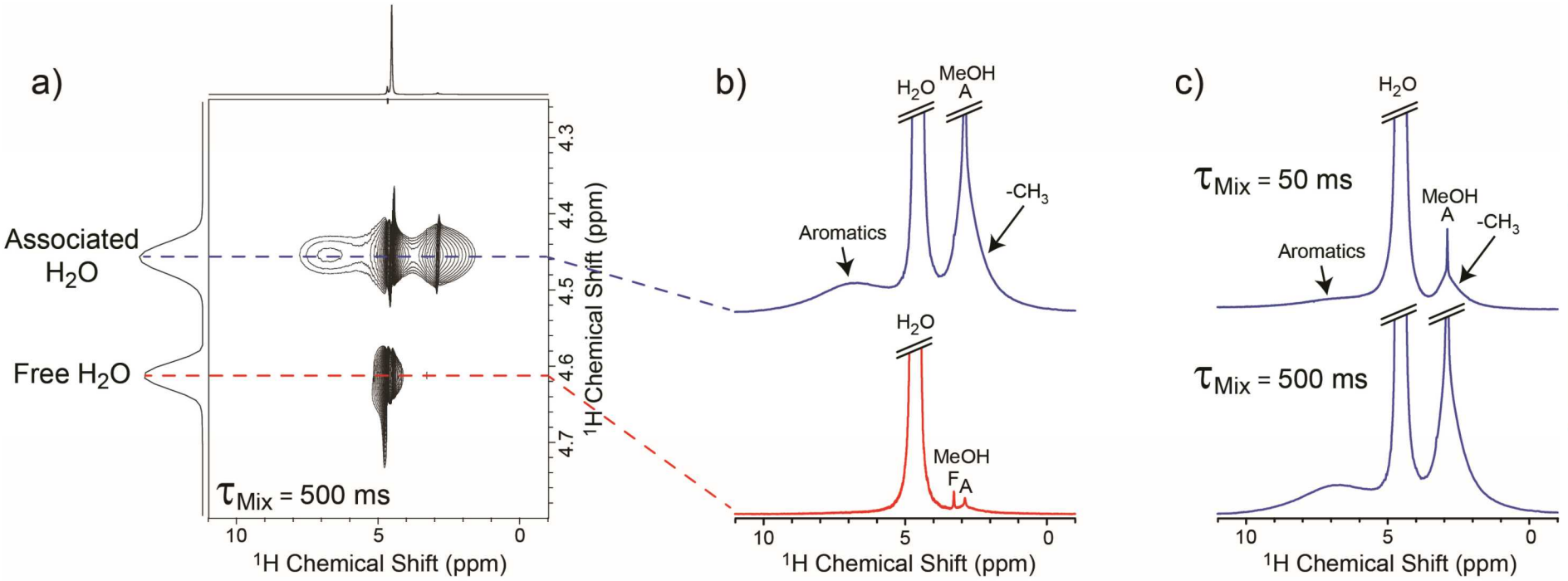

- **The 2D NOESY data (faster spinning speeds) reveal correlation between the associated species (both H_2O and MeOH) and the membrane.**
- **Short mixing times suggest near the cation ($N(CH_3)_3^+$).**
- **Free species do not reveal any strong NOE correlations.**

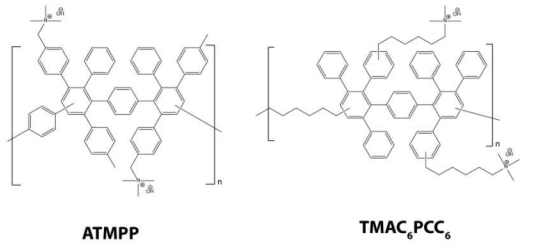

2D ^{1}H-^{1}H Exchange/NOESY Studies

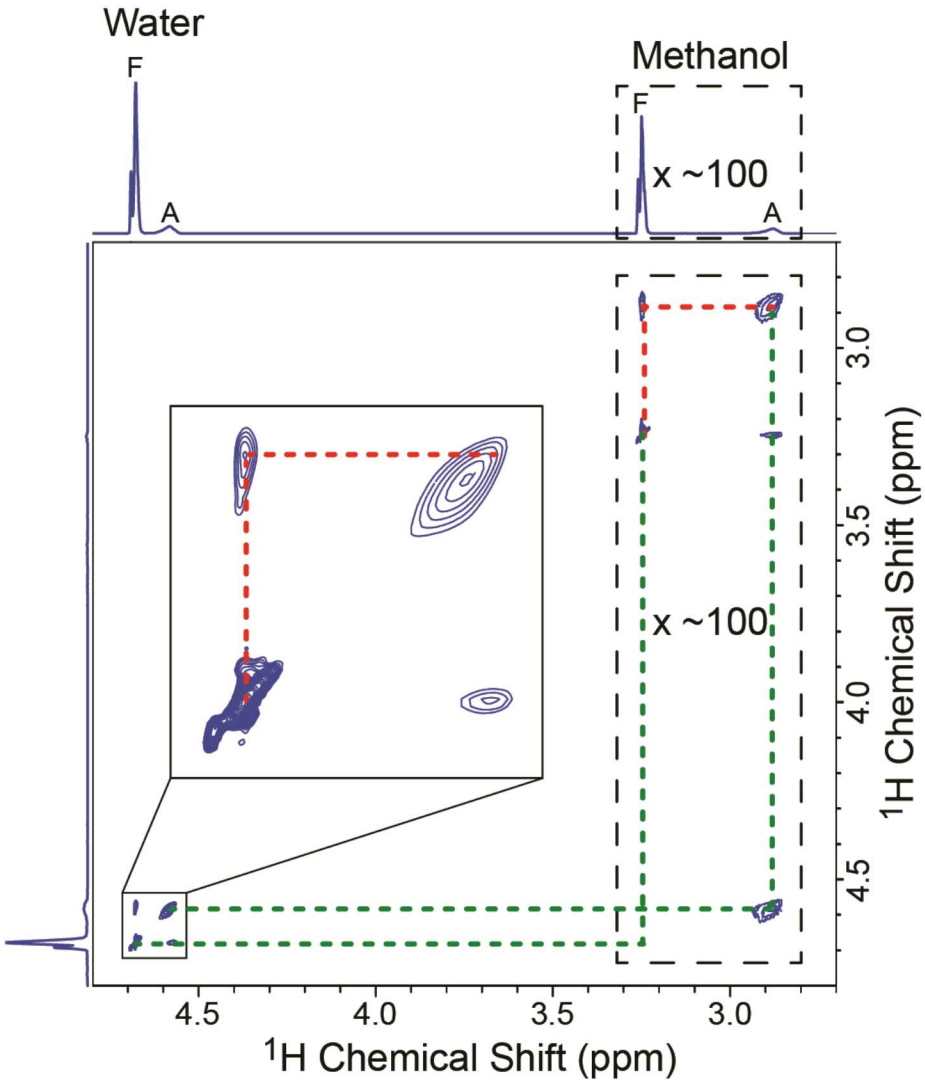

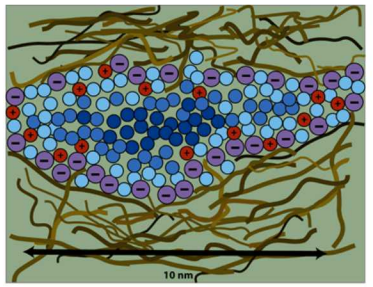

- Free and associated domains exist.
- These domains show some exchange.
- Associated water and MeOH in close contact with membrane.

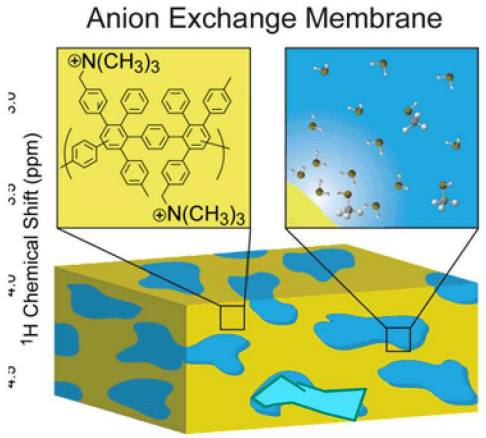

2D ^{1}H-^{1}H Exchange/NOESY Studies

$$\frac{I_{CP}(\tau_{mix})}{I_{Diag}(\tau_{Diag})} = 1 - \exp[-\sigma\tau_{mix}]$$

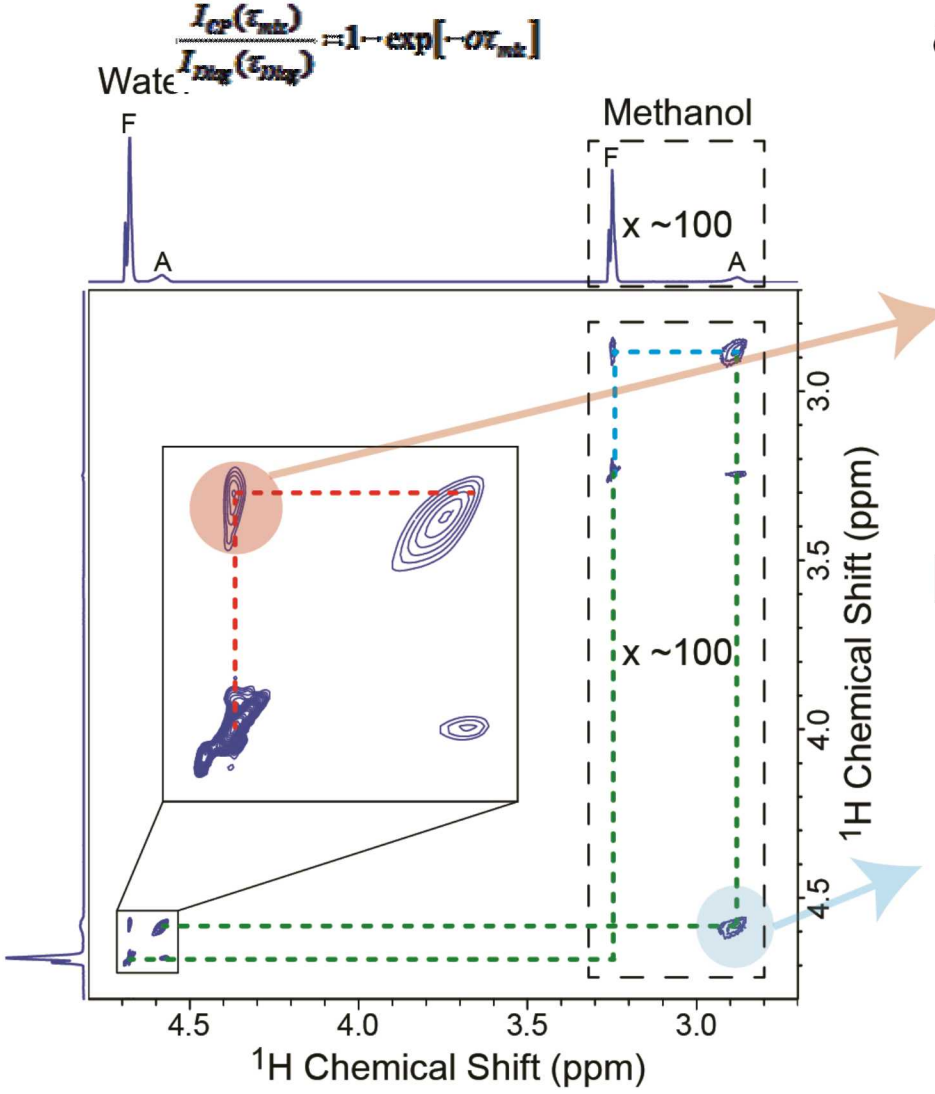

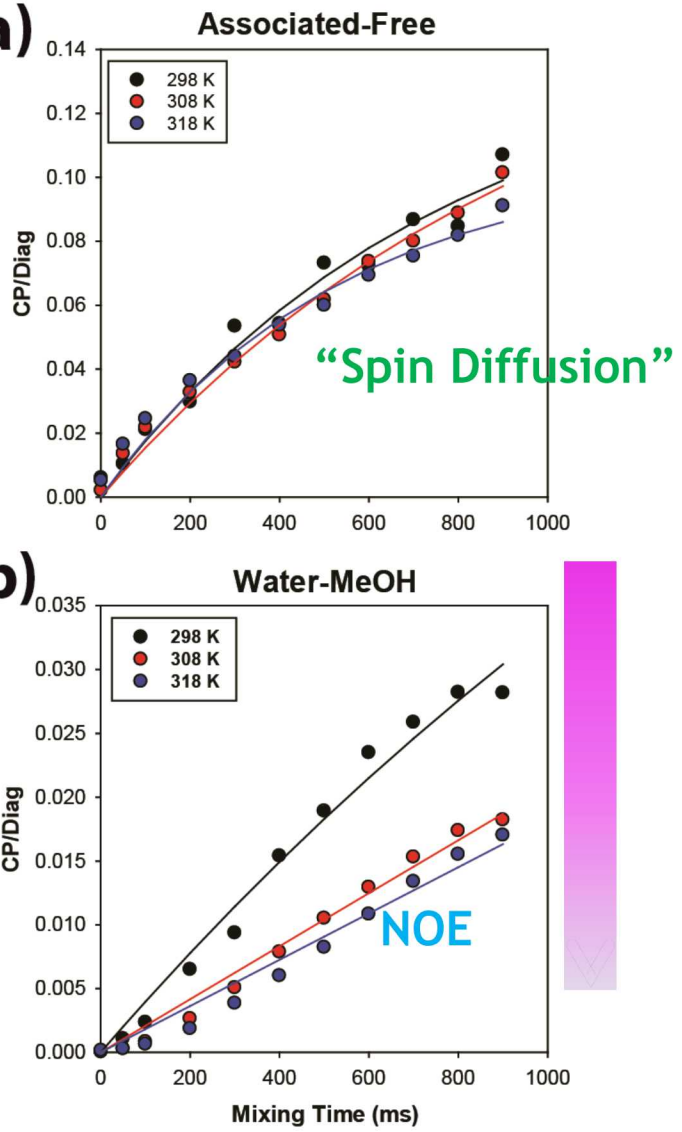

Diffusion Analysis of Individual Species

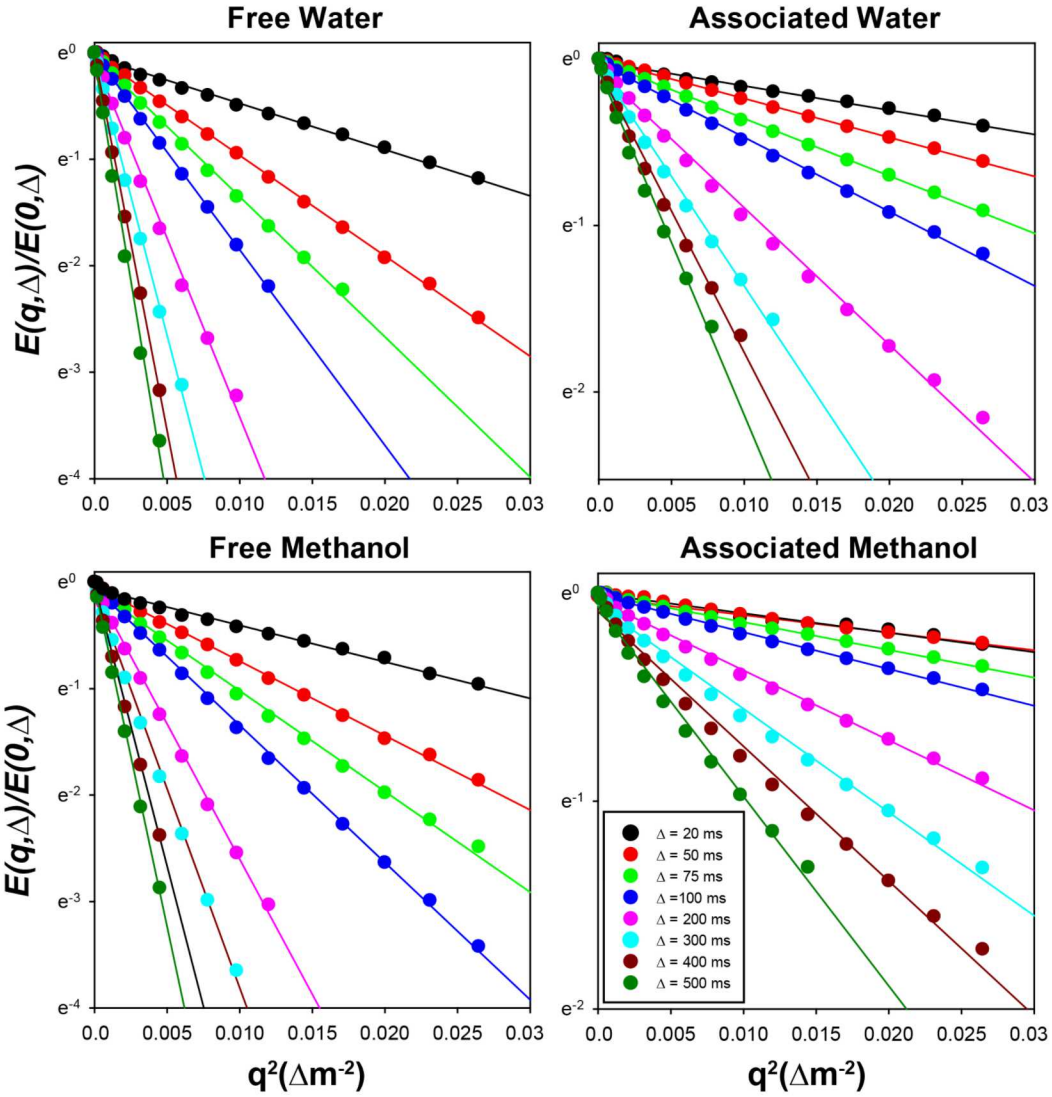

$$\left\langle R^2(\Delta)\right\rangle = -6\ln\left[E(q,\Delta)/E(0,\Delta)\right]/q^2$$

$$\left\langle R^2\right\rangle = 6Dt$$

$$\left\langle z_M^2(\Delta)\right\rangle = -2\ln\left[E(q,\Delta)/E(0,\Delta)\right]/q^2$$

$$\left\langle z_M^2\right\rangle = 2D_\alpha t^\alpha$$

- **Associated diffusion is an order of magnitude slower than free species (Water and MeOH).**
- **MeOH diffusion slower than Water in both environments.**
- **The ratio of D_{assoc}/D_{free} is much smaller for MeOH, suggesting preferential association with membrane.**

Todd M. Alam and Michael R. Hibbs, "Characterization of Heterogeneous Solvent Diffusion Environments in Anion Exchange Membranes", *Macromolecules*, **47**, 1073-1084 (2014). http://dx.doi.org/10.1021/ma402528v

Anomalous Diffusion?

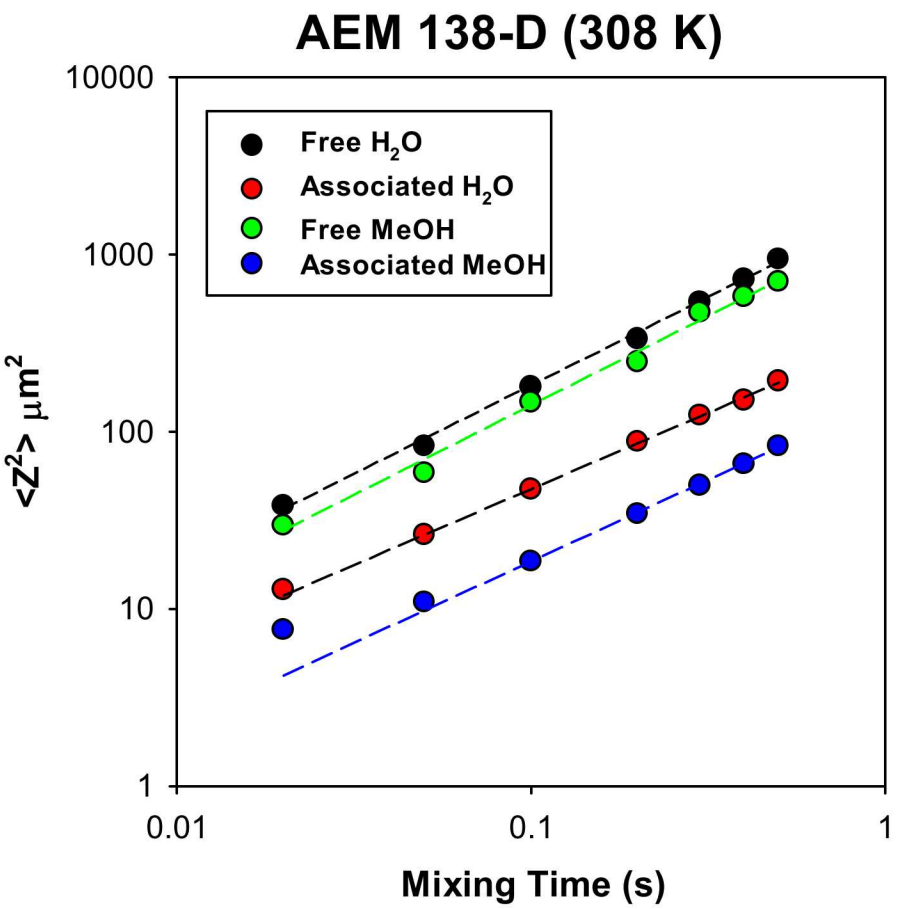

Anomalous diffusion can be expressed can be expressed through the power law.

$$\left\langle z^2 \right\rangle = 2D_\alpha \Delta^\alpha$$

α = 1, normal diffusion
α < 1, sub-diffusive
α ~ 0.7 2D fractal

Disappears with increasing temperature.

Diffusion Analysis of Individual Species

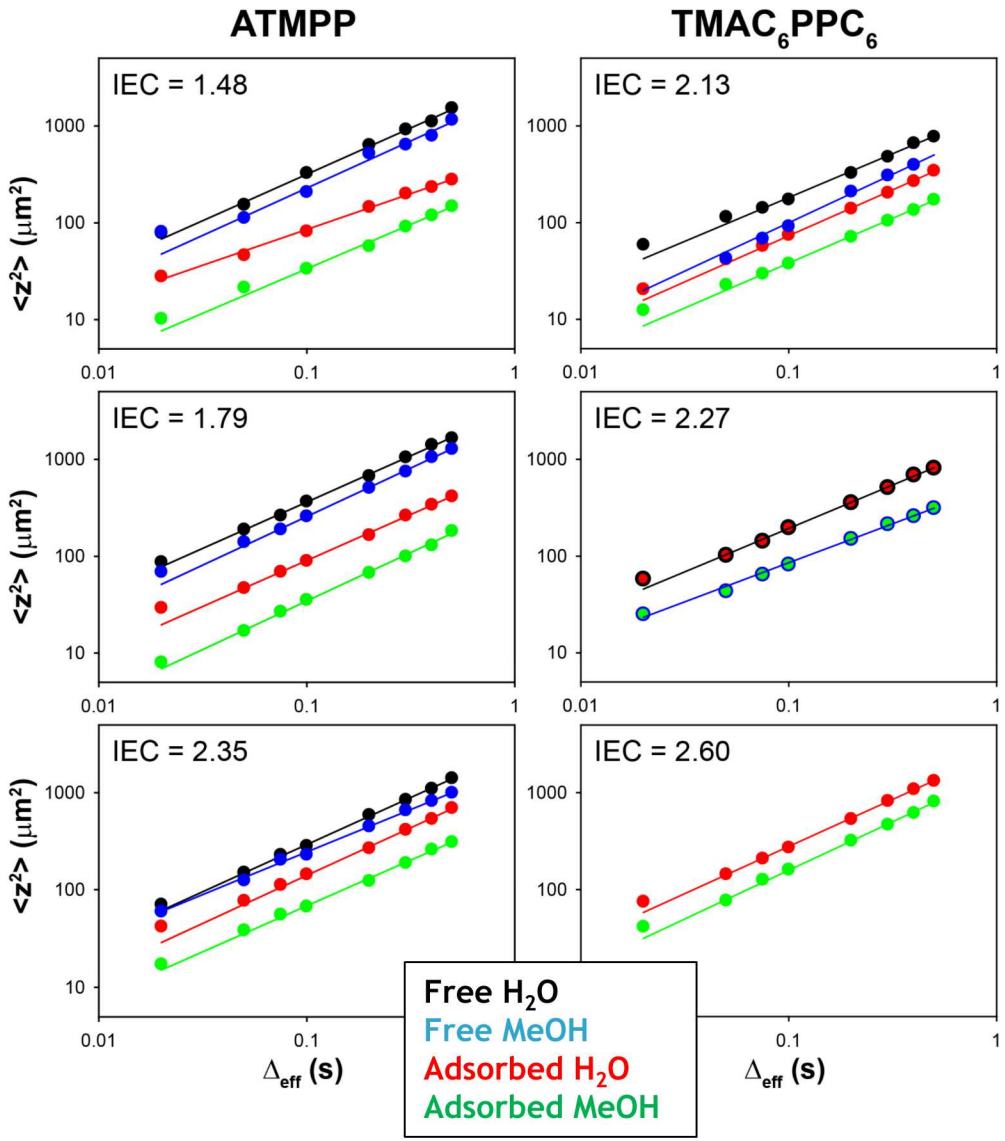

- Extract $\langle z^2 \rangle$ from multiple different Δ delays in PFG NMR
- Evaluate possibility of anomalous diffusion ($\alpha \neq 1$).
- Most systems show normal diffusion. As expected in these membranes.
- Associated water environment reveal fractal diffusion at lower hydration/temperatures.
- Activation energies (E_a) higher for associated species.

Todd M. Alam and Michael R. Hibbs, "Characterization of Heterogeneous Solvent Diffusion Environments in Anion Exchange Membranes", *Macromolecules*, **47**, 1073-1084 (2014). http://dx.doi.org/10.1021/ma402528v

Diverge…. In the time remaining

HRMAS PFG NMR

Solvent Diffusion in 3D Printed Advanced Manusfactured (AM) Materials

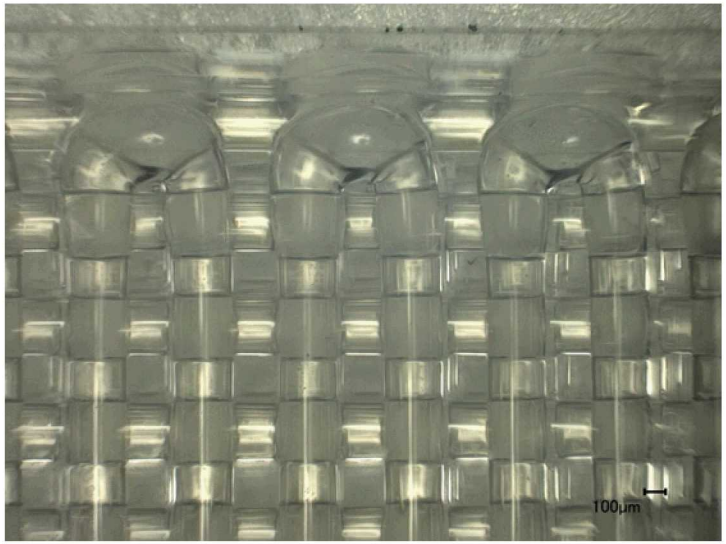

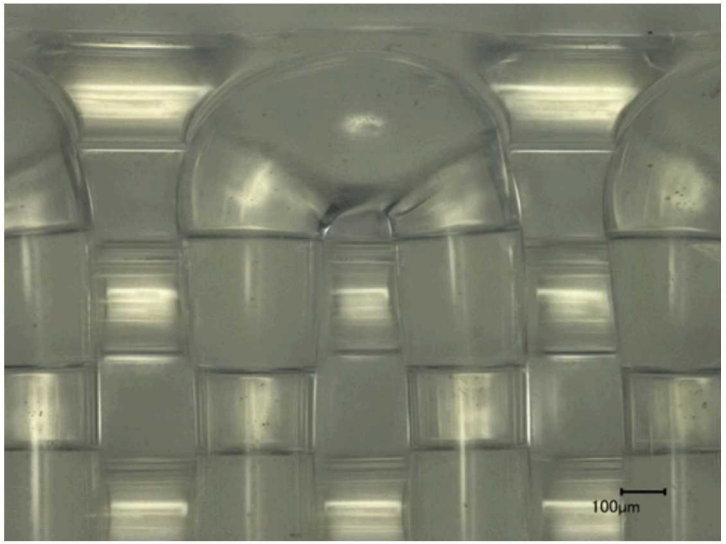

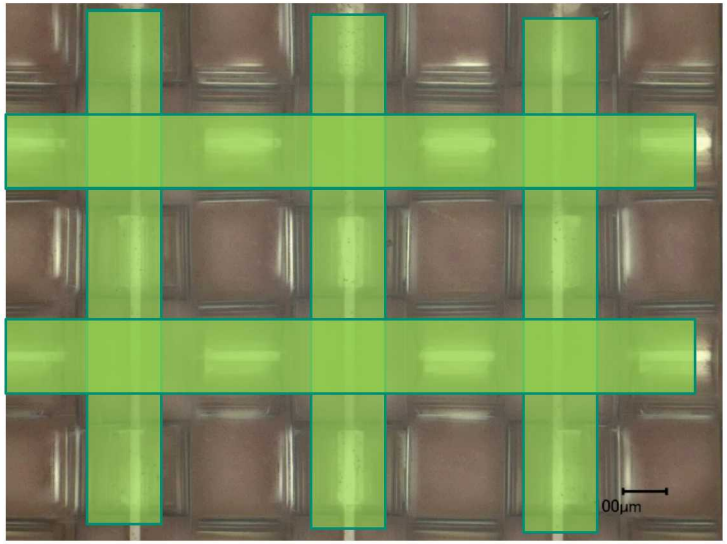

- Direct-write of Corning SE1700 siloxanes.
- Multi-layer (4 to 8 layers).
- Variable write and spacing (200 - 400 µm).
- Different cure protocol.
- *Diffusion of different penetrants?*

Penetrant Diffusion in 3D Printed Silicones

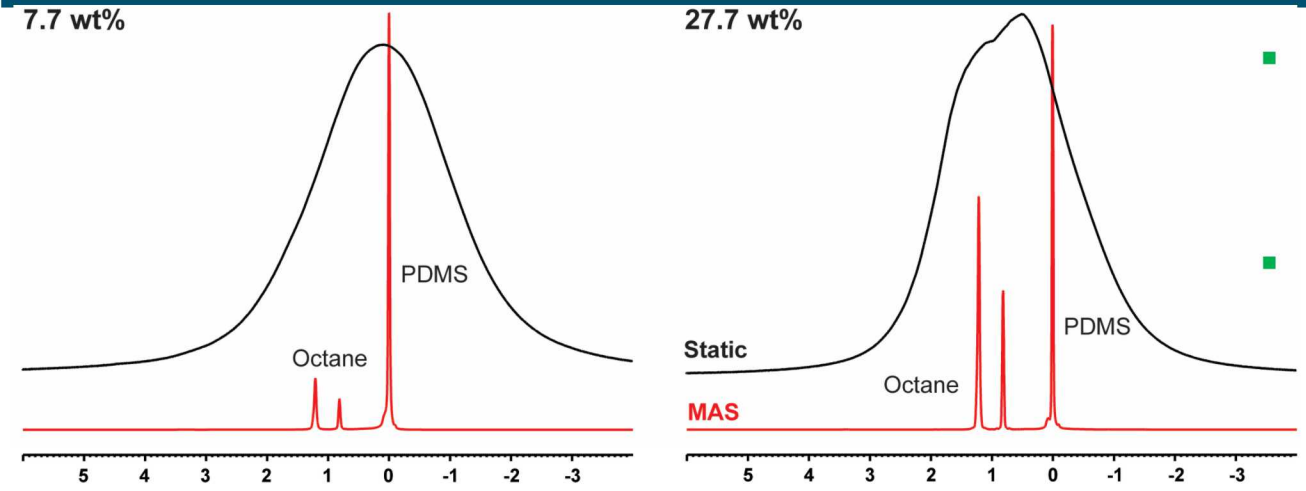

- HRMAS NMR allows resolution of penetrant diffusion.
- Especially at low swelling concentrations (Q).

Dow Corning SE1700

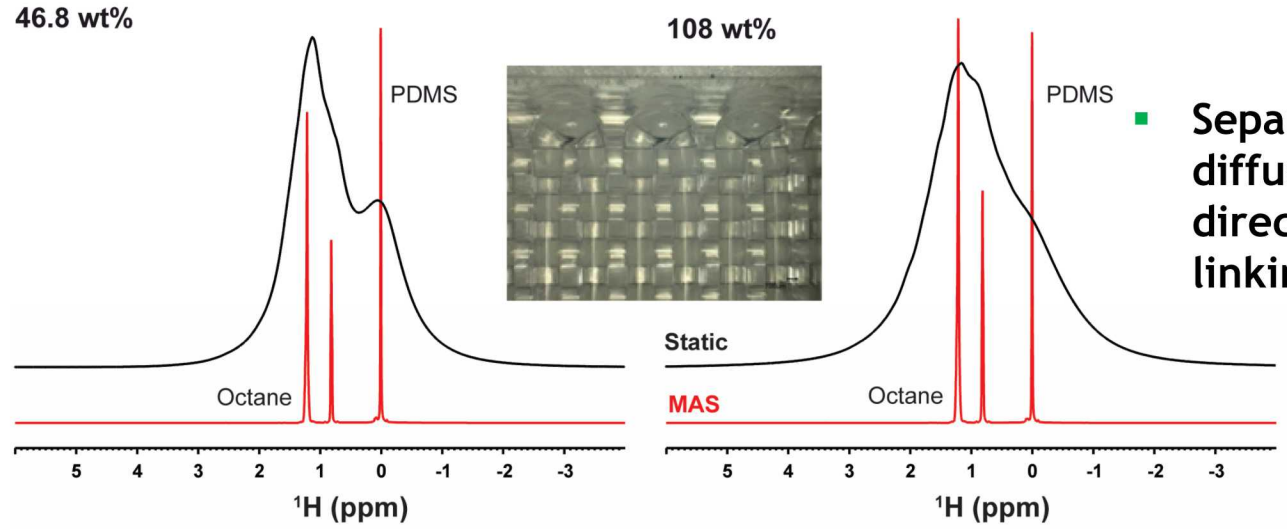

- Separation in static PFG NMR diffusion experiments impacted directly by degree of PDMS cross-linking.

Overlap in Diffusion Signal Decay

HRMAS NMR PFG Diffusion

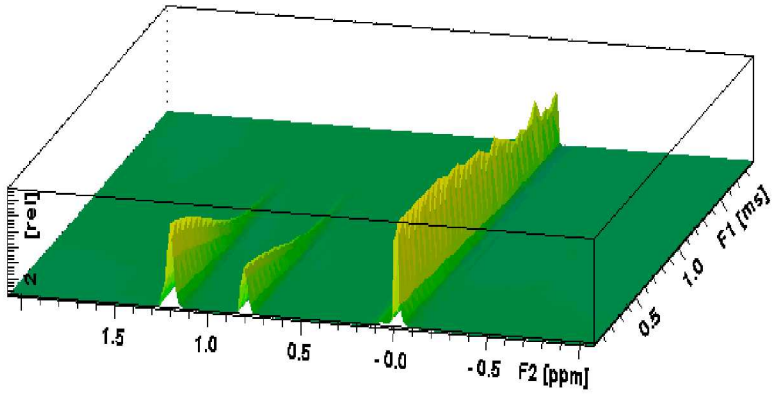

- No need to separate/extract slowly decaying siloxane signal from mobile octane penetrant.

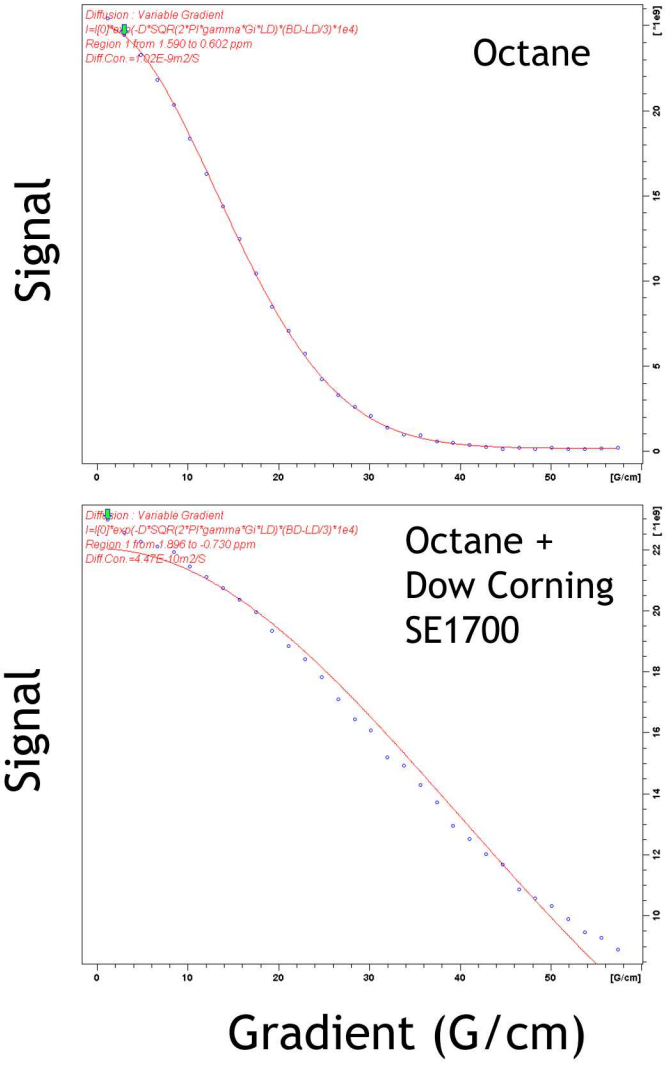

Diffusion of Penetrants in Polymers

Linear PDMS

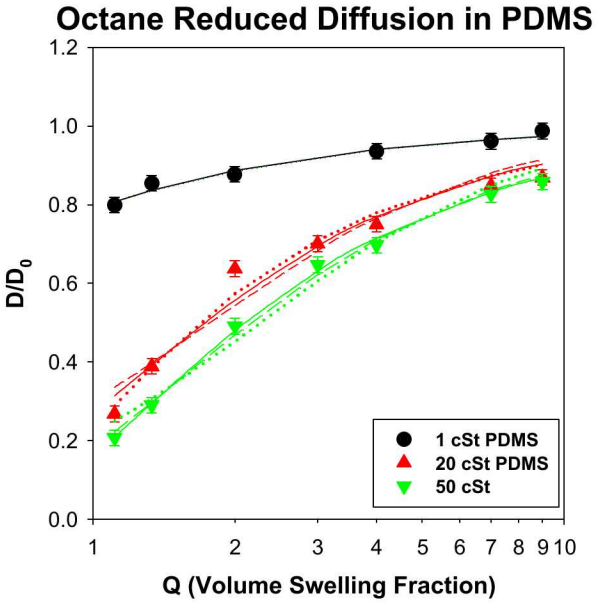

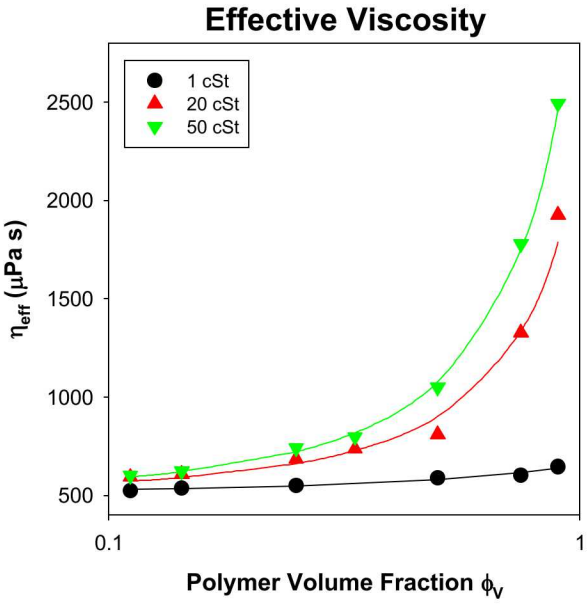

- Diffusion is dependent on concentration of penetrant!
- Behavior varies with the polymer/penetrant system.
- "Local" effective viscosity can extracted from D/D_0.

Fujita (Free Volume)

$$\frac{D}{D_0} = \exp\left\{\frac{-B\left(f_s - f_p\right)}{\left(Q-1\right)f_s^2 + f_s f_p}\right\}$$

$$Q = \frac{1}{\varphi_p} = \frac{V}{V_0} = \frac{\left(V_s + V_p\right)}{V_p}$$

Phillies (Stretch Exponential)

$$\frac{D}{D_0} = \exp\left\{-\alpha Q^{-v}\right\}$$

Petit (Hydrodynamic)

$$\frac{D}{D_0} = \frac{1}{1+\alpha Q^{-2v'}}$$

$$D = kT/\zeta$$

[1] Vrentas, Duba (1977) *J. Polym. Sci.*, **126**, 177-186. [2] Phillies, (1989) *J. Phys. Chem.*, **93**, 5029-5039.
[3] Petit, Roux, Zhu, MacDonald (1996), *Macromolecules*, **29**, 6031-6036.

Diffusion of 3D Printed Siloxanes

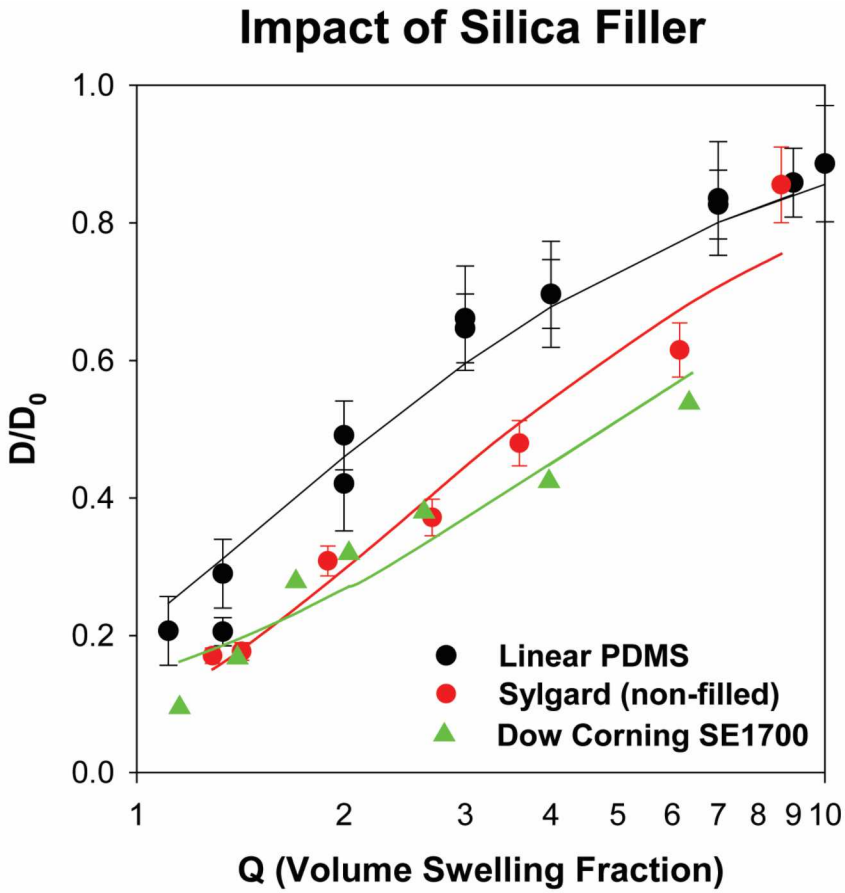

- Reduction diffusion in filled PDMS is present.
- Differences increase with degree of swelling.

Diffusion of 3D Printed Siloxanes

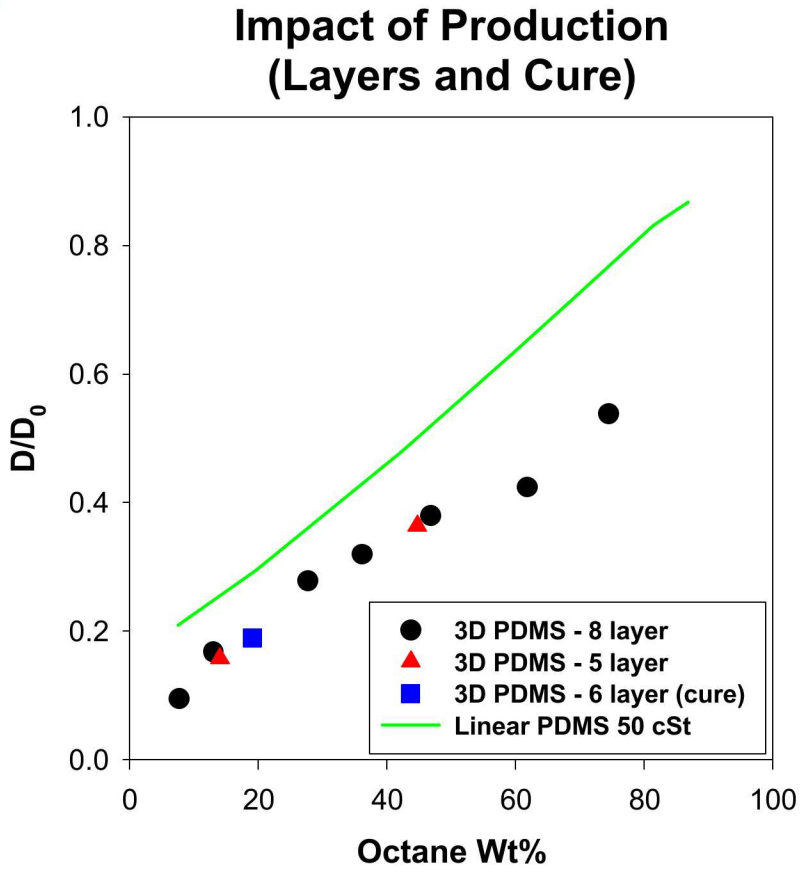

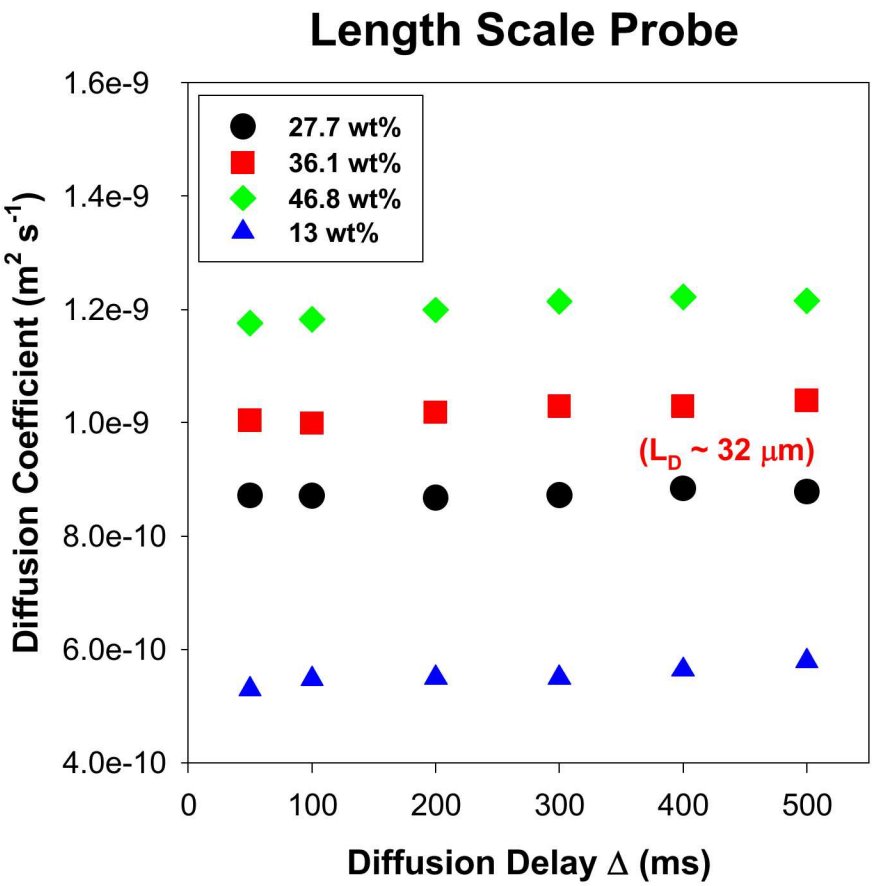

- No impact on number of direct-write layers on overall diffusion.
- No restricted diffusion on 10-50 μm length scale (homogeneous diffusion).
- Diffusion is not the answer to the residual stress effects (….layer gradient….)

Penetrant Mixtures in Swollen Siloxanes

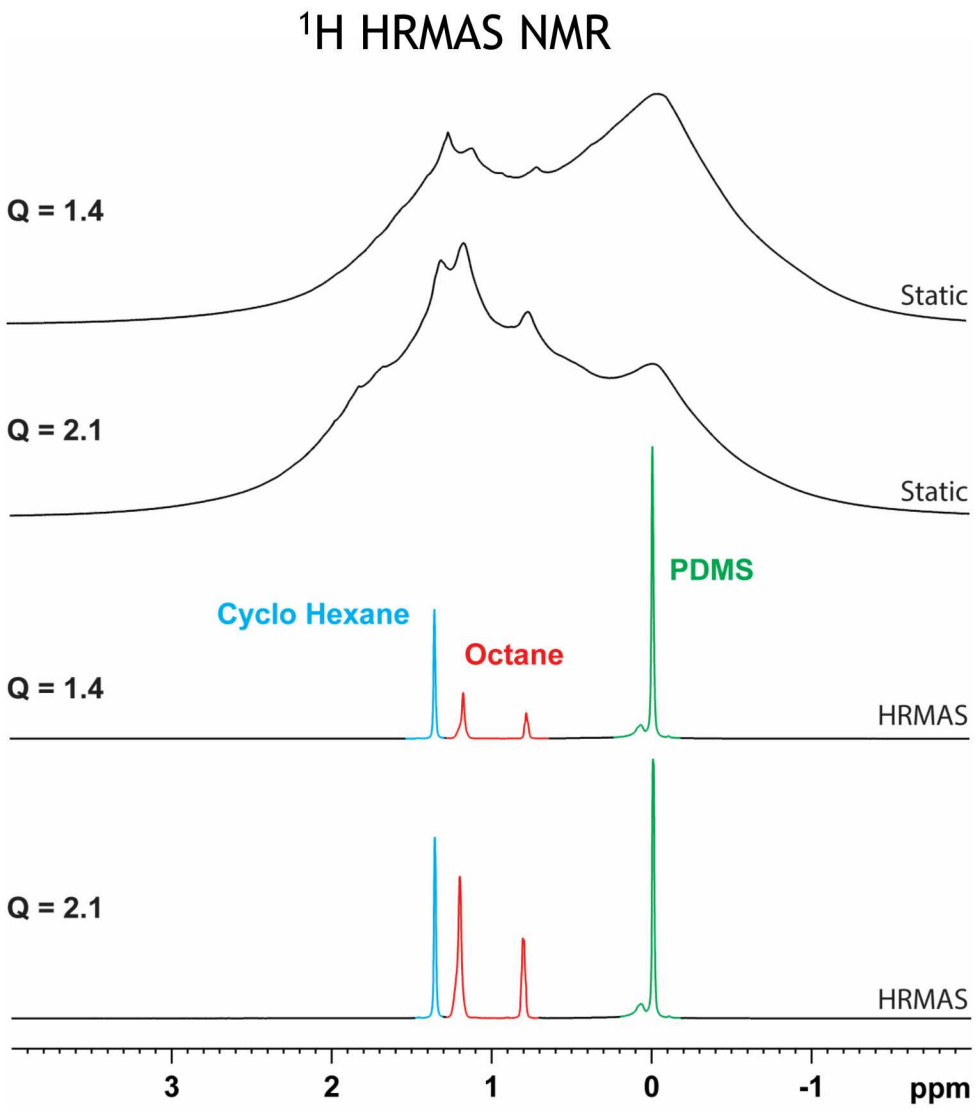

- Different penetrants are unresolved under static conditions.
- Well resolved under HRMAS allowing individual diffusion constants to be measures.
- Also reveals differential PDMS species in swollen material.

Diffusion for Penetrant Mixtures

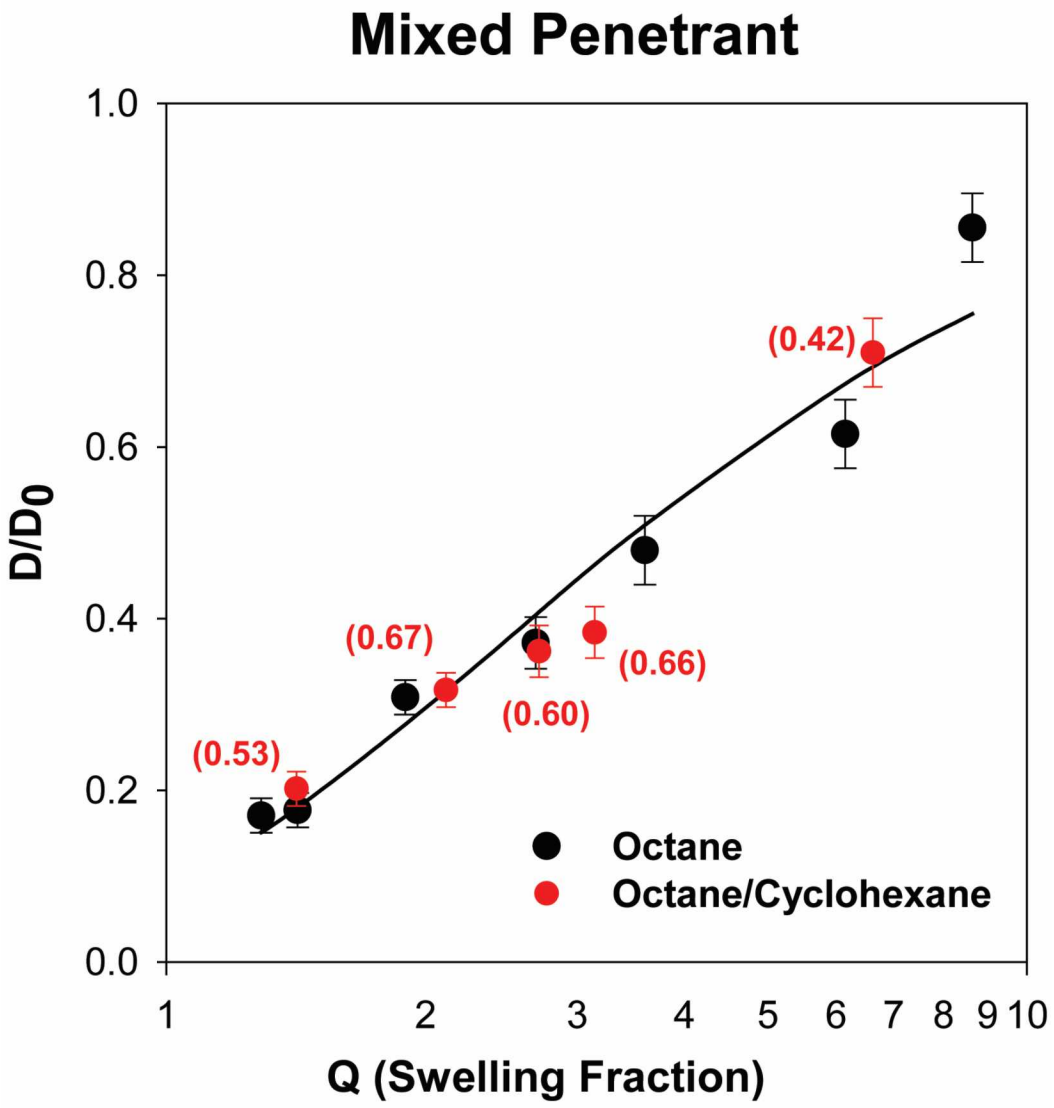

- Diffusion of penetrants not strongly impact by solvent fraction [octane/(octane+cyclohexane).
- Diffusion well described by simple free volume description.
- *Need to investigate non-ideal solvent mixtures to identify preferential surface interactions.*

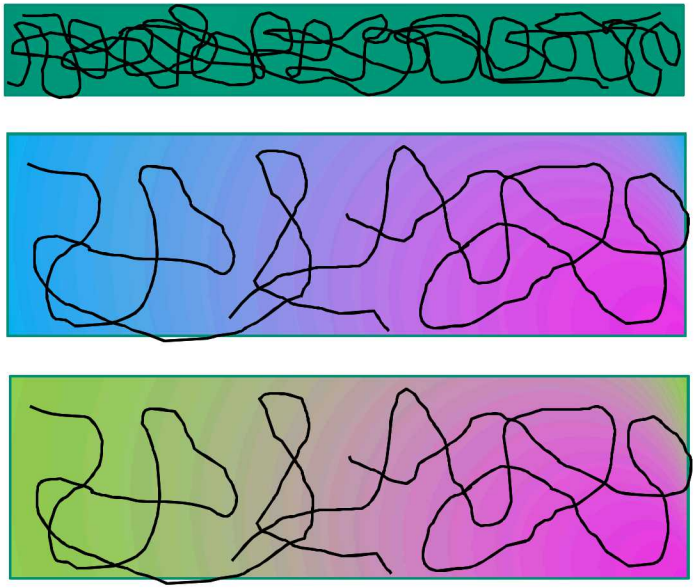

Resolution in Nanoporous Membrane Polymer Composites

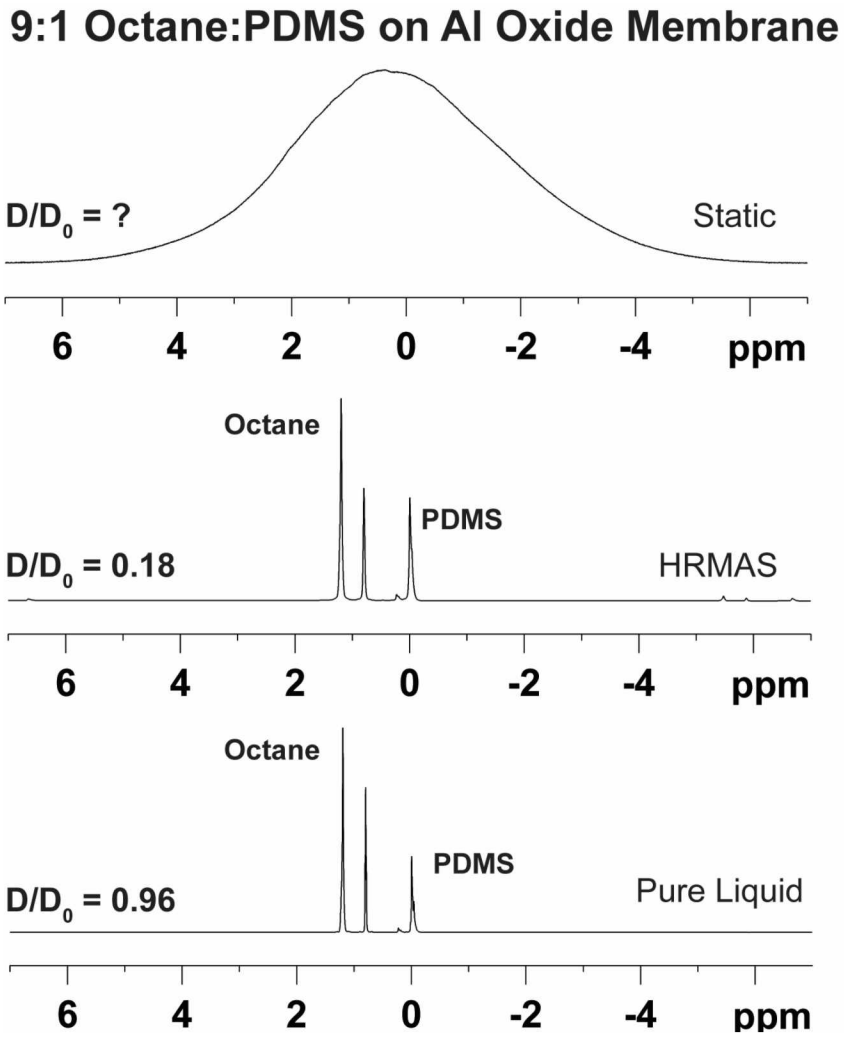

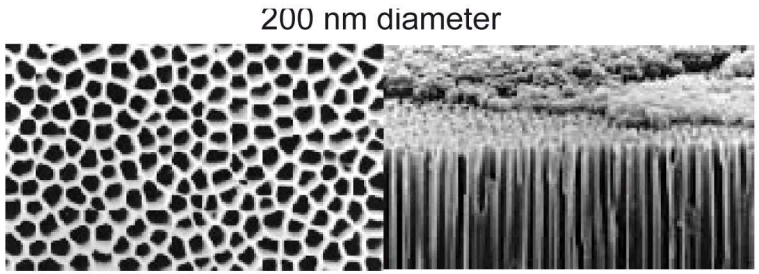

- Example of surface interactions and confinement impacting diffusion.
- Adsorption into Al oxide membrane reduces diffusion of octane by a factor 5.
- Not a simple free volume effect!

HRMAS NMR Diffusometry in Materials

- "Identification of Multiple Diffusion Rates in Mixed Solvent Anion Exchange Membranes Using High Resolution MAS NMR", *ACS Macro Letters*, **1**, 910-914 (2012).
- "Characterization of Heterogeneous Solvent Diffusion Environments in Anion Exchange Membranes", *Macromolecules*, **47**, 1073-1084 (2014)

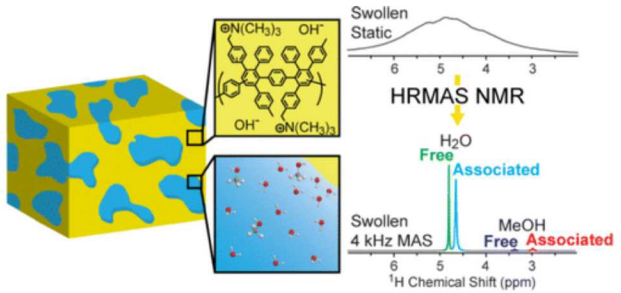

- "Characterization of Free, Restricted and Entrapped Water Environments in Poly(N-Isopropyl Acrylamide) Hydrogels via ^{1}H HRMAS PFG NMR Spectroscopy", *J. Polymer Science: Polymer Physics*, **52** 1521-1527 (2014).

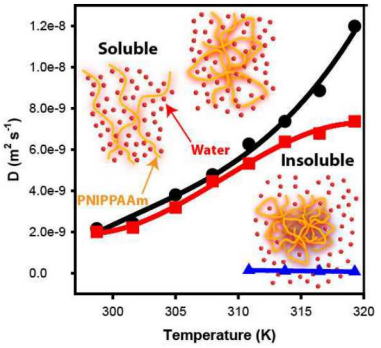

- "The Effect of Curvature on the Dynamic and Diffusional Properties of Phospholipids on Silica Materials using HRMAS NMR", *In Preparation*

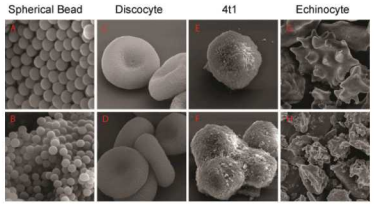

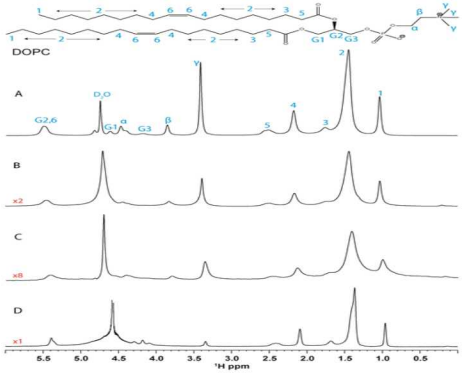

- "Measuring In-Pore Diffusion of Carbonate Solvent Mixtures in Nanoporous Carbon", *Chem. Phys. Lett*, **658**, *51-57*(2016).

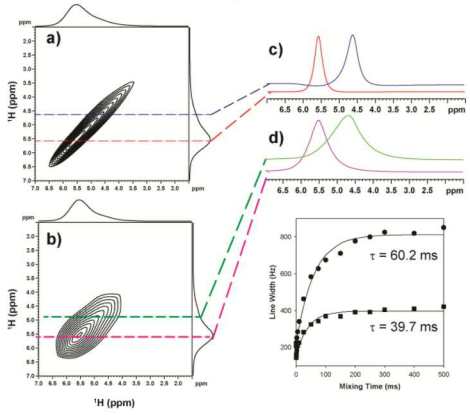

Diffusion in Nanoporous Membrane Polymer Composites (20 nm)

Reduced Diffusion in Aluminum Oxide Membranes

$$\zeta_{avg} = \frac{V_{surf}\zeta_{surf} + V_{free}\zeta_{free}}{\left(V_{surf} + V_{free}\right)}$$

Reduction due to polymer free volume

Reduction (PDMS) due to surface induced friction

Reduction due to surface induced friction

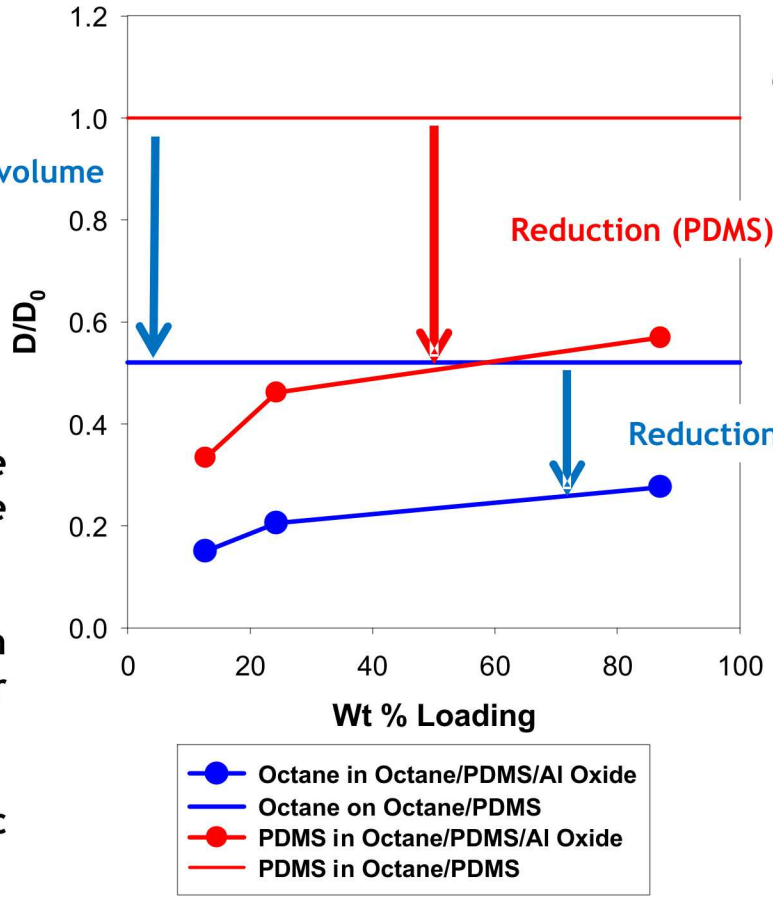

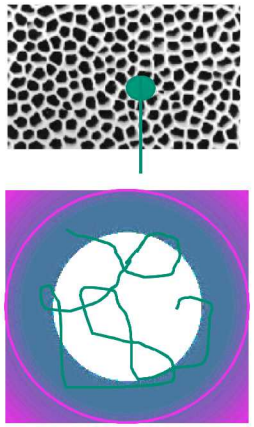

- Cleary an impact of the confinement near the surface.
- Ratio of surface friction reduction similar for PDMS and Octane.
- Not resolvable in static PFG experiment.

Grotthuss Mechanism

Grotthuss Mechanism

Proton_Zundel.gif

Ab Initio Calculations
Water Adsorption Energies & Hydrogen Bonding Types

$$\Delta E_{\text{Ads}}^{\text{Opt}} = E\left(\text{Clutser}+n\text{H}_2\text{O}\right) - E^{\text{Opt}}\left(\text{Cluster}\right) - \sum_{i=1}^{N} E^{\text{Opt}}\left(\text{H}_2\text{O}\right)$$

DFT 6-311**

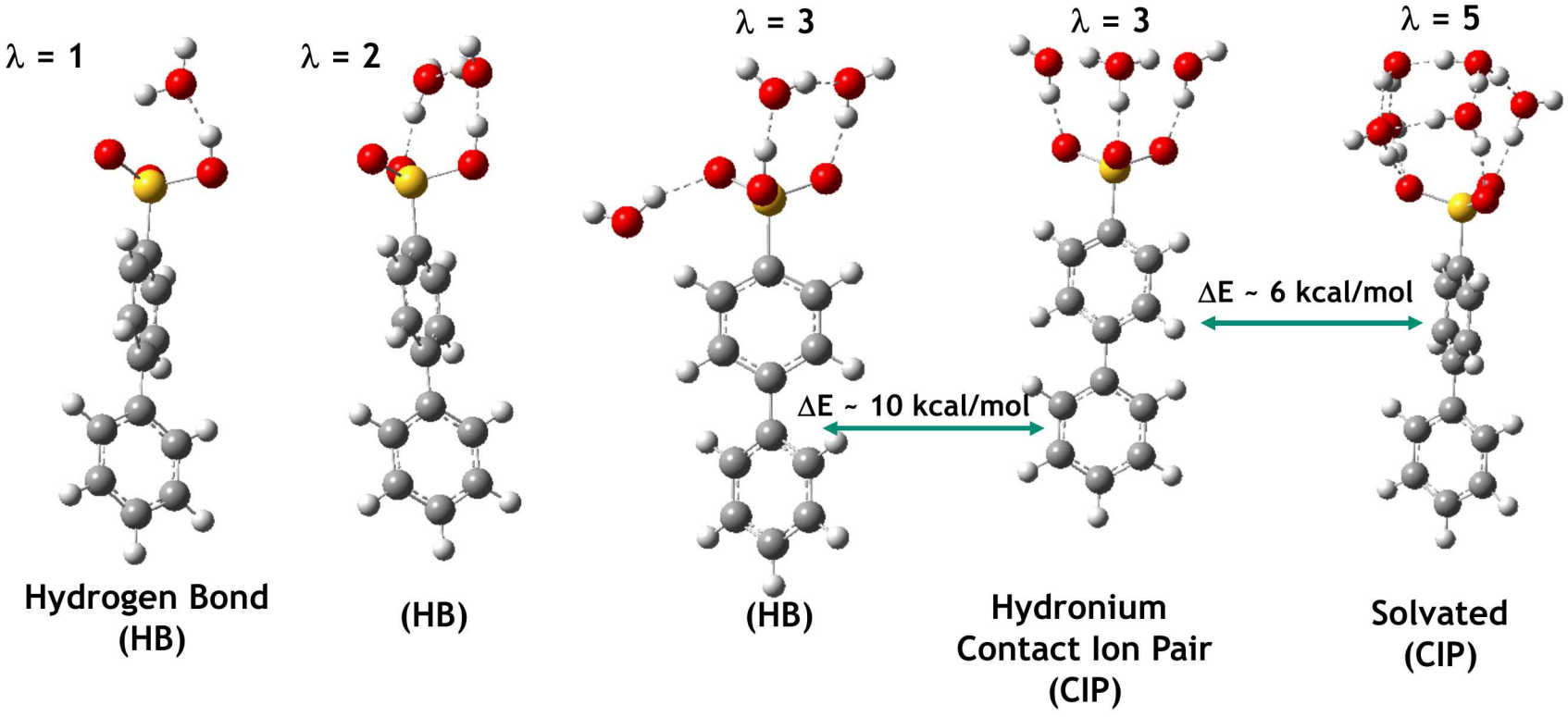

For small clusters very limited structural impact!

T. M. Alam "Ab Initio Study of Sulfonic Acid Micro-Hydration in Sulfonated Diels Alder Poly(Phenylene) Polymers", J. Phys. Chem. C (2018) *Submitted*

Large Water/Acid Clusters (from MD Simulations)

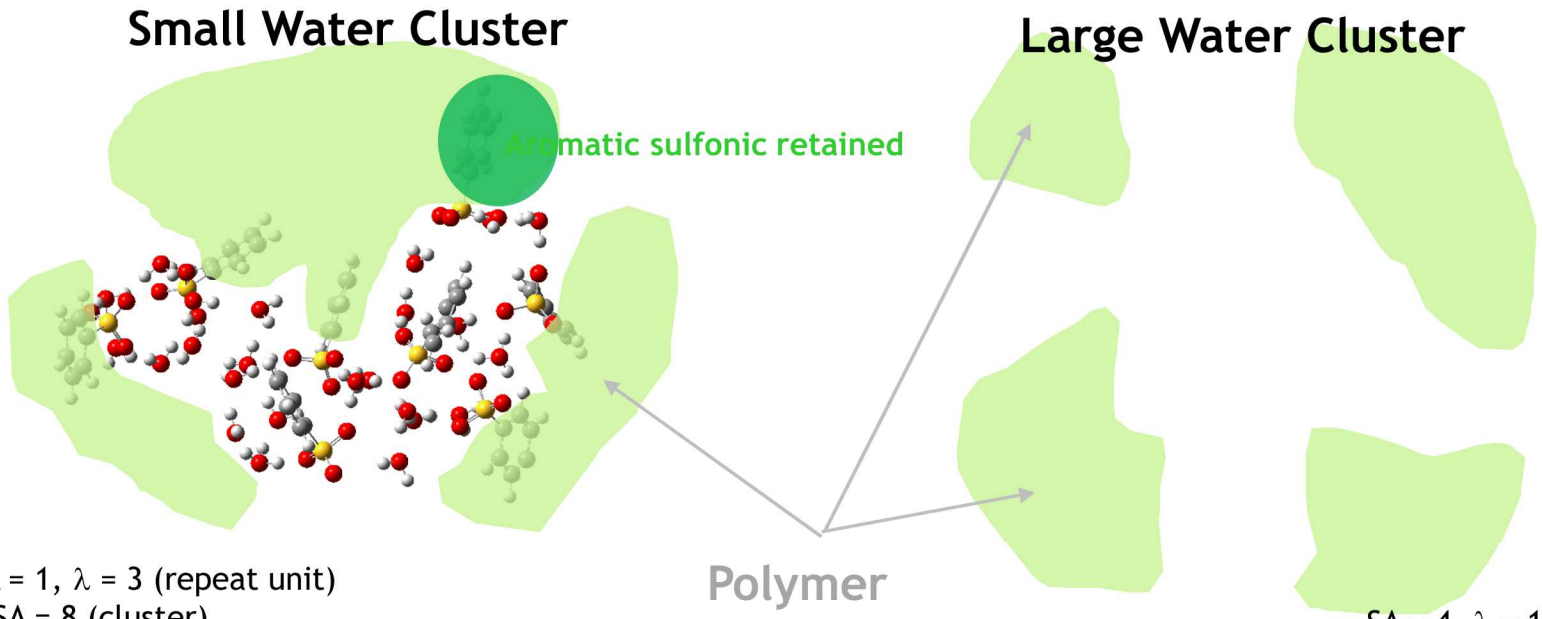

SA = 1, λ = 3 (repeat unit)
# SA = 8 (cluster)
17 H_2O, 8 H_3O^+
Gyration = 7.6 Angstroms

SA = 4, λ = 10 (repeat unit)
# SA =11 (cluster)
42 H_2O, 11 H_3O^+
Gyration = 7.7 Angstroms

Adsorption energies determined for each individual H_2O/H_3O^+

$$\Delta E_{\text{Ads}}^{Total} = \Delta E_{Ads}^{H_3O^+} + \Delta E_{Ads}^{H_2O} = \sum_{j=1}^{n} \Delta E_{Ads}^{H_3O^+}(j) + \sum_{i=1}^{m} \Delta E_{Ads}^{H_2O}(i)$$

$$\Delta E_{\text{Ads}}^{H_2O}(i) = E\left(\text{Cluster}\left[m\text{H}_2\text{O}\right]\right) - E\left(\text{Cluster}\left[(m-1)\text{H}_2\text{O}(i)\right]\right) - E^{Opt}\left(\text{H}_2\text{O}\right)$$

$$\Delta E_{\text{Ads}}^{H_3O^+}(j) = E\left(\text{Cluster}\left[n\text{H}_3\text{O}^+\right]\right) - E\left(\text{Cluster}\left[(n-1)\text{H}_3\text{O}^+(\text{j})\right]\right) - E^{Opt}\left(\text{H}_3\text{O}^+\right)$$

T. M. Alam "Ab Initio Study of Sulfonic Acid Micro-Hydration in Sulfonated Diels Alder Poly(Phenylene) Polymers", J. Phys. Chem. C (2018) *Submitted*

Adsorption Energies
Large Water/Acid Clusters from MD Simulations

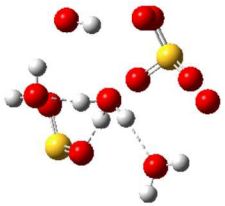

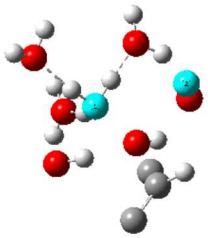

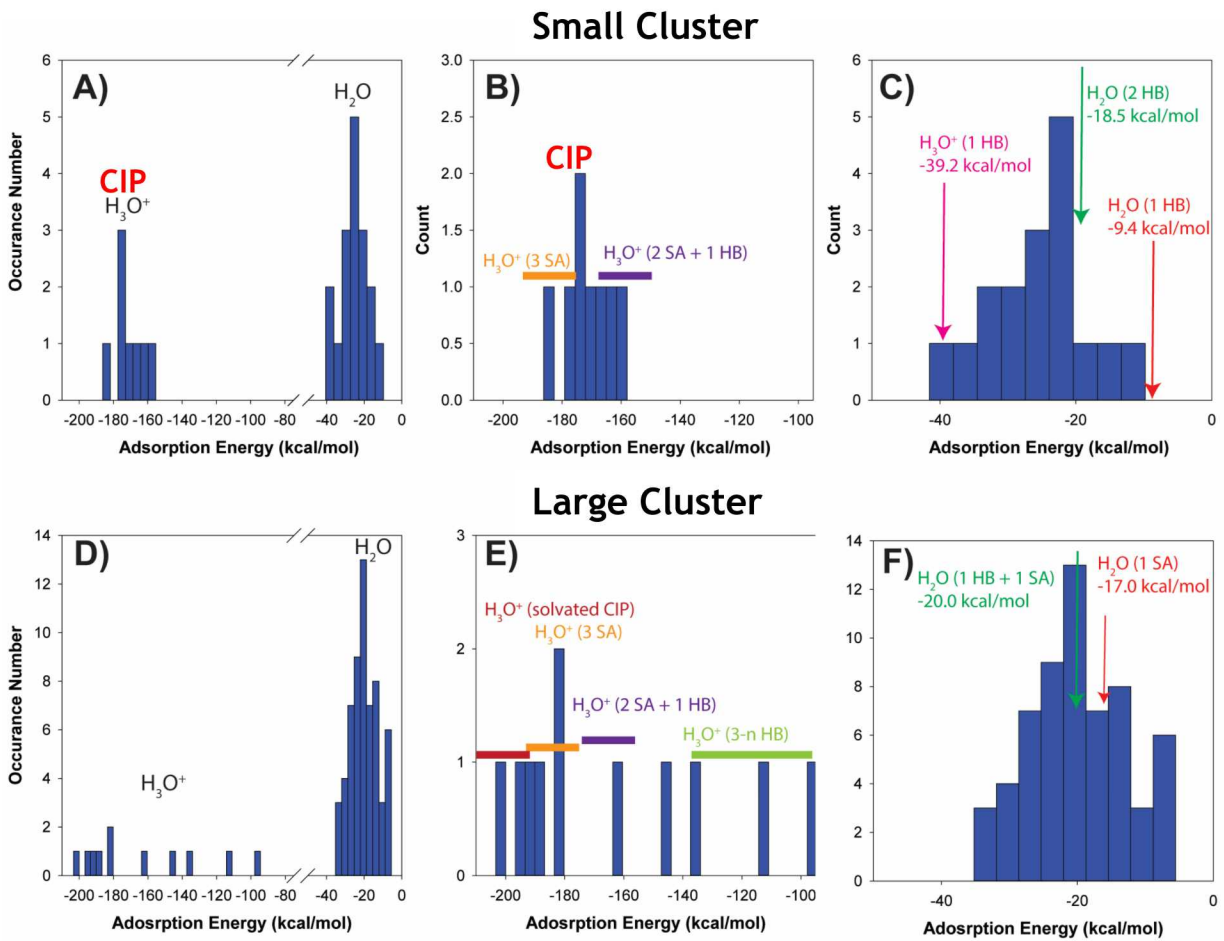

Todd M. Alam, "Computational Study of Microhydration in Sulfonated Diels-Alder Poly(phenylene) Polymers", J. Phys. Chem. A, 122, 3927-3938 (2018). DOI: 10.1021/acs.jpca.8b01354

- Increasing hydration allows formation of solvate CIP – large adsorption energy.
- Inter-chain coordination of H_2O/H_3O^+ important!
- This driving force counteracted by chain energetics maximizing all HB interactions.

^{1}H Magic Angle Spinning (MAS) NMR

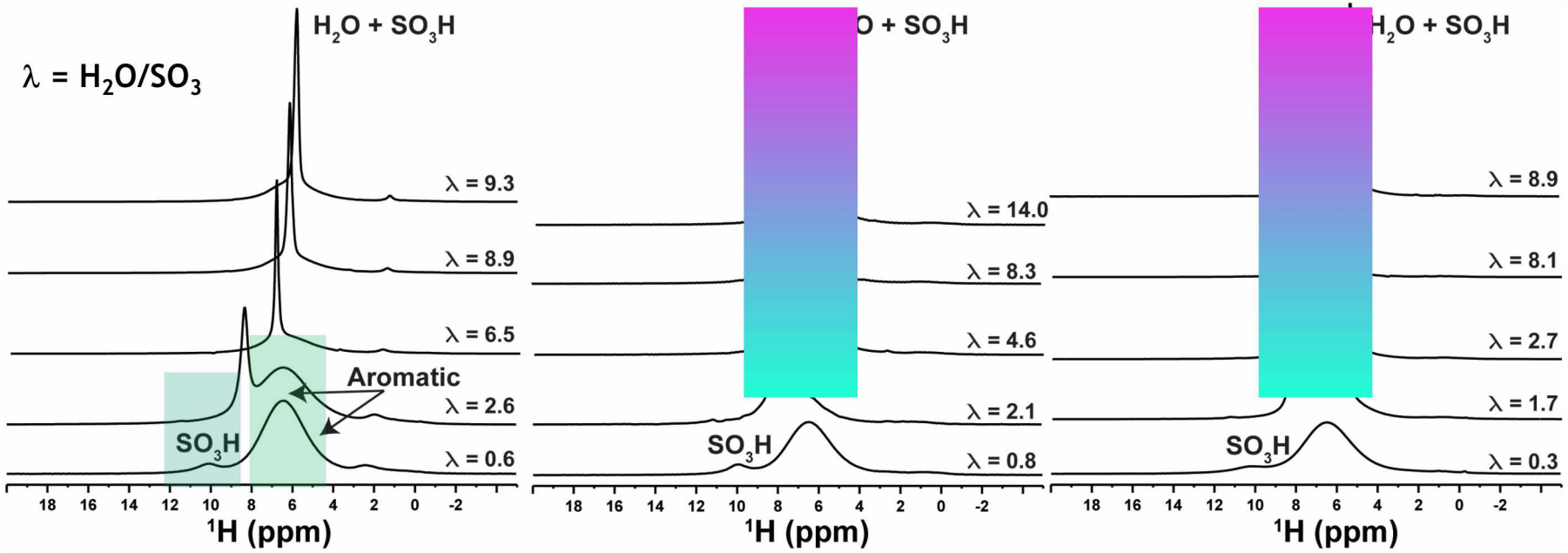

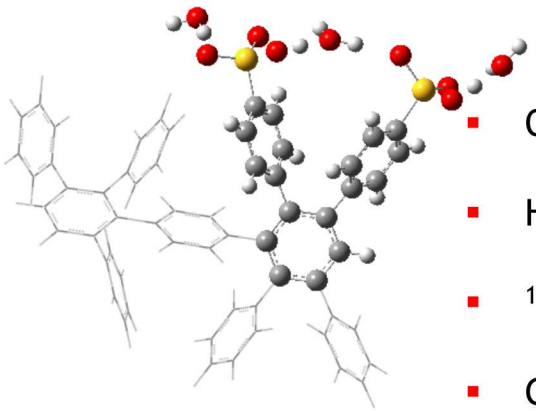

- Only 3 ^{1}H environments (aromatic, H_2O, SO_3H).
- H_2O+SO_3H in rapid exchange (single resonance)
- ^{1}H NMR chemical shift reflects relative concentration of SO_3^- coordination.
- Can chemical shift be related to “average” hydrogen bond strength?
- Similar information from IR?

Chemical Shift Hydrogen Bond Stength Correlations

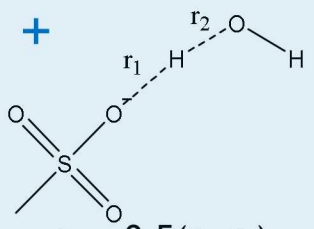

$q_1 = 0.5(r_1 - r_2)$

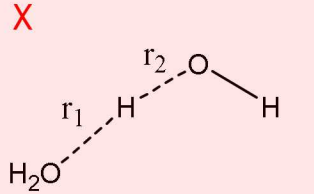

$q_1 = 0.5(r_1 - r_2)$

$$\delta(^1\mathrm{H}) = a + b\exp\left[-cq_1^2\right]$$

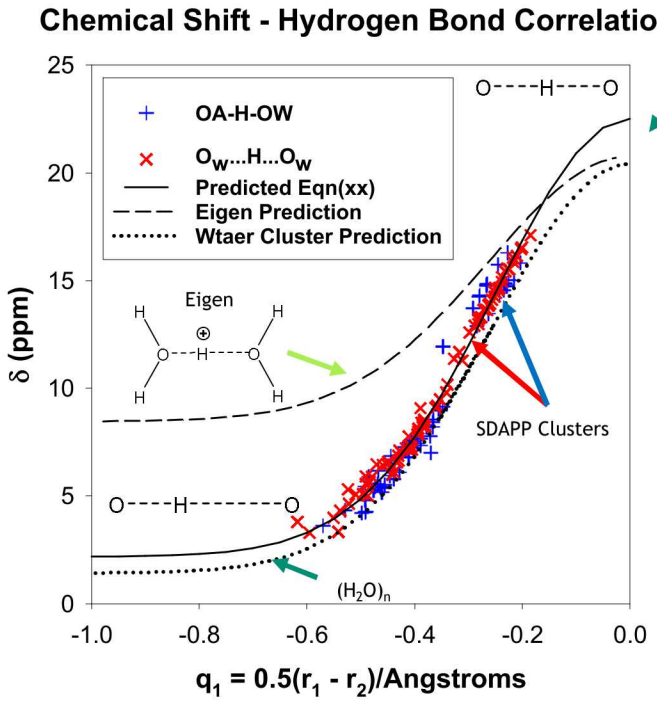

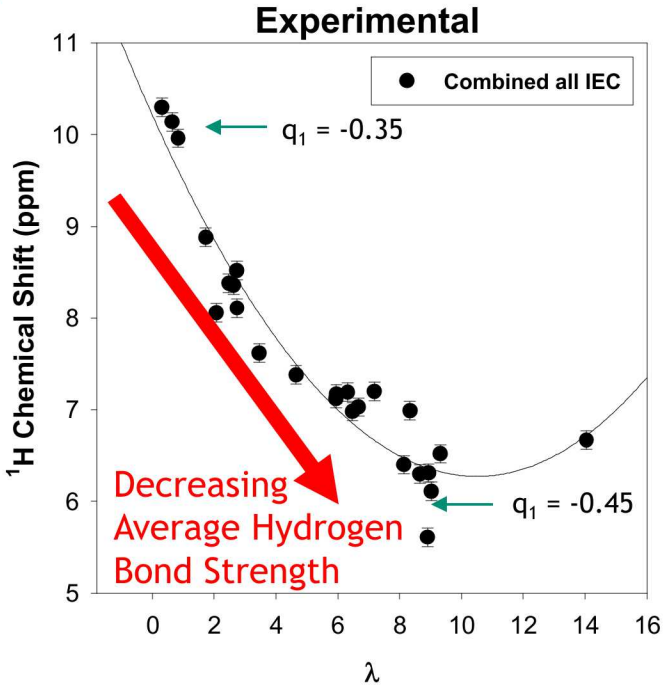

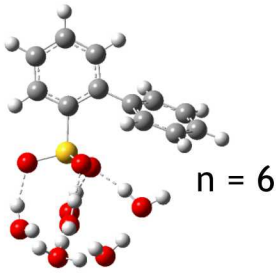

- *Ab initio* ^{1}H chemical shift calculations for all SDAPP $_n(H_2O)$ clusters (n = 1 to 6).
- Correlations follow definition of Limbach and company.
- Experimental is a dynamic average over all H environments, but provides a measure of the changing hydrogen bond strengths with hydration.
- Reduction in hydrogen bond strength → increase in Grotthuss mechanism (proton defect).

H.-H. Limbach, P. M. Tolstoy, N. Perez-Hernandez, J. Guo, I. G. Shenderovich, G. S. Denisov, "OHO Hydrogen Bond Geometries and NMR Chemical Shifts: From Equilibrium Structures to Geometric H/D Isotope Effects, with Application for Water, Protonated Water and Compressed Ice", *Israel J. Chem.*, **49**, 199-216 (2009).

Activation Energies

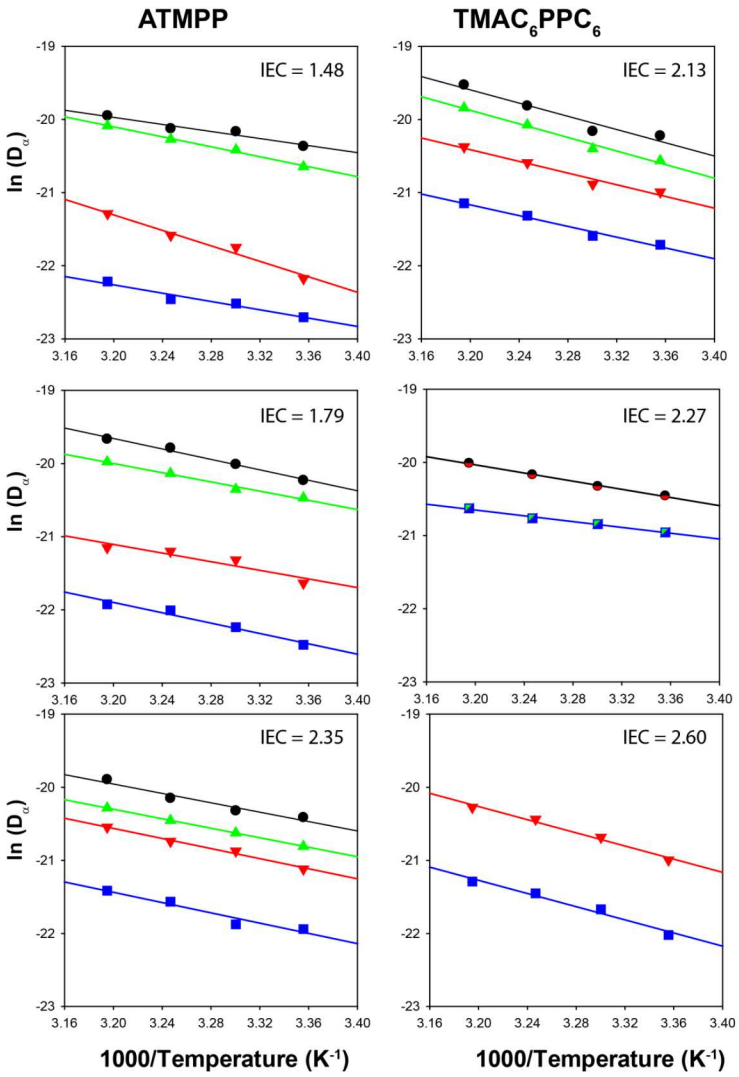

Sample (IEC)	E_a (kJ/Mol)			
	F-H_2O	A-H_2O	F-MeOH	A-MeOH
1N MeOH	26.0	--	27.0	--
ATMPP (1.48)	20.0		28.3	23.6
ATMPP (1.79)	29.7	24.5	26.2	29.4
ATMPP (2.35)	26.7	28.7	27.0	29.2
$TMAC_6PCC_6$ (2.13)	37.6		38.6	30.6
$TMAC_6PCC_6$ (2.27)	--	23.2	--	16.5
$TMAC_6PCC_6$ (2.60)				

- Results similar to Nafion and Nafion composites.
- No direct comparison because individual water environments not investigated.

NMR Spin Diffusion Analysis

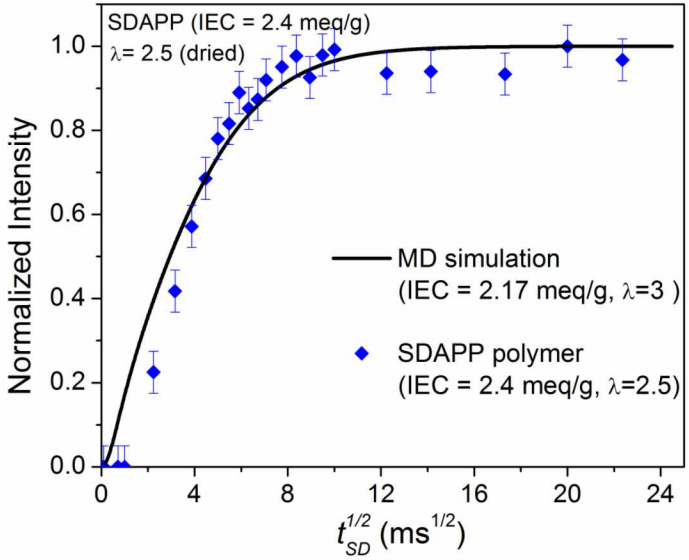

Proportion to Interface Surface Area

Density & Volume Fraction

Very structure/model specific

$$\frac{M_B(t_{SD})}{M_B(t_{SD}\to\infty)} \approx \frac{S}{V_{total}}\sqrt{t_{SD}}\,\frac{2}{\sqrt{\pi}}\left(\frac{\rho_{HA}\phi_A+\rho_{HB}\phi_B}{\phi_A\phi_B}\right)\left[\frac{\sqrt{D_AD_B}}{\rho_{HA}\sqrt{D_A}+\rho_{HB}\sqrt{D_B}}\right]-O\left(\sqrt{t_{SD}}^2\right)$$

Spin Diffusion Constants

$$d = 2\varepsilon\phi_B\frac{V_{total}}{S}$$

For Simple Models Related to Domain Size

^{13}C MAS NMR - Looking for Dynamics…

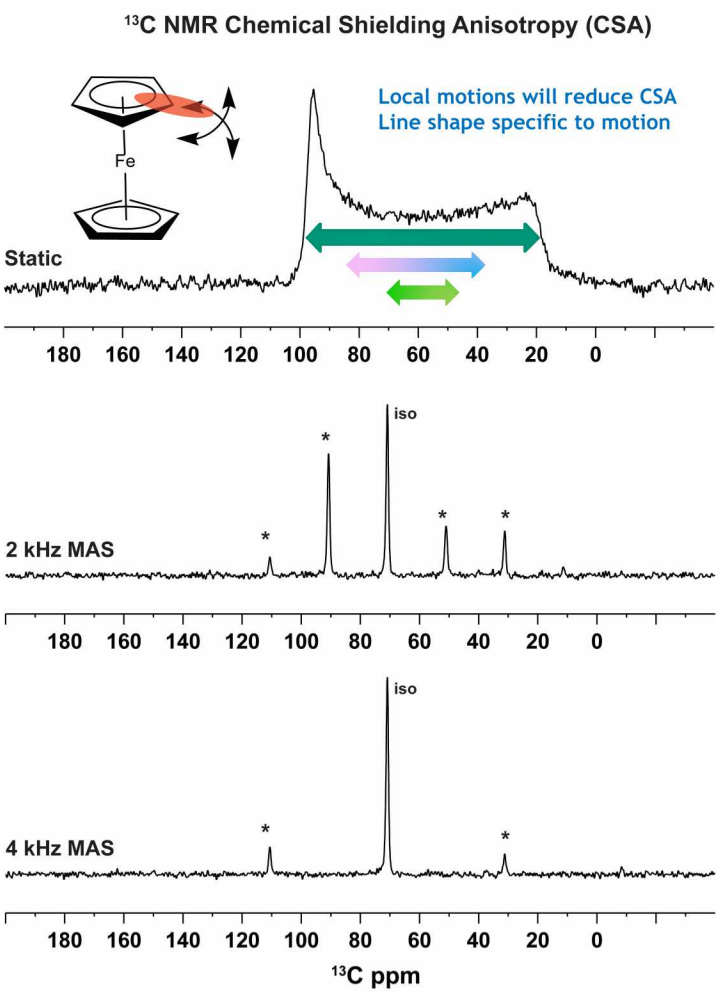

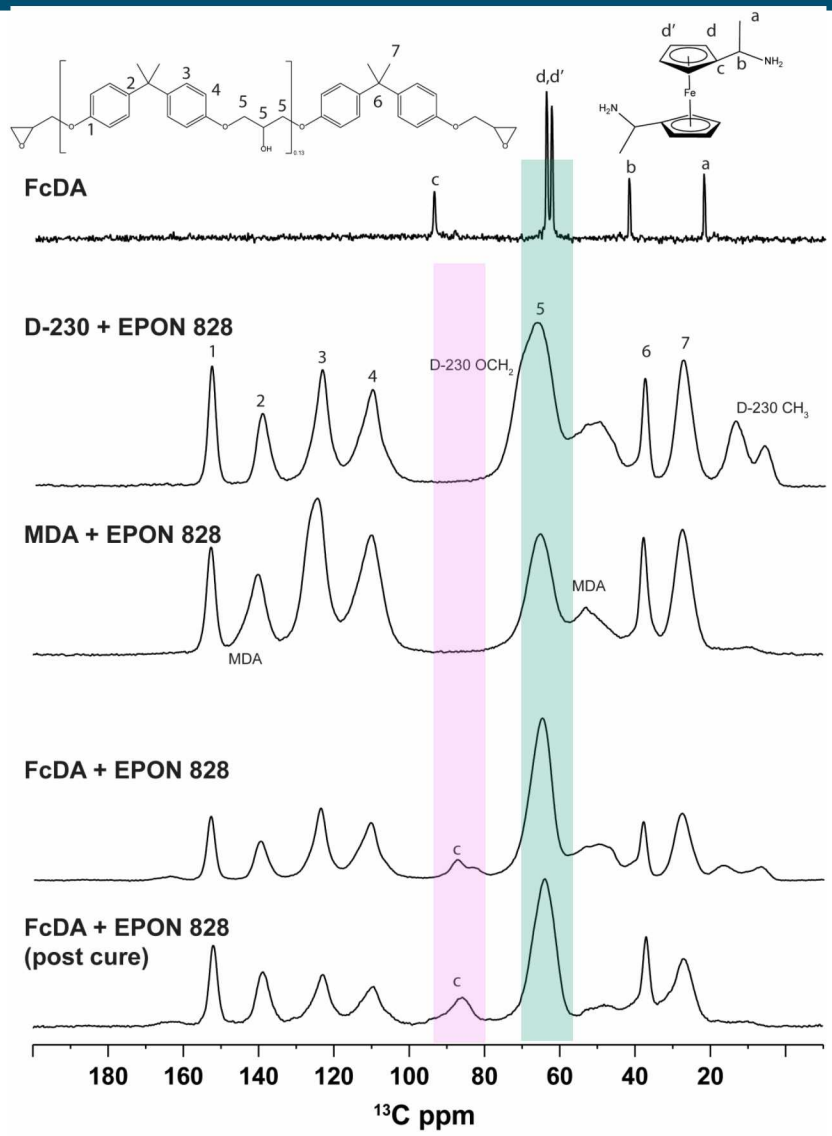

Solution ^{13}C NMR Reveals Multiple Conformers

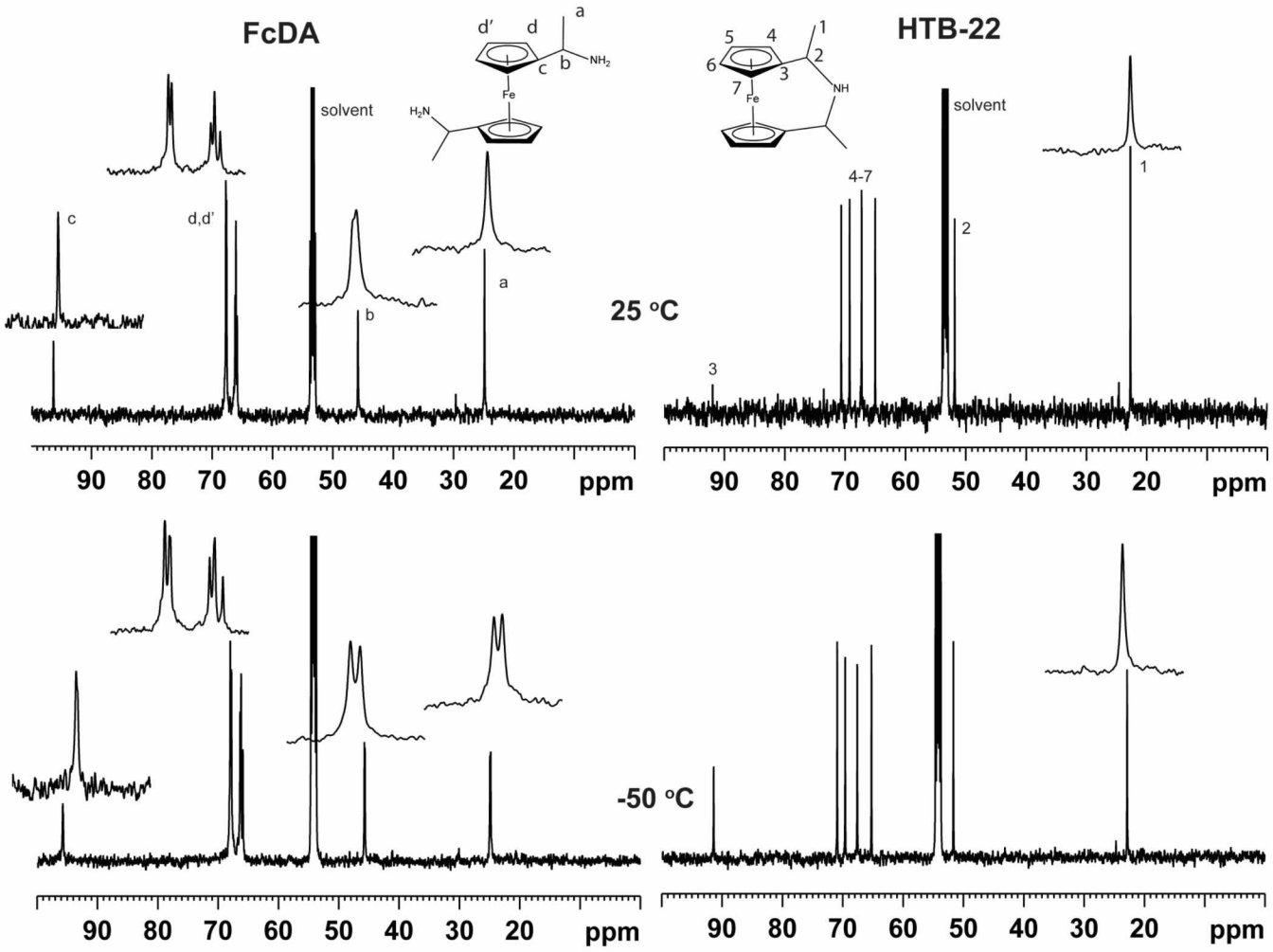

^{1}H NMR - DQ NMR During Cure

Cure Kinetics Followed by Segmental Topology

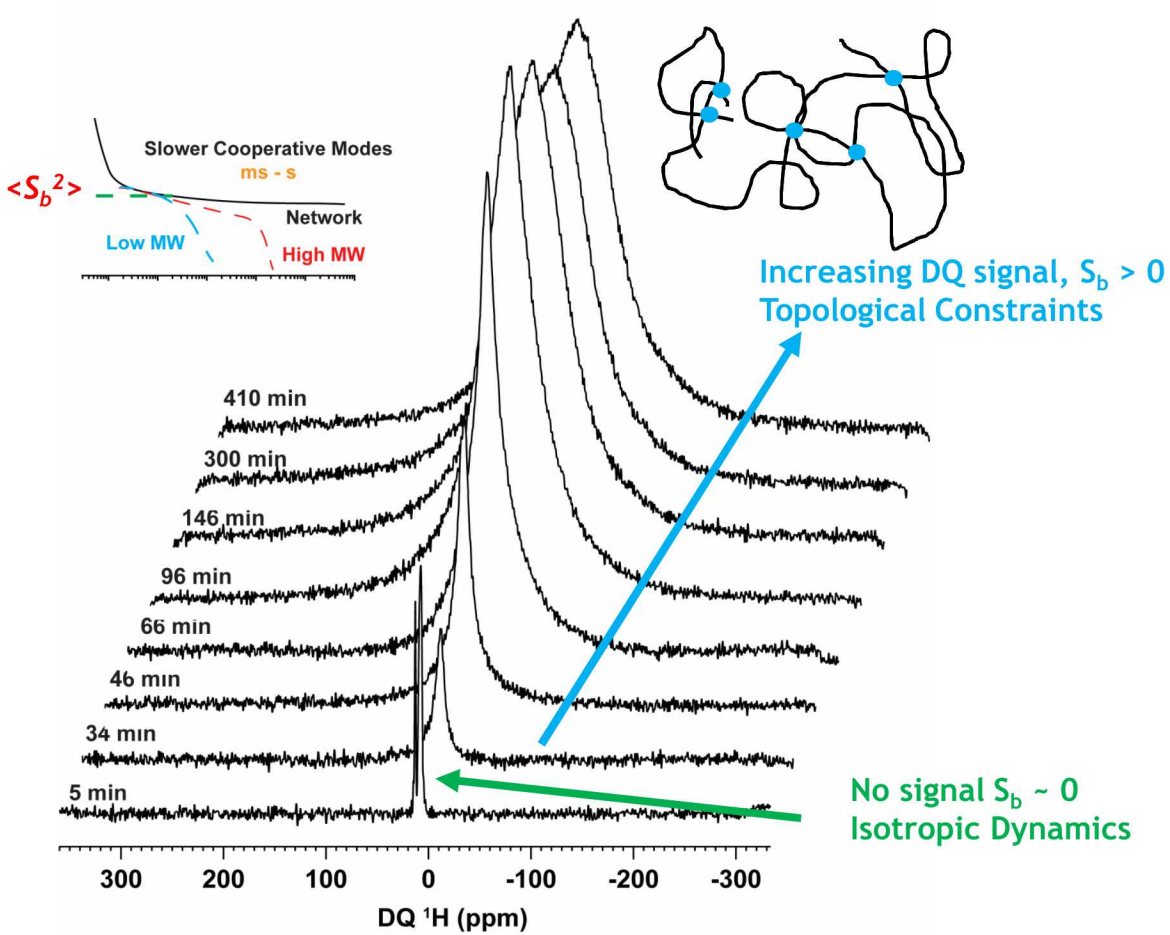

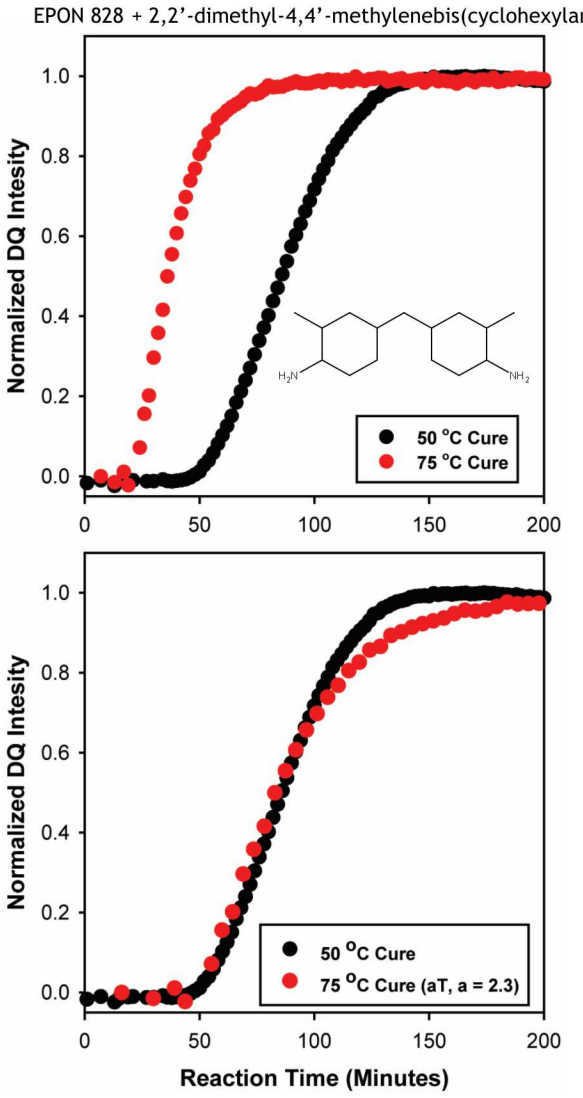

Martin-Gallego, M.; González-Jiménez, A.; Verdejo, R.; Lopez-Manchado, M. A.; Valentin, J. L., Epoxy resin curing reaction studied by proton multiple-quantum NMR. Journal of Polymer Science Part B: Polymer Physics 2015, 53 (18), 1324-1332.

^{1}H NMR - DQ NMR Fully Cure

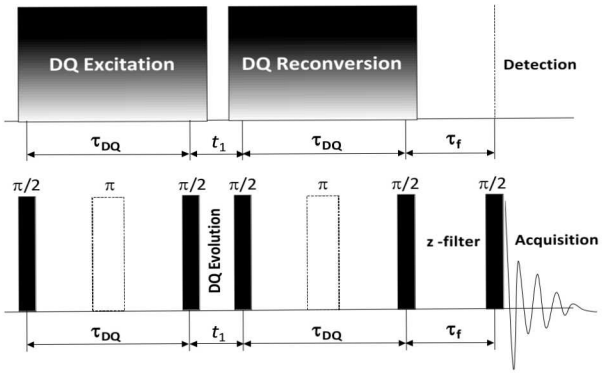

$$I_{nDQ} = \frac{I_{DQ}}{I_{DQ} + I_{ref} - B\exp\left[-2\tau_{DQ}/T_2\right]}$$

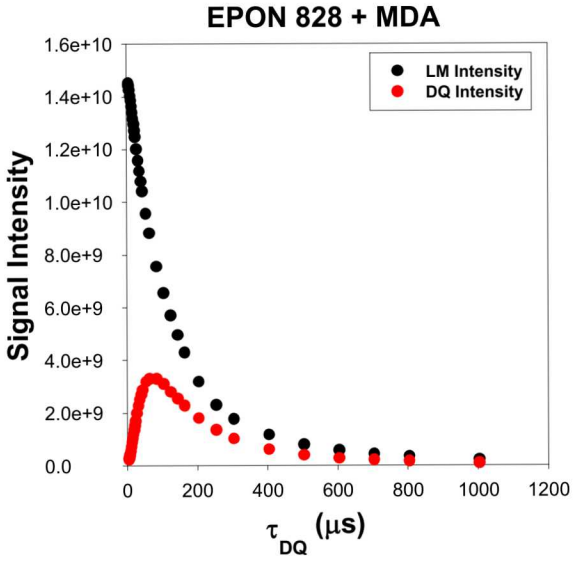

Raw DQ Data

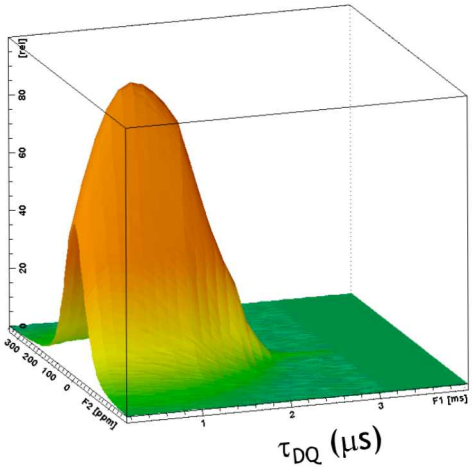

$$I_{nDQ} \rightarrow D_{res}$$

$$S_b = \frac{D_{res}}{D_{Static}}$$

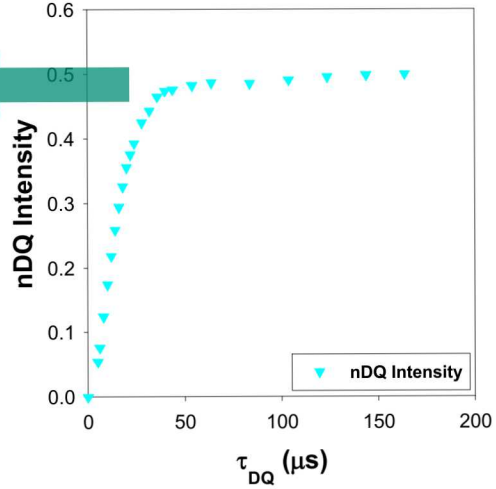

Normalized DQ Data

DQ ^{1}H NMR
Extraction of Effective Dipolar Coupling

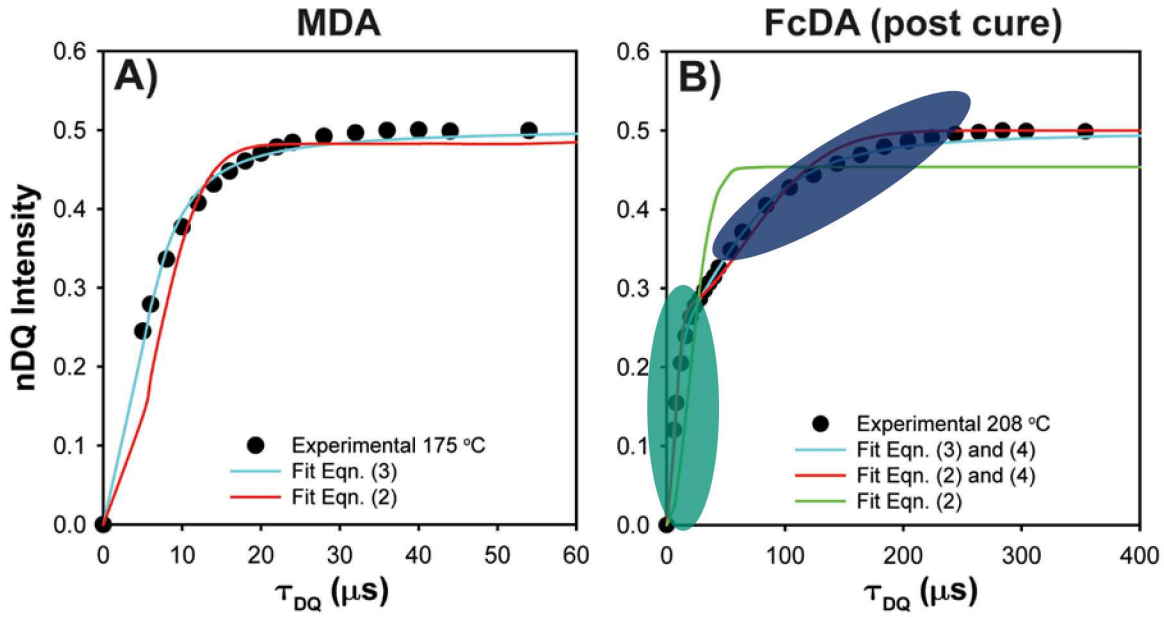

Gaussian Buildup

$$I_{nDQ}\left(D_{res}\right)=\frac{1}{2}\left(1-\exp\left\{-\frac{2}{5}D_{res}\tau_{DQ}^{2}\right\}\right)$$

Gaussian-Distributed Buildup

$$I_{nDQ}\left(\bar{D}_{res},\sigma_{D}\right)=\frac{1}{2}\left(1-\exp\left\{-\frac{\frac{2}{5}\bar{D}_{res}^{2}\tau_{DQ}^{2}}{1+\frac{4}{5}\sigma_{D}^{2}\tau_{DQ}^{2}}\right\}\left[1+\frac{4}{5}\sigma_{D}^{2}\tau_{DQ}^{2}\right]^{-1/2}\right)$$

$$I_{nDQ}\left(D_{res}^{(1)},D_{res}^{(2)},f\right)=f\,I_{nDQ}\left(D_{res}^{(1)}\right)+\left(1-f\right)I_{nDQ}\left(D_{res}^{(2)}\right)$$

DQ ^{1}H NMR Distribution of D_{res}

Fredholm Integral Equation

Experimental DQ buildups

Distribution of D_{res}

$$g(\tau_{DQ}) = \int_0^\infty K\left[D_{res}, \tau_{DQ}\right] f(D_{res})\, dD_{res}$$

Kernel

$$K\left[D_{res}, \tau_{DQ}\right]$$

Gaussian Buildup Kernal

$$I_{nDQ}(D_{res}) = \frac{1}{2}\left(1 - \exp\left\{-\frac{2}{5} D_{res} \tau_{DQ}^2\right\}\right)$$

"Abragam-like" (A-1) Kernel

$$I_{nDQ}(\tau_{DQ}, D_{res}) = \frac{1}{2}\left(1 - \exp\left\{-\left(0.378 D_{res} \tau_{DQ}\right)^{1.5}\right\}\right) \times \cos[0.583] D_{res} \tau_{DQ}$$

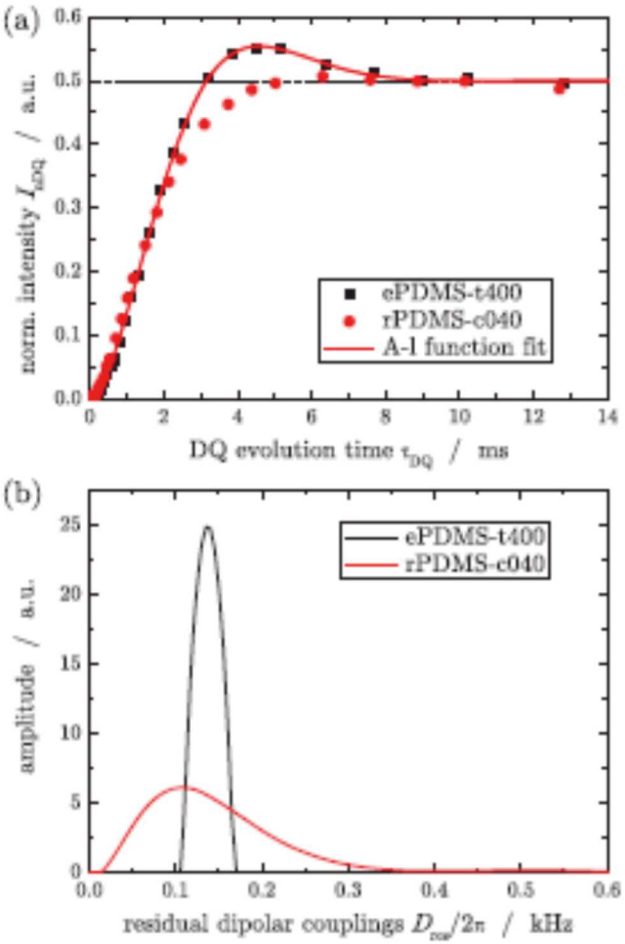

Chassé, W.; Valentín, J. L.; Genesky, G. D.; Cohen, C.; Saalwächter, K., Precise dipolar coupling constant distribution analysis in proton multiple-quantum NMR of elastomers. *The Journal of Chemical Physics* **2011**, *134* (4), 044907.